$P2Y_2$ NUCLEOTIDE RECEPTOR UP-REGULATION AND FUNCTION IN SUBMANDIBULAR GLAND EPITHELIUM

A dissertation presented to

the Faculty of the Graduate School

University of Missouri-Columbia

In Partial Fulfillment

of the Requirements for the Degree

Doctor of Philosophy

---

by

Ann Marie Schrader-Ratchford

Dr. Gary A. Weisman, Dissertation Supervisor

Dr. Robert W. Lim, Dissertation Supervisor

MAY 2005

ACKNOWLEDGEMENTS

There are many people in my life who have helped me become the person that I am, and have helped me attain the goals that I have achieved thus far. While here at the University of Missouri, I have met many friends, most of whom are members of the Departments of Medical Pharmacology and Physiology, and Biochemistry, all of whom have had an impact on my career here as a graduate student. First, I'd like to thank fellow classmate Youn Ju Lee and long-time friend and classmate Travis Hillen. Hanging out with each of them and having conversations about classes, research, and miscellaneous topics have been very helpful and enjoyable. Along with Youn Ju and Travis, I would like to thank the other fellow graduate students who are too numerous to name individually, but who have all made my time here a joyful experience. Next, I would like to acknowledge the office staff, Pamela Burgess and Donna Taylor-Stearns for always helping me, especially after the retirement of my advisor, Dr. John Turner. Dr. John Turner was my dissertation advisor for my first three years here, and I am thankful to him for the excellent scientific advice he has given me during that time. Many of the faculty members have helped me as well, not only as mentors, but also as friends. For this, I am eternally grateful. I would especially like to thank Dr. Judith Cole for fostering my goal of becoming a teacher and allowing me to lecture in the nursing pharmacology course; Dr. Robert Lim for taking over as my departmental advisor and giving excellent advice; and Dr. Gary Weisman for accepting me into his lab and leading my research project to completion. Dr. Gary Weisman has been an invaluable source of guidance and support in my development as a scientist during my last years here. Along with Dr. Robert Lim

and Dr. Gary Weisman, I would like to express my gratitude to the other members of my committee Dr. Stephen Halenda, Dr. Leonard Forte, and Dr. Laurie Erb for their contributions to my dissertation project. Next, I would like to thank my lab members in both the 'Turner lab' and the 'Weisman lab' who have provided an excellent working environment that is both professional and fun. In particular I would like to acknowledge Olga Baker and Jean Camden who have been great friends and a constant support for me emotionally and professionally. We have had some great times attending international meetings, discussing research projects, and celebrating good times. Jean especially, was an immense help after Dr. John Turner retired, and has been a constant source of inspiration.

Finally, I would like to thank my parents, Kenneth and Rita Schrader. They are a constant source of love, encouragement, and support, which has driven me to do the best that I can. I am also grateful to my husband, Nathan Ratchford and my siblings, Tina, Paul, Bob, Beth, and Alisa who are an endless source of inspiration, encouragement, and comic relief. Together, my parents, siblings, and Nathan have given me a source of solidarity and confidence to tackle any task ahead of me.

TABLE OF CONTENTS

ACKNOWLEDGEMENTS…….. iii

ABSTRACT……..….. vii

LIST OF TABLES…… .. ix

LIST OF FIGURES……..……...…. x

LIST OF ABBREVIATIONS……..… xiii

CHAPTER

1. INTRODUCTION……...…. 1

Salivary glands…… 1

Sjögren's syndrome……. 8

NOD.B10 mice……..… 9

P2 nucleotide receptors……. 15

$P2Y_2$ receptors in salivary glands……. 19

Experimental approach……...… 26

2. $P2Y_2$ NUCLEOTIDE RECEPTOR UP-REGULATION IN SUBMANDIBULAR GLAND CELLS FROM THE NOD.B10 MOUSE MODEL OF SJÖGRENS SYNDROME……. 27

Abstract……..…… 28

Introduction…… 29

Materials and Methods……..…….. 32

Results……..……. 38

Discussion……..……... 53

3. MATRIX METALLOPROTEASE- AND EGFR-DEPENDENT ERK1/2 ACTIVATION BY $P2Y_2$ NUCLEOTIDE RECEPTORS IN A HUMAN SUBMANDIBULAR GLAND CELL LINE…… .57

Abstract…….… 58

Introduction……... 60

Methods……... ….63

Results…… .68

Discussion…… 102

4. CONCLUDING REMARKS…….. 107

REFERENCES……...… 118

CURRICULUM VITA …… 133

ACADEMIC ABSTRACT

Sjögren's Syndrome (SS) is an autoimmune disease that specifically targets exocrine glands, including salivary glands, and results in an impairment of secretory function. The $P2Y_2$ nucleotide receptor is a 7 transmembrane spanning G protein-coupled receptor activated equipotently by extracellular ATP and UTP. $P2Y_2$ receptors are up-regulated in response to stress or injury in a variety of tissues including rat aorta after balloon angioplasty (Seye et al., 1997), collared rabbit carotid arteries (Seye et al., 2002), in myocardium from the left ventricle of rats with congestive heart failure (Hou et al., 1999), in a rat model of renal ischemic reperfusion (Kishore et al., 1998), in activated mouse thymocytes (Koshiba et al., 1997), and in submandibular glands under stress conditions (Turner et al., 1997; Ahn et al., 2000). Therefore, it was assessed whether $P2Y_2$ receptor expression was altered in submandibular glands (SMGs) of the NOD.B10 mouse model of primary SS as compared to SMGs of normal C57BL/6 mice. Results indicated that $P2Y_2$ receptor mRNA and activity are up-regulated in SMG of the SS mouse model, but not in SMG of normal mice. Other uridine nucleotide receptors, i.e., $P2Y_4$ and $P2Y_6$ receptors, showed no significant differences in expression between SMG cells of C57BL/6 or NOD.B10 mice, suggesting that only the $P2Y_2$ nucleotide receptor was up-regulated in NOD.B10 mice. Taken together, these results indicate that up-regulation of functional $P2Y_2$ receptors occurs in SMGs of the NOD.B10 mouse model of SS and warrant further studies to elucidate the function of $P2Y_2$ receptors in SS.

Recently, $P2Y_2$Rs have been shown to transactivate growth factor receptors and their signaling pathways via RAFTK (PYK2) and src (Soltoff, 1998; Liu et al., 2004). Additionally, transactivation of the epidermal growth factor receptor (EGFR) by other G protein-coupled receptors has been shown to be dependent on the proteolytic release of EGFR ligands such as heparin binding epidermal growth factor (HBEGF) (Prenzel et al., 1999; Pierce et al., 2001). Utilizing the human submandibular gland (HSG) cell line, we found that activation of the $P2Y_2$R by its agonist UTP causes phosphorylation of the EGFR and the extracellular-signal regulated kinases, ERK1/2, and downstream transcription factors ELK and P90RSK in a time-dependent manner. The EGFR inhibitor AG1478 blocked UTP-stimulated phosphorylation of the EGFR and ERK1/2. Moreover, TAPI-2, a matrix metalloprotease (ADAM17) inhibitor, and ADAM10 and ADAM17 siRNA also inhibited UTP-stimulated phosphorylation of the EGFR and ERK1/2. The src inhibitor PP2 inhibited UTP-stimulated ERK1/2, but not EGFR phosphorylation. Other results indicate that $P2Y_2$R-mediated ERK1/2 activation occurs by two distinct pathways, a rapid src- and PKC-dependent pathway and a slower response requiring ADAM10 and ADAM17 metalloprotease activity, EGFR transactivation and extracellular calcium. These studies suggest that $P2Y_2$Rs may be a promising target in treatments for Sjögren's syndrome.

LIST OF TABLES

Table Page

Table 1. Comparison between human Sjögren's syndrome (SS) and murine autoimmune exocrinopathy (AEC)…….…… 11

Table 2. P2X and P2Y receptors are classified according to their agonist rank order potencies……..……. 22

LIST OF FIGURES

Figure Page

Figure 1. Diagram of human salivary glands…….. 4

Figure 2. Structure of salivary glands…….. 6

Figure 3. Time line for biochemical and physiological changes related to the development of loss of secretory function observed in the Sjögren's syndrome-like disease of non-obese diabetic (NOD) mice…….. ….13

Figure 4. P2 receptors…….. ……17

Figure 5. The structure of the human $P2Y_2$ receptor……... 24

Figure 6. Detection of $P2Y_2$receptor mRNA in SMG cells from NOD.B10 and C57BL/6 mice by RT-PCR……. 39

Figure 7. Detection of $P2Y_2$ receptor mRNA in SMG slices from NOD.B10 or C57BL/6 mice by *in situ* hybridization…….……..41

Figure 8. Detection of $P2Y_4$ and $P2Y_6$ receptor mRNA in mouse SMG cells from NOD.B10 and C57BL/6 mice by RT-PCR……43

Figure 9. $P2Y_2$ receptor activity in SMG cells isolated from NOD.B10 and C57BL/6 mice……. 47

Figure 10. Percentage of UTP-responsive SMG cells from NOD.B10 or C57BL/6 mice …….……..49

Figure 11. $P2Y_6$ receptor activity in SMG cells from NOD.B10 and C57BL/6 mice……...51

Figure 12. Concentration-dependence of UTP-induced phosphorylation of EGFR, ERK1/2, and downstream targets of ERK1/2, p90RSK and ELK in HSG cells……..…..69

Figure 13. Time-dependence of UTP-induced phosphorylation of EGFR, ERK1/2, and the downstream targets of ERK, p90RSK and ELK in HSG cells...…….71

Figure 14. Detection of $P2Y_2$ and $P2Y_6$ but not $P2Y_4$ receptor mRNA in HSG cells, and of detection $P2Y_2$ but not $P2Y_6$ receptor activity…….73

Figure 15. The EGFR autophosphorylation inhibitor AG1478 affects only the slow phase of UTP-induced ERK1/2 phosphorylation in HSG cells..77

Figure 16. The src inhibitor PP2 affects only the rapid phase of UTP-induced ERK1/2 phosphorylation in HSG cells …….. 79

Figure 17. TAPI-2, a selective inhibitor of ADAM17, inhibits the EGFR-dependent phase of UTP-induced ERK1/2 phosphorylation in HSG cells ……83

Figure 18. CMK, a furin inhibitor, inhibits the EGFR-dependent phase of UTP-induced ERK1/2 phosphorylation in HSG cells…….85

Figure 19. ADAM10 and ADAM17 siRNAs inhibit UTP-induced ERK1/2 phosphorylation in HSG cells ……..…..…87

Figure 20: Anti-growth factor antibodies do not inhibit UTP-induced phosphorylation of the EGFR in HSG cells ……..…….90

Figure 21. UTP-induced ERK1/2 phosphorylation is not dependent on intracellular calcium……94

Figure 22: UTP-induced ERK1/2 phosphorylation due to EGFR transactivation is dependent on extracellular calcium ……..…..…96

Figure 23: Rapid UTP-induced ERK1/2 phosphorylation is dependent on PKC.97

Figure 24: Model for $P2Y_2R$-mediated EGFR transactivation and ERK1/2 phosphorylation ……...……..….99

Figure 25. $P2Y_2Rs$ do not promote cleavage of pro-caspase-3 in HSG cells...109

Figure 26. Effect of resveratrol on $P2Y_2R$ agonist-induced increases of $[Ca^{2+}]_i$ and $P2Y_2R$ mRNA expression in rat SMG cells after 48 h in culture…….114

LIST OF ABBREVIATIONS

ADAM10	a disintegrin and metalloprotease 10
ADAM17	a disintegrin and metalloprotease 17
ADP	adenosine 5'-diphospate
AEC	Autoimmune Exocrinopathy
AR	amphiregulin
ATP	adenosine 5'-triphosphate
BCIP	5-bromo-4-chloro-3-indolyl phosphate toluidine salt
BSA	bovine serum albumin
BzATP	benzoylbenzoyl-ATP
cAMP	adenosine 3',5'-cyclic monophosphate
Caspases	cysteine proteases with aspartate specificity
COX-2	cyclooxygenase-2
DIG	digoxigenin
DMEM-F12	Dulbecco's modified Eagle's medium-Ham's F-12
DNase	ribonuclease-free deoxyribonuclease
EDRF	endothelium derived relaxing factor, also known as nitric oxide
EGF	epidermal growth factor
EGFR	epidermal growth factor receptor
ERK1/2	extracellular regulated kinases 1 and 2
FBS	fetal bovine serum
G3PDH	glyceraldehyde-3-phosphate dehydrogenase

GPCR	G protein-coupled receptor
GTP	guanosine 5'-triphospate
HBEGF	heparin binding EGF-like growth factor
HEPES	N-2-hydroxyethylpiperazine-N'-2-ethane-sulfonic acid
$[Ca^{2+}]_i$	intracellular calcium concentration
IFNγ	interferon gamma
IP_3	inositol 1,4,5-trisphosphate
JNK	c-Jun N-terminal kinase
MAPK	mitogen activated protein kinase
MEK1/2	ERK kinase
MHC	major histocompatability complex
MMPs	matrix metalloproteases
mRNA	messenger RNA
NBT	nitro blue tetrazolium chloride
NO	nitric oxide
NOD	non-obese diabetic
p38MAPK	p38 mitogen activated protein kinase
p90RSK	p90 ribosomal S6 kinase
PAR	parotid gland
PDGF	platelet derived growth factor
PDGFR	platelet derived growth factor receptor
PKC	protein kinase C
PLA2	phospholipase A2

PLCβ	phospholipase Cβ
PLD	phospholipase D
PMA	phorbol 12-myristate 13-acetate
PYK2	proline rich tyrosine kinase 2
RAFTK	related adhesion focal tyrosine kinase
RT-PCR	reverse transcription-polymerase chain reaction
SAPK	stress activated protein kinase
SDS-PAGE	sodium dodecyl sulfate-polyacrylamide gel electrophoresis
siRNA	small interference RNA
SH3	src homology 3
SMG	submandibular gland
SS	Sjögren's syndrome
TBST	tris-buffered saline containing Tween 20
TGFα	transforming growth factor alpha
TNFα	tumor necrosis factor alpha
UDP	uridine 5'-diphosphate
UTP	uridine 5'-triphosphate
VCAM	vascular cell adhesion molecule
VEGFR	vascular endothelial growth factor receptor

CHAPTER 1

INTRODUCTION

This dissertation examines the role of $P2Y_2$ nucleotide receptor expression in salivary glands, particularly in a mouse model of the autoimmune salivary gland disease Sjögren's syndrome (see Chapter 2). The signal transduction pathways downstream of $P2Y_2$ receptor activation in salivary gland cells are also considered (see Chapter 3). Chapter 1 concerns background information about the structure and function of salivary glands, the etiology of Sjögren's syndrome, the utility of the NOD.B10 mouse model of Sjögren's syndrome, the structure and function of P2 nucleotide receptors, particularly the $P2Y_2$ subtype, and $P2Y_2$ receptor signaling in salivary glands in relation to salivary gland function.

Salivary glands

The salivary glands secrete saliva, a physiologically active product that continually bathes the teeth and oral mucosa. Some functions of saliva include: 1) aiding in digestion of starchy food particles; 2) lubrication of food to facilitate swallowing, and lubrication of the oral cavity to facilitate speech; 3) providing anti-microbial action that is both bacteriostatic and bacteriocidal; and 4) protection against tooth demineralization [1]. The saliva is composed of water, salts, and mucins that coat and protect the lining of the teeth and cavity walls, lysozymes, lactoferrins, and peroxidases that retard bacterial growth, and other proteins such as amylases that facilitate digestion of carbohydrates.

There are three pairs of major salivary glands, the submandibular, parotid, and sublingual glands, that together contribute to saliva production to varying degrees and supply saliva components (see Figure 1). There are also minor salivary glands located on the tongue, palate, and buccal and labial mucosa that contribute small amounts of saliva. The smallest of the paired glands, the sublingual glands, are inferior to the tongue and contribute 5% of total salivary secretion. The parotid glands, situated anteroinferiorly to the ear, are the largest of the salivary glands, and contribute 20% of total saliva secretion. The submandibular gland is located inferior to the jaw and contributes 70% of the saliva produced [2].

The three types of salivary glands are comprised primarily of two cell types: acinar cells, either mucosal or serosal, and ductal cells, either intercalated, striated, or excretory (see Figure 2). The acinar cells are stimulated by neurotransmitters acting on receptors that stimulate secretion by increasing the intracellular Ca^{2+} concentration to activate Ca^{2+}-activated Cl^- channels, and by generating the ion gradients that facilitate water flow to the luminal side of the glandular structure. These ion gradients promote the transport of secretagogues through the ductal structures where the ionic content of saliva portion is modified by selective ion reabsorption into the cells. The final product flows to the mouth cavity where it lubricates the oral surfaces and aids in digestion of food particles.

Each salivary gland contributes to saliva production in different ways due to the type of acinar cells that comprise the individual glands. The sublingual gland, mostly composed of mucous acinar cells, produces a mucous or viscous

secretion. The parotid gland, formed mostly of serous acinar cells, generates a watery secretion. Finally, the submandibular gland, composed of both serous and mucous acinar cells, secretes a fluid that is a mixture of both mucous and serous saliva.

Figure 1. Diagram of human salivary glands. The three major paired salivary glands are the submandibular, parotid, and sublingual glands [3]. The submandibular, parotid, and sublingual glands produce 70%, 20%, and 5% of the total saliva, respectively. The minor salivary glands contribute the remaining 5% of the saliva. A cross section of the submandibular gland in the bottom right panel shows the two types of acinar cells, mucosal and serosal.

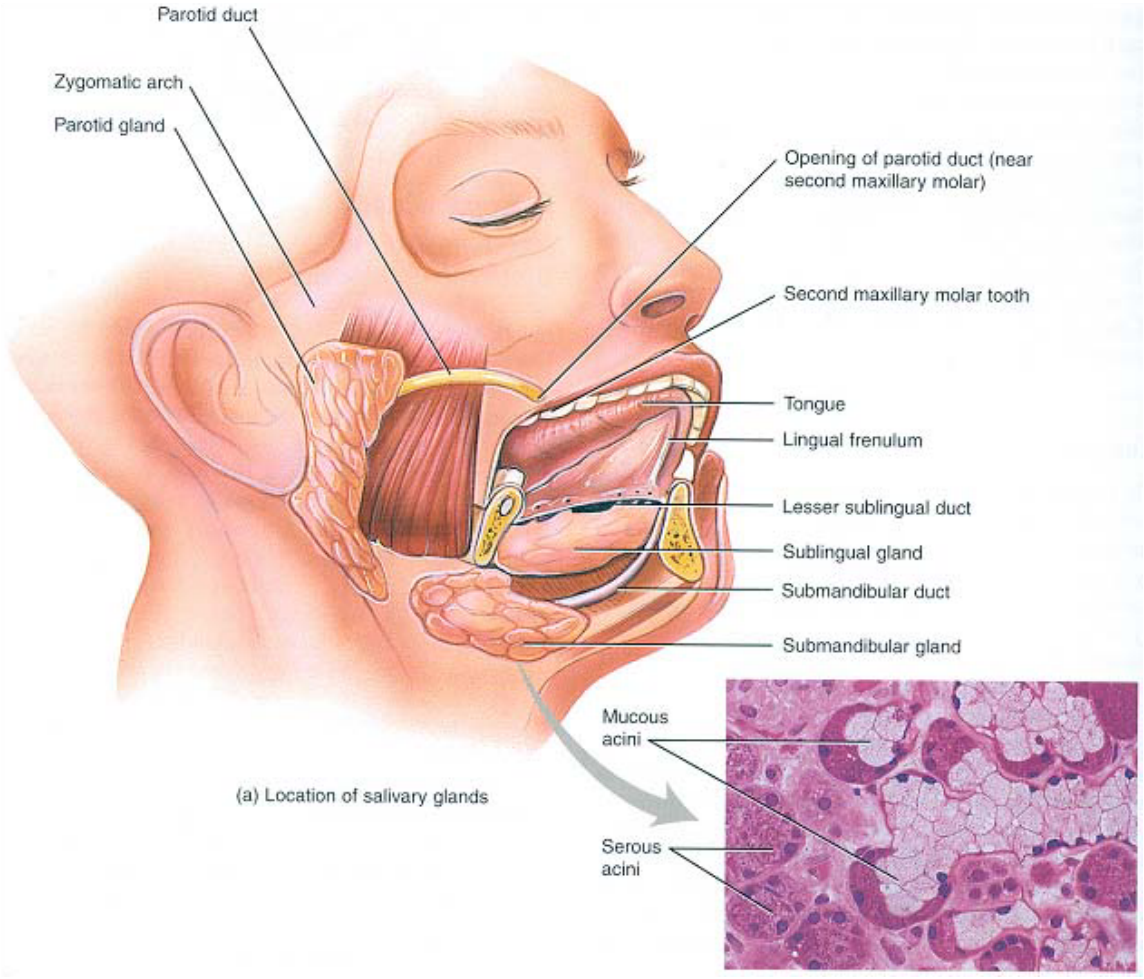
Parotid duct
Zygomatic arch
Parotid gland
Opening of parotid duct (near second maxillary molar)
Second maxillary molar tooth
Tongue
Lingual frenulum
Lesser sublingual duct
Sublingual gland
Submandibular duct
Submandibular gland
Mucous acini
Serous acini
(a) Location of salivary glands

Figure 2. Structure of salivary glands. The salivary glands are composed of two types of acinar cells, serosal and mucosal, and three types of ductal cells, intercalated, striated, and excretory [4].

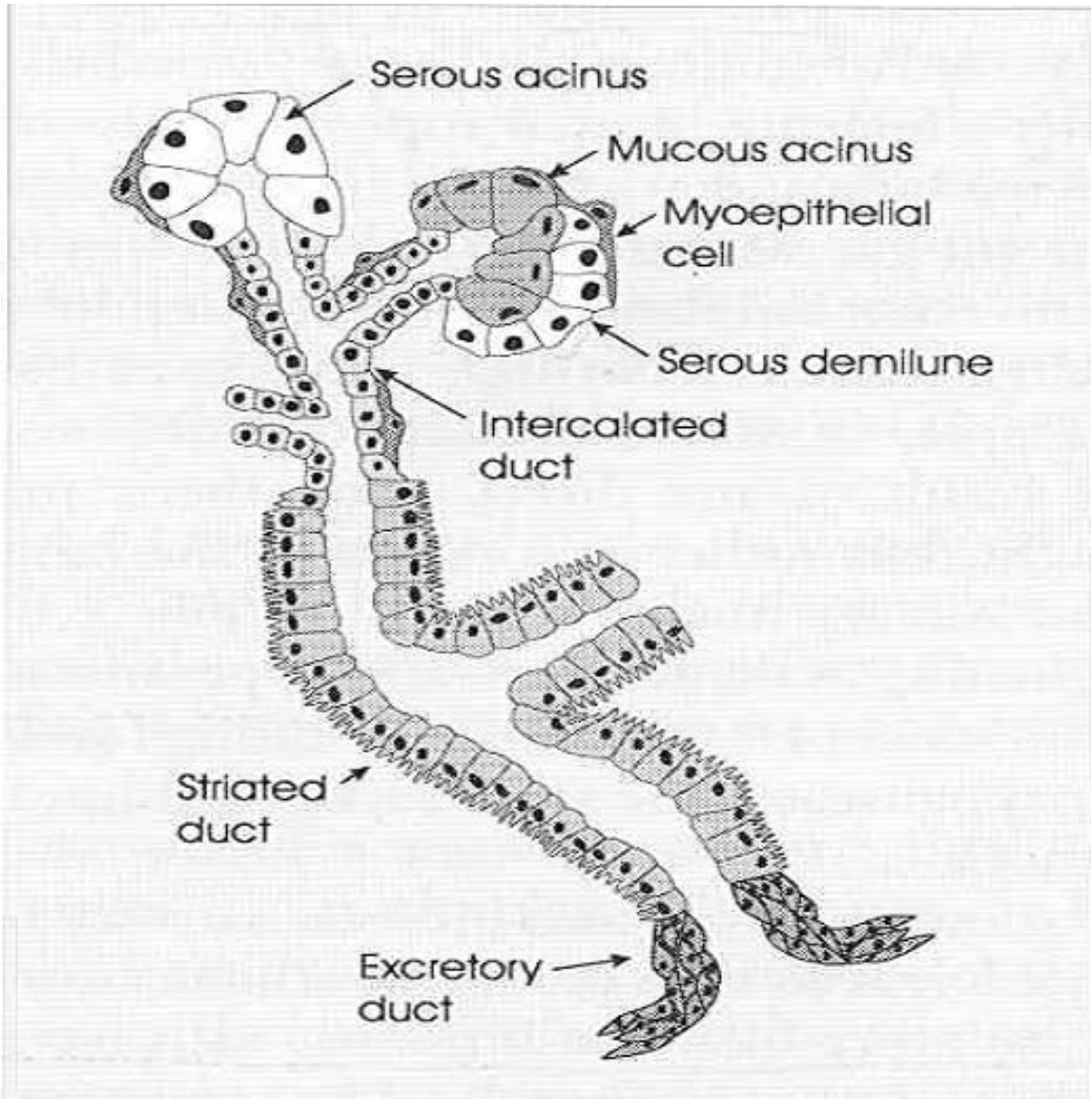
Serous acinus
Mucous acinus
Myoepithelial cell
Serous demilune
Intercalated duct
Striated duct
Excretory duct

Sjögren's syndrome

Sjögren's syndrome (SS) is an autoimmune disease in which immune cells invade the salivary and lacrimal exocrine glands. The syndrome is named after Dr. Henrik Sjögren, a Swedish ophthalmologist who described the symptoms in his thesis work in 1933 [5]. Earlier, in 1926, Henri Gougerot, a French ophthalmologist published the observation of what is now known as SS (the combinatorial presentation of the symptoms of dry eyes, dry mouth, and pain in several joints), although the disease is named after Sjögren who reported more cases, surpassed in number only by the Mayo Clinic, Rochester, USA [5]. SS is characterized by xerostomia (dry mouth) and xerophthalmia (dry eyes) and affects more than a million people in the United States, predominantly female (90%). Dryness of the mucosal surfaces serviced by exocrine glands such as skin, gastrointestinal tract, lungs, and other tissues has also been observed in patients with SS [6]. About 50% of the time, SS occurs alone and is termed primary SS, and 50% of the time, it occurs in the presence of another connective tissue disease and is termed secondary SS. The four most common diagnoses that co-exist with SS are rheumatoid arthritis, systemic lupus, systemic sclerosis (scleroderma), and polymyositis/dermatomyositis [7].

Pathogenesis of SS occurs in two phases: an asymptomatic phase in which epithelial cells of exocrine tissues undergo dedifferentiation accompanied by elevated apoptosis, and a secondary phase in which organ autoantigens result in the activation of T-and B-cells, and the generation of autoantibodies [8]. The presence of autoantibodies to the cell surface muscarinic receptor, M3,

correlates with the hallmark clinical symptom of secretory dysfunction [9-11]. In addition, alterations in glandular innervation of the exocrine tissues in SS patients have been detected [11-14].

Histopathological analysis of minor salivary glands from SS patients shows primarily $CD4^+$ T-cell lymphocytes [15]. Infiltrates appear as peri-ductal and peri-vascular foci within the glandular architecture of the salivary and lacrimal glands. Serological evaluations show the presence of rheumatoid factor, hypergammaglobulinaemia, and specific anti-nuclear antibodies to nuclear proteins such as SS-A/Ro and SS-B/La [7], as well as antibodies against α-fodrin [16], carbonic anhydrase II [17], and the muscarinic M3 receptor [9-11, 18].

To investigate the etiology of SS, several mouse models have been developed, including MRL/lpr, New Zealand white/New Zealand black (NZW/NZB), NFS/sld, and the non-obese diabetic (NOD) mouse. Despite the apparent similarities between SS and the several animal models, only the NOD mouse has been shown to demonstrate a corresponding loss of secretory function that parallels the temporal progression of lymphocytic infiltrates in these tissues [11, 19-21]. For this reason, the NOD mouse has emerged as an excellent model for the study of the pathogenesis of SS-like disease.

NOD.B10 mice

The NOD mouse model most closely matched to primary SS is the NOD.B10 mouse model, which displays a similar disease called Autoimmune Exocrinopathy (AEC) [18]. NOD.B10 mice, unlike the parental NOD mice, do not

display diabetes but retain the impaired ability to secrete saliva and tears. This makes them an excellent model for primary SS [18]. The biochemical and immunological similarities between human SS and AEC in the NOD mouse include the presence of lymphocytic infiltrates correlated with the impairment of secretory function and tear formation, as well as the presence of autoantibodies [18], as shown in Table 1. Since NOD-scid (severe combined immunodeficiency) mice lack the ability to generate functional B- and T-lymphocytes due to the introduction of a homozygous mutation at the scid locus, scientists are able to separate abnormalities that are caused by genetic changes from those caused by the immune system. Interestingly, despite the changes in exocrine tissue homeostasis, NOD-scid mice do not lose secretory capacity with increasing age, although there is a decline in the acinar to ductal cell ratio due to acinar cell death [11, 22, 23]. This suggests that AEC may occur in two phases, the first being triggered by genetic abnormalities and the second being triggered by an immune response, as shown in Figure 3 [8]. Nod.Igm null mice lacking functional B-lymphocytes but not T-lymphocytes, retain the capacity to secrete saliva, even though glandular homeostasis is altered in a similar manner to NOD and NOD-scid mice [11, 24]. This suggests that B-cells and autoantibodies may play a primary role in establishing decreased secretory function.

Table 1. Comparison between human Sjögren's syndrome (SS) and murine autoimmune exocrinopathy (AEC).

Sjögren's syndrome (SS)	Autoimmune exocrinopathy (AEC)
Lacrimal glands	
Decreased tear formation	Decreased tear formation (30%)
Lymphocytic infiltrates	Lymphocytic infiltrates
Salivary glands	
Lymphocytic foci of PAR, SMX	Lymphocytic foci of SMX and minor salivary glands
Loss of secretory response in all glands	Loss of secretory response in all glands (90%)
Salivary gland enlargement	Same gland size or decrease
Fas:FasL expressed on epithelial cells	Fas:FasL expressed on epithelial cells
Elevated levels of caspase and MMP (metalloproteinase)	Elevated levels of caspase and MMP (metalloproteinase)
Saliva	
Temporal decline in amylase activity	Temporal decline in amylase activity
Serum	
Anti-muscarinic (M3) receptor	Anti-muscarinic (M3) receptor

Figure 3. Time line for the biochemical and physiological changes related to the development of loss of secretory function observed in the Sjögren's syndrome-like disease of non-obese diabetic (NOD) mice. These same events may be operative in the glandular epithelial cells of human patients [8].

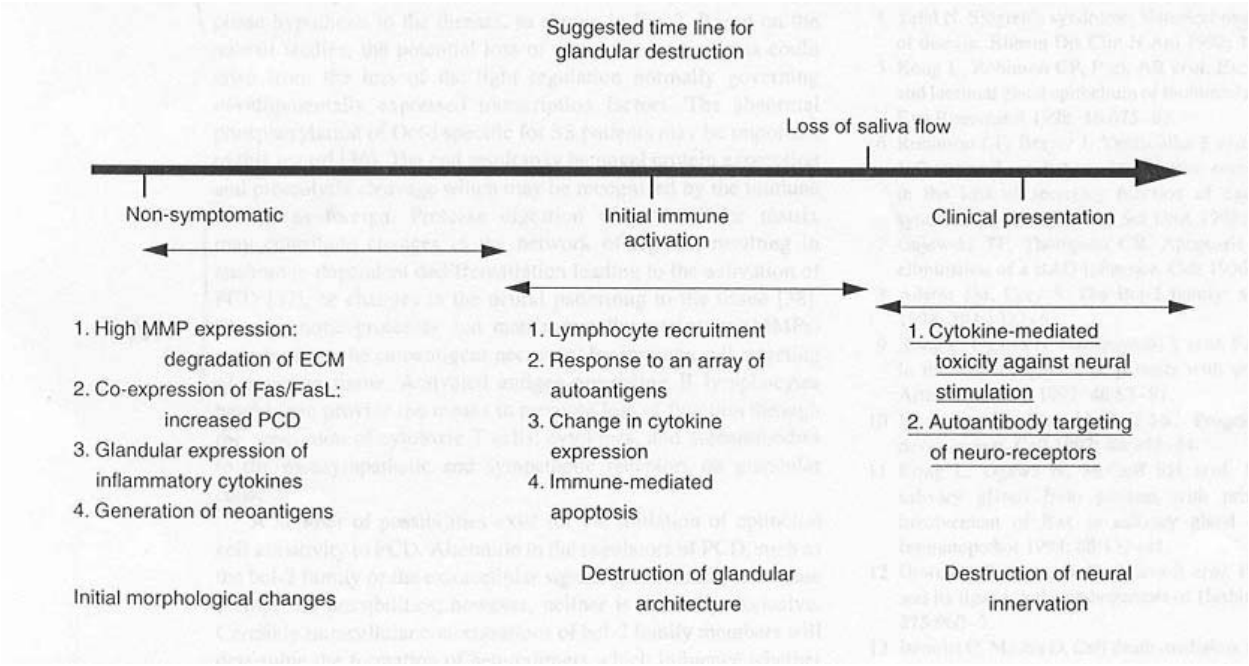
Suggested time line for glandular destruction
Loss of saliva flow
Non-symptomatic
Initial immune activation
Clinical presentation
1. High MMP expression: degradation of ECM
2. Co-expression of Fas/FasL: increased PCD
3. Glandular expression of inflammatory cytokines
4. Generation of neoantigens
1. Lymphocyte recruitment
2. Response to an array of autoantigens
3. Change in cytokine expression
4. Immune-mediated apoptosis
1. Cytokine-mediated toxicity against neural stimulation
2. Autoantibody targeting of neuro-receptors
Initial morphological changes
Destruction of glandular architecture
Destruction of neural innervation

P2 nucleotide receptors

Biological sources of extracellular nucleotides include the release of ATP from contracting skeletal muscle contraction, from stimulated sensory nerves, and from a variety of cell types in response to mechanical stress or injury [25]. Extracellular nucleotides are important signaling molecules that mediate a variety of physiological effects by acting on cell surface nucleotide receptors. These nucleotide receptors, known as P2 receptors, are activated by the extracellular nucleotides ATP, ADP, UTP, or UDP and can mediate a variety of effects including smooth muscle contraction, neurotransmission, exocrine and endocrine secretion, immunoreactivity, inflammation, platelet aggregation, cell proliferation, and modulation of cardiac function [25-29]. P2 receptor subtypes are classified according to their molecular structures, effector systems, and pharmacological profiles. Based on these criteria, P2 nucleotide receptors can be divided into two families: ligand-gated ion channels (P2X receptors) and G protein-coupled P2Y receptors (see Figure 4, [30]).

Members of the P2X receptor family are ATP-gated ion channels that mediate rapid increases (within 10 ms) in the plasma membrane permeability of Na^+, K^+, and Ca^{2+} cations [31-33]. Functional P2X receptors are comprised of hetero- or homo-multimers [25]. Each subunit has 379 to 472 amino acids and consists of 2 transmembrane-spanning α helices with a large extracellular domain containing a number of disulfide bonds [25, 34].

In contrast to P2X receptors, P2Y receptors respond to ATP and other adenine and uridine nucleotides and have slower response times (less than 100

ms) due to coupling to heterotrimeric GTP-binding proteins (G proteins) proteins and their second messenger systems [25, 35]. Members of the P2Y receptor family have 308 to 377 amino acids (masses of 41 to 53 kDa after glycosylation), and are comprised of 7 transmembrane-spanning domains.

The families of P2 receptors (P2X and P2Y) can be further subdivided into subtypes based upon distinct rank order of agonist potencies for each receptor. Currently, seven P2X receptor subtypes ($P2X_{1-7}$) and eight P2Y receptor subtypes ($P2Y_1$, $P2Y_2$, $P2Y_4$, $P2Y_6$, $P2Y_{11}$, $P2Y_{12}$, $P2Y_{13}$, $P2Y_{14}$) have been cloned. The rank order of agonist potencies for the above receptors are listed in Table 2. Of the P2Y receptors, $P2Y_1$, $P2Y_2$, $P2Y_4$, $P2Y_6$, and $P2Y_{11}$ receptors are coupled to the phospholipase C (PLC) signaling pathway leading to inositol 1,4,5-trisphosphate (IP_3)-dependent increases in $[Ca^{2+}]_i$ and diacylglycerol-dependent activation of protein kinase C (PKC). The $P2Y_{11}$ receptor is also positively coupled to adenylyl cyclase. $P2Y_{12}$, $P2Y_{13}$, and $P2Y_{14}$ receptors couple to the G_i protein signaling pathway that inhibits adenylyl cyclase [36].

Figure 4. P2 receptors. P2 receptors are classified into two families: P2X receptors are ligand-gated ion channels, and P2Y receptors are G protein-coupled receptors.

P2X
($P2X_{1-7}$)
ligand-gated ion channels

P2Y
($P2Y_{1, 2, 4, 6, 11, 12, 13, 14}$)
G protein-coupled receptors

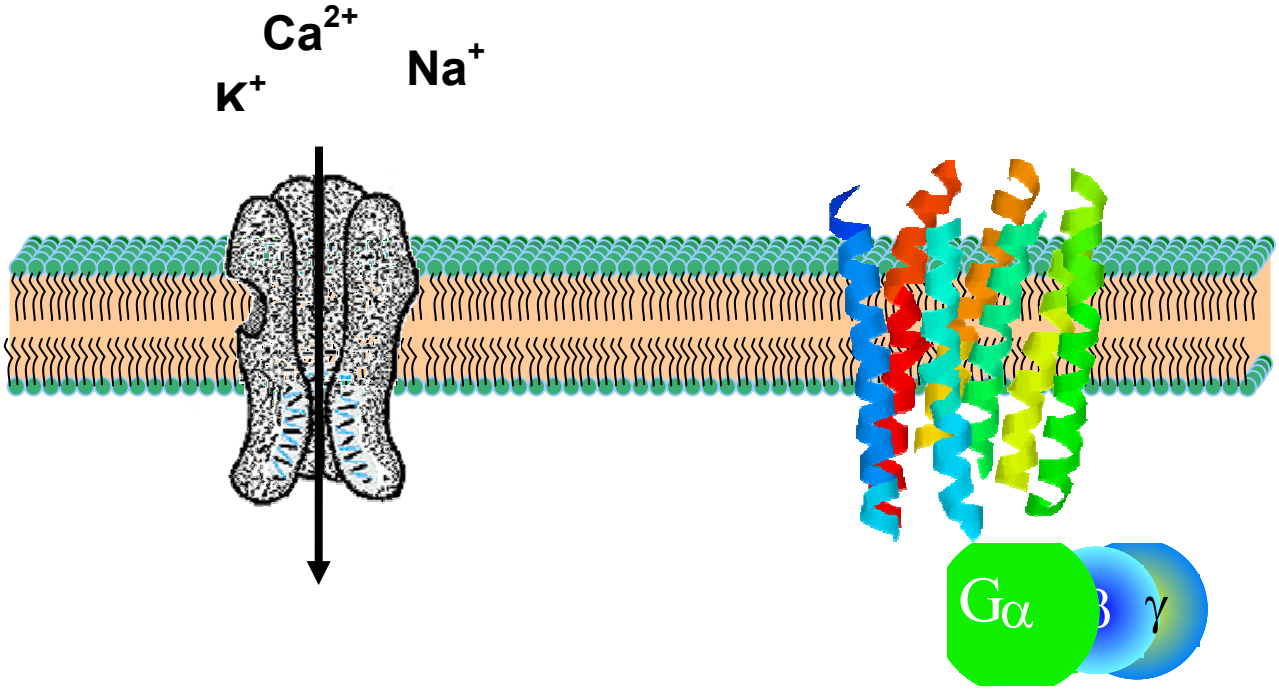

$P2Y_2$ receptors in salivary glands

In salivary glands, four subtypes of P2 receptors have been identified: $P2X_4$, $P2X_7$, $P2Y_1$ (in developing glands), and $P2Y_2$ (up-regulated in response to stress). The rank order of agonist potencies for the four above-mentioned receptors are listed in bold in Table 2 [37, 38]. Through changes in $[Ca^{2+}]_i$ and other mechanisms, P2 receptors appear to regulate salivary cell volume, ion and protein secretion, and the permeability of small molecules possibly related to cytotoxicity [38, 39]. The roles of P2 receptors in regulating saliva secretion have not been reported, however, the ability of nucleotides to increase second messenger levels, ion fluxes, and protein secretion in salivary gland cells suggests that P2 receptors modulate the production and composition of saliva [38].

Recombinant and endogenous $P2Y_2$ receptors couple to PLCβ via G_{q11} protein to mediate phosphoinositol 4,5-bisphosphate hydrolysis leading to IP_3-dependent Ca^{2+} mobilization, and diacylglycerol-dependent activation of PKC, and $P2Y_2$ receptors also can couple to $G_{i/o}$ proteins by an integrin-dependent mechanism [32, 40]. $P2Y_2$ receptor-mediated activation of G_{q11} protein and PLCβ also stimulates PLA2, Ca^{2+}-dependent K^+ channels, and generation of endothelium-derived relaxing factor (EDRF) [25, 32, 40]. The specific downstream response to activation by $P2Y_2$ receptors of a given signaling pathway is partially dependent on the cell type in which the $P2Y_2$ receptor is expressed. In NCB-20 cells, and renal mesangial cells, $P2Y_2$ receptors stimulate the inhibition of cAMP formation accompanied by elevations in $[Ca^{2+}]_i$ [41, 42]. In

airway epithelial cells, $P2Y_2$ receptor activation mediates the gating of Ca^{2+}-dependent Cl^- channels that in turn promote fluid secretion [43, 44]. In rat hypothalamus, $P2Y_2$ receptors mediate depolarization of supraoptic neurosecretory cells by opening a nonselective cation channel [45]. $P2Y_2$ receptor also couple to activation of PLD and stimulation of phosphatidylcholine breakdown [46, 47], by a mechanism that is Ca^{2+}-independent [48]. In addition, protein tyrosine phosphorylation and MAPK activation can occur in response to $P2Y_2$ receptor-mediated activation of PKC, independent of IP_3, $[Ca^{2+}]_i$ [49], or without activation of PKC due to stimulation of stress-activated protein kinases [50].

The ERK pathway plays an important role in the regulation of gene expression that controls many cellular processes including growth and differentiation. In cultured aortic smooth muscle cells and in activated thymocytes, $P2Y_2$ receptors mediate an increase in the expression of immediate-early and delayed-early cell cycle-dependent genes [51]. Since ERK is activated in response to a wide range of cellular stresses and since $P2Y_2$ receptors are up-regulated in response to injury or stress [52-58], it is logical to assume that $P2Y_2$ receptors can activate the ERK pathway. Indeed, the ability of $P2Y_2$ receptors to activate ERK has been reported [59-61]. Activation of ERK by the $P2Y_2$ receptor can occur via EGFR transactivation [60], in part through binding of Src to SH3 binding domains in the C-terminal tail of the $P2Y_2$ receptor, ([62]; see Figure 5). $P2Y_2$ receptor-mediated EGFR transactivation in human salivary gland (HSG) cells has been investigated (see Chapter 3).

To analyze the function of the $P2Y_2$ receptor, a $P2Y_2$ receptor knockout mouse has been developed by Homolya et al. (1999) that displays reduced chloride secretion in airway epithelial cells, confirming the importance of the $P2Y_2$ receptor in regulating epithelial chloride secretion [63, 64]. In the ocular mucosa, $P2Y_2$ receptor activation increases salt, water, and mucous secretion [65]. The $P2Y_2$ receptor also regulates fluid and electrolyte (chloride) secretion in the colon and gallbladder, pancreatic and bile ducts [37], and airway epithelium where fluid secretion is accompanied by mucin glycoprotein release from epithelial goblet cells [66]. $P2Y_2$ receptor activation also promotes inflammation in vascular human coronary artery endothelial cells (HCAEC) that occurs through the SH3 binding domain-dependent transactivation of vascular epidermal growth factor receptor type 2 (VEGFR-2) [67], leading to increases in the expression of vascular cell adhesion molecule (VCAM-1) and recruitment of monocytes [53, 67]. In addition to intracellular C-terminal SH3 binding domains, the $P2Y_2$ receptor also contains an Arg-Gly-Asp (RGD)-sequence in the first extracellular loop that has been shown to interact with $\alpha_v\beta_3/\beta_5$ integrins [40] to regulate nucleotide-induced cell chemokinesis and chemotaxis [68, 69], responses associated with inflammation [70].

Table 2. P2X and P2Y receptors are classified according to their rank order of agonist potencies. Table 2 shows the rank order of agonist potencies of the cloned P2 receptor subtypes [37].

Receptor Subunit	Rank Order of Agonist Potency
$P2X_1$	2-MeSATP>ATP>α,β-meATP
$P2X_2$	2-MeSATP>ATP (α,β-meATP inactive)
$P2X_3$	2-MeSATP>ATP>α,β-meATP
$P2X_4$	ATP>2-MeSATP>α,β-meATP
$P2X_5$	ATP>2-MeSATP>ADP
$P2X_6$	ATP>2-MeSATP>ADP
$P2X_7$	BzATP, ATP>2-MeSATP>ADP
Receptor Subtype	
$P2Y_1$	2-MeSADP>ATP>ADP (UTP inactive)
$P2Y_2$	UTP=ATP>>2-MeSATP
$P2Y_4$	UTP>ATP=ADP
$P2Y_6$	UDP>UTP>ADP
$P2Y_{11}$	ATP>2-MeSATP>ADP
$P2Y_{12}$	2MeSATP=2MeSADP>ADP
$P2Y_{13}$	2MeSATP=2MeSADP>ADP>ATP
$P2Y_{14}$	UDP-glucose>UDP-galactose

Figure 5. The structure of the human $P2Y_2$ receptor. The $P2Y_2$ receptor is a seven transmembrane spanning receptor containing SH3 binding domains (yellow) in the C-terminal tail, and an integrin ($\alpha_v\beta_3/\beta_5$) binding domain (red) in the first extracellular loop [40, 62]. We have incorporated a hemagglutinin epitope tag at the N-terminus of the recombinant $P2Y_2$ receptor (green) and amino acids required for receptor activation are shown in orange [71].

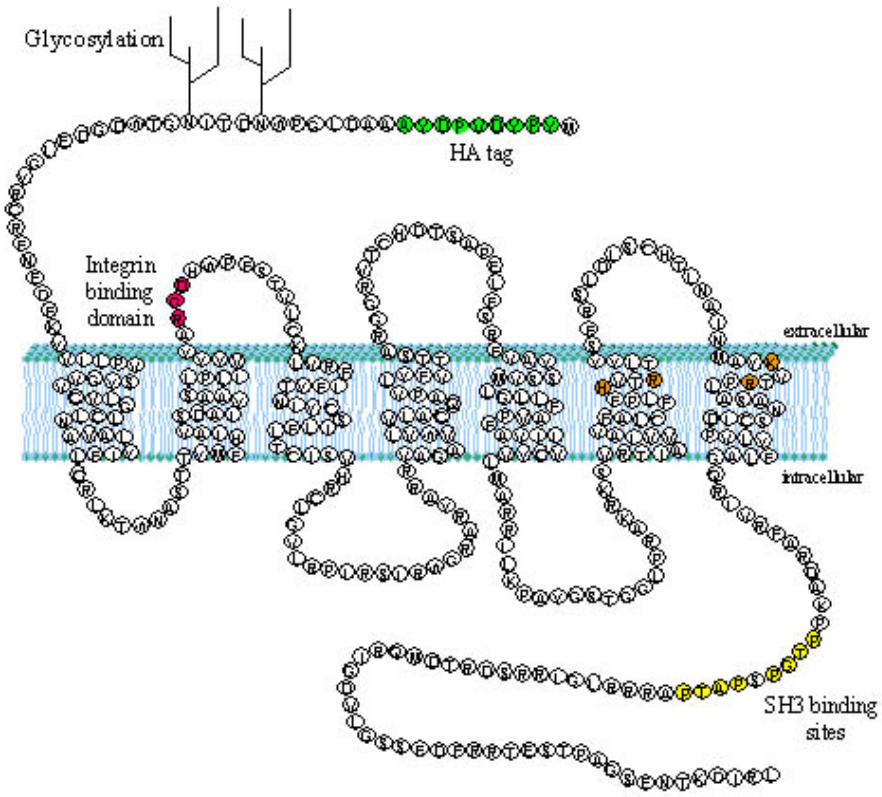
Glycosylation
HA tag
Integrin
binding
domain
extracellular
intracellular
SH3 binding
sites

***Experimental approach*:**

The research described in this dissertation includes the analysis of $P2Y_2$ receptor up-regulation in salivary gland cells of the NOD.B10 mouse model of the autoimmune disease Sjögren's syndrome (SS) (Chapter 2), and the investigation of novel signaling pathways and related responses that are coupled to activation by the up-regulated $P2Y_2$ receptors in salivary gland cells (Chapter 3). Chapter 4 of the dissertation contains concluding remarks and describes preliminary data indicating that the botanical anti-oxidant resveratrol can block stress-induced $P2Y_2$ receptor up-regulation in salivary gland.

CHAPTER 2

$P2Y_2$ nucleotide receptor up-regulation in submandibular gland cells from the NOD.B10 mouse model of Sjögren's syndrome

ABSTRACT

Sjögren's syndrome (SS) is an autoimmune disease that specifically targets exocrine glands, including salivary glands, and results in an impairment of secretory function. $P2Y_2$ nucleotide receptors for extracellular ATP and UTP are up-regulated in response to stress or injury in a variety of tissues including submandibular glands (SMGs) [38, 52, 53, 55-58]. **Objective**: To assess whether $P2Y_2$ receptor expression is up-regulated in SMGs of the NOD.B10 mouse model of primary SS as compared to SMGs of normal C57BL/6 mice. **Design:** SMG cells were isolated from normal C57BL/6 and diseased NOD.B10 mice. $P2Y_2$ receptor mRNA expression was determined by reverse transcription-polymerase chain reaction (RT-PCR) and *in situ* hybridization, whereas functional $P2Y_2$ receptor activity was analyzed by measuring UTP-induced increases in $[Ca^{2+}]_i$. **Results:** In contrast to SMG cells from C57BL/6 mice, SMG cells from 4-19 week-old NOD.B10 mice exhibited increased $P2Y_2$ receptor mRNA localized to both ductal and acinar cell types. The levels of mRNA for other uridine nucleotide receptors, i.e., $P2Y_4$ and $P2Y_6$ receptors, showed no significant differences between SMG cells of C57BL/6 and NOD.B10 mice, suggesting that only the $P2Y_2$ receptor was up-regulated in NOD.B10 mice. Moreover, $P2Y_2$ receptor activity in SMG cells from NOD.B10 mice increased with age (i.e., disease progression). **Conclusion:** $P2Y_2$ receptor up-regulation in SMGs is associated with the SS phenotype in NOD.B10 mice, which encourages further attempts to determine the role of this pathway in the development of SS.

INTRODUCTION

Extracellular nucleotides mediate a variety of biological effects by acting on cell surface P2 nucleotide receptors. P2 receptors, when activated by ligands including ATP, ADP, UTP, and UDP, can stimulate smooth muscle contraction, neurotransmission, exocrine and endocrine secretion, immune responses, inflammation, platelet aggregation, and cardiac function [25]. Biological sources of extracellular nucleotides include release from contracting skeletal muscle and activated sensory nerves, aggregating platelets and a variety of cell types in response to mechanical stress or injury [25, 72, 73]. P2 receptors have been classified into two families: P2X ligand-gated ion channels and P2Y G-protein-coupled receptors. In mammalian salivary glands, four subtypes of P2 receptors have been identified: $P2X_4$, $P2X_7$, $P2Y_1$, and $P2Y_2$ [38].

$P2X_4$ and $P2X_7$ receptors are non-selective cation channels activated by ATP with high and low affinities, respectively. Activation of these receptors leads to an elevation in the intracellular Ca^{2+} concentration, $[Ca^{2+}]_i$, due to calcium influx, a response that is inhibited by extracellular Mg^{2+} [74, 75].

$P2Y_1$ and $P2Y_2$ receptors are coupled primarily to the G_q family of G proteins that activate phospholipase C-dependent increases in $[Ca^{2+}]_i$ [32, 76]. $P2Y_1$ receptors have a distinctive rank order of agonist potencies: 2-MeSATP>2-MeSADP>ADP>ATP, as do $P2Y_2$ receptors: UTP=ATP>UDP. $P2Y_1$ receptors are expressed in rat SMGs and have been suggested to play a role in salivary gland development [77]. We have found that $P2Y_1$ receptors were most active in SMG cells isolated from immature animals, but as the gland developed the Ca^{2+}

response to $P2Y_1$ receptor agonists diminished [77]. In 4 week-old rats, SMGs exhibited only a moderate response to $P2Y_1$ receptor activation, as compared to the strong response in SMGs from newborn rats. $P2Y_2$ nucleotide receptor expression was barely detectable in normal salivary glands, but was up-regulated upon disruption of tissue homeostasis by various methods [52, 54, 78]. Previously, we have shown that enzymatic dispersal and culture of cells from rat submandibular, parotid, or sublingual glands, up-regulated $P2Y_2$ receptor mRNA expression and activity as a function of time in culture [54]. $P2Y_2$ receptor up-regulation also occurred in rat salivary glands *in vivo* 3 days after SMG ductal ligation [52]. Upon removal of the ligature, $P2Y_2$ receptors were down-regulated to basal levels. $P2Y_2$ receptors also are up-regulated in rat vascular neointima after balloon angioplasty [58], in collared rabbit carotid arteries [53], in myocardium from the left ventricle of rats with congestive heart failure [55], in a rat model of renal ischemic reperfusion [56], and in activated mouse thymocytes [57], suggesting that $P2Y_2$ receptor up-regulation occurs in response to tissue damage and disease.

Sjögren's syndrome (SS) is an autoimmune disease in which the salivary and lacrimal glands are targeted by the immune system for destruction, leading to an impairment of saliva and tear secretion, respectively [7]. SS is characterized by xerostomia (dry mouth) and xerophthalmia (dry eyes) and affects more than a million people in the United States, predominantly (90%) females. The NOD.B10 mouse, which develops an autoimmune exocrinopathy (AEC) similar to SS around 8 weeks of age, is an accepted experimental model

for primary SS [11, 19-21, 79]. NOD.B10 mice, as compared to normal C57BL/6 mice, exhibit a parallel decrease in fluid secretion and an increase in lymphocytic infiltration in exocrine glands [11, 19-21, 79]. We postulated that $P2Y_2$ receptor up-regulation may play a role in development of the SS phenotype, and therefore we analyzed $P2Y_2$ receptor expression in NOD.B10 mice.

METHODS

Materials

Chromatographically purified collagenase was purchased from Worthington Biochemical (Freehold, NJ). Fura 2-AM was purchased from Molecular Probes (Eugene, OR). Alkaline phosphatase-conjugated sheep anti-digoxigenin antibody, NBT/BCIP Substrate, Dig Wash and Block Buffer Set were obtained from Roche Applied Science (Mannheim, Germany). The cDNA synthesis kit was obtained from BD Biosciences (Palo Alto, CA). Oligonucleotide primers were purchased from Integrated DNA Technologies, Inc. (Coralville, IA). RNase-free DNase and Lig'nScribe kit were purchased from Ambion (Austin, TX). RNeasy kit was purchased from Qiagen (Chatsworth, CA). Taq DNA polymerase was obtained from Gibco BRL/Invitrogen (Carlsbad, CA). All other reagents were purchased from Sigma Chemical Co. (St. Louis, MO) unless otherwise stated.

Animals

NOD.B10 and C57BL/6 mice were purchased from Jackson Laboratories, Bar Harbor, ME. Animals that were sex and age matched were used at 4 and 14 weeks post-partum for RT-PCR and intracellular free Ca^{2+} concentration measurements. Animals at 19 weeks post-partum were used for *in situ* hybridization experiments. Protocols conformed to Animal Care and Use guidelines of the University of Missouri-Columbia.

Preparation of dispersed cell aggregates from mouse SMG

Cell aggregates were prepared from glands isolated from mice, as described earlier for rats with a few minor variations [80]. Briefly, sex and age matched animals were anesthetized with Nembutal pentobarbital sodium injection (125 mg/kg body weight), bled, and salivary glands were excised. Glands were minced and placed in dispersion medium containing collagenase and hyaluronidase at 37˚C [80] for 35 min. Minced samples were dispersed by passage through a 10 ml pipette after 15, 25, and 35 min in dispersion buffer. The dispersed cell aggregates were washed with assay buffer [120 mM NaCl, 4 mM KCl, 1.2 mM $MgSO_4$, 1.2 mM KH_2PO_4, 1 mM $CaCl_2$, 10 mM glucose, and 15 mM N-2-hydroxyethylpiperazine-N'-2-ethane-sulfonic acid (HEPES), pH 7.4] containing 1% (w/v) bovine serum albumin (BSA) and filtered through a nylon mesh. The cell preparation was washed twice and resuspended in assay buffer containing 0.1% (w/v) BSA and used for measurements of $[Ca^{2+}]_i$. For RNA isolation, cells were pelleted and suspended in RNA lysis buffer (Buffer RLT from Qiagen RNeasy Mini kit with 140 μM β-mercaptoethanol).

Intracellular free Ca^{2+} concentration measurements

The $[Ca^{2+}]_i$ was quantified in single cells within acinar and ductal clusters with the Ca^{2+}-sensitive fluorescent dye fura 2, using an InCyt Dual-Wavelength Fluorescence Imaging System (Intracellular Imaging, Cincinnati, OH). Dispersed cell aggregates in assay buffer were incubated with 2.0 μM fura 2-acetoxymethyl ester (fura 2-AM) for 30 min at 37˚C, washed, transferred to coverslips treated

with Cell-Tak (Becton Dickinson Labware, Bedford, MA) according to the manufacturer's instructions, and incubated for 20 min at 37˚C. Coverslips with adherent cells, acinar and ductal, were positioned on the stage of a fluorescence microscope and stimulated with agonists at 37˚C, as described in the figure legends. Cells were exposed to 340/380 nm light and fluorescence emission at 505 nm was converted to $[Ca^{2+}]_i$ using a standard curve created with solutions containing known concentrations of Ca^{2+}. Increases in $[Ca^{2+}]_i$ were measured by subtracting basal $[Ca^{2+}]_i$ from the peak $[Ca^{2+}]_i$ measurement. The percentage of cells that responded to UTP was also determined. Viable cells were identified by responsiveness to carbachol and non-responding cells were eliminated.

RT-PCR

Total RNA was extracted from cells using a RNeasy kit, followed by treatment with ribonuclease-free deoxyribonuclease (DNase). The quantity and quality of the RNA was assessed by spectrophotometry and agarose gel electrophoresis after DNase treatment. cDNA synthesis was performed using a first-strand cDNA synthesis kit with 1 μg of total RNA and oligo dT primer. Ten percent of the cDNA was used as template in the PCR. For amplification of $P2Y_2$ receptor cDNA, the upstream primer, 5'-CTTCAACGAGGACTTCAAGTACGTGC-3', and the downstream primer, 5'-CATGTTGATGGCGTTGAGGGTGTGG-3', were used to amplify a 778-bp fragment. For amplification of $P2Y_4$ receptor cDNA, the upstream primer, 5'-CCACCTACATGTTCCACCTGGCA-3', and the downstream primer, 5'-

GAAGCAGACAGCAAAGACAGTCA-3', were used to amplify a 555-bp fragment. For amplification of $P2Y_6$ receptor cDNA, the upstream primer, 5'-TGCCACCCACCACCTGTGTCTACCG-3', and the downstream primer, 5'-AGTAGAAGAGGATGGGGTCCAGCAC-3', were used to amplify an 871-bp fragment. For amplification of G3PDH cDNA, the upstream primer, 5'-TGAAGGTCGGTGTCAACGGATTTGGC-3', and the downstream primer, 5'-CATGTAGGCCATGAGGTCCACCAC-3', were used to amplify a 983-bp fragment. The PCR reaction contained 2.5 units of Taq polymerase, 2 mM $MgCl_2$, and 20 pmol of each primer in a 50 μl reaction volume. The PCR conditions were as follows: 1 min at 94˚C, then 30 cycles (for $P2Y_2$, G3PDH) or 35 cycles (for $P2Y_4$, $P2Y_6$) of denaturation for 1 min at 94˚C, annealing for 1 min at 60˚C, and extension for 1 min at 72˚C, followed by a 7 min extension at 72˚C. The resulting products were resolved on a 2% (w/v) agarose ethidium bromide gel. cDNA derived from total RNA isolated from human 1321N1 astrocytoma cells transfected with either $P2Y_2$, $P2Y_4$, or $P2Y_6$ receptor cDNA [71, 81] was used as a positive control. The amplified bands were visualized with ultraviolet light, and the relative densities were quantified using the Gel Doc 2000 gel documentation system (Bio-Rad, Hercules, CA).

In situ hybridization

A 250 bp fragment of mouse $P2Y_2$ receptor cDNA was generated by PCR using a plasmid containing mouse $P2Y_2$ receptor cDNA as template. A T7 promoter was ligated to the PCR fragment (25 ng) using the Lig'nScribe kit,

according to the manufacturer's instructions, to yield both antisense and sense PCR templates that were used (1 μg) to generate $P2Y_2$ riboprobes using a Digoxigenin RNA labeling kit (Roche Applied Science).

Preparation of the mouse SMG tissue slides and the *in situ* hybridization techniques were performed according to a protocol described previously [52] with a few variations. Briefly, tissue sections on slides were fixed, washed, and prehybridized with hybridization solution [4X SSC, 0.5X Denhardt's, 1 mM EDTA, 10 mM phosphate buffer, pH 7.0, 0.1 mg/ml salmon sperm DNA, 0.1 mg/ml yeast tRNA, 100 mg/ml dextran sulfate, and 50% (v/v) deionized formamide] for at least 3 h at 50°C in a humidified chamber. Riboprobes (400 ng/ml antisense or sense) in hybridization buffer were heated for 5 min at 65°C, quenched on ice, and added to the tissue sections after removal of the buffer used in the prehybridization step. Tissue sections were covered with HybriSlip (RPI, Mount Prospect, IL) and hybridized overnight at 50°C in a humidified chamber. The following day, tissue sections were washed and incubated for 1 h at room temperature with alkaline phosphatase-conjugated anti-digoxigenin antibody diluted 1:5000 in blocking buffer (supplied in the DIG Wash and Block Buffer Set). Then, sections were washed and incubated with nitro blue tetrazolium chloride/5-bromo-4-chloro-3-indolyl phosphate toluidine salt (NBT/BCIP) in detection buffer (DIG Wash and Block Buffer Set) for 17 h in the dark at room temperature according to the manufacturer's instructions. The reaction was stopped, and the sections were counterstained with nuclear fast red (Zymed, San

Francisco, CA) and mounted with Histomount mounting solution (Zymed) following the manufacturer's instructions.

RESULTS

Age-dependent increases in $P2Y_2$ receptor mRNA expression in SMG from NOD.B10, but not C57BL/6 mice.

Results indicated that $P2Y_2$ receptor mRNA expression increased relative to G3PDH mRNA in freshly dispersed SMG cells from NOD.B10 mice between 4 and 14 weeks of age (Figure 6). In contrast, there was relatively little $P2Y_2$ receptor mRNA expression detected in SMG cells from C57BL/6 mice, and the level of expression relative to G3PDH mRNA did not change with age (Figure 6). When normalized to G3PDH mRNA, there was a relative two-fold increase in $P2Y_2$ receptor mRNA in SMG cells from 14 week-old NOD.B10 mice, as compared to C57BL/6 mice of the same age (Figure 6, bottom panel).

Tissue localization of $P2Y_2$ receptor mRNA was determined by *in situ* hybridization with a $P2Y_2$-specific antisense riboprobe and SMG slices from NOD.B10 mice. Results showed that $P2Y_2$ receptor mRNA was localized to both ductal and acinar cell types (Figure 7A). Furthermore, SMG slices isolated from C57BL/6 mice again showed relatively little $P2Y_2$ receptor mRNA expression (Figure 7B), as compared to SMG from NOD.B10 mice.

The relative mRNA levels of the other uridine nucleotide receptors, $P2Y_4$ and $P2Y_6$, were measured in freshly dispersed SMG cells from 14 week-old NOD.B10 and C57BL/6 mice. $P2Y_6$ receptor mRNA was expressed at similar levels in SMG cells from NOD.B10 and C57BL/6 mice, and $P2Y_4$ receptor mRNA was not detectable (Figure 8).

Figure 6. Detection of $P2Y_2$ receptor mRNA in SMG cells from NOD.B10 and C57BL/6 mice. mRNA was isolated from SMG cells of 4 or 14 week-old NOD.B10 (B10) and C57BL/6 (B6) mice and cDNA was synthesized and amplified by RT-PCR using primers specific for $P2Y_2$ or G3PDH cDNA (see Methods). PCR products were gel electrophoresed and the amplified $P2Y_2$ receptor cDNA was expressed relative to G3PDH cDNA after densitometric scanning (bottom panel). mRNA isolated from human 1321N1 cells expressing the recombinant $P2Y_2$ nucleotide receptor served as a positive control; PCR of RNA samples incubated in the absence of reverse transcriptase (-RT) served as a negative control. Data shown in the top panel are representative of 4 experiments. The bottom panel represents the relative densities of $P2Y_2$ specific PCR products amplified from 14 wk B10 RNA, normalized to the relative densities of PCR products amplified from 14 wk B6 RNA. The data are expressed as the means +/- SE of results from 4 experiments.

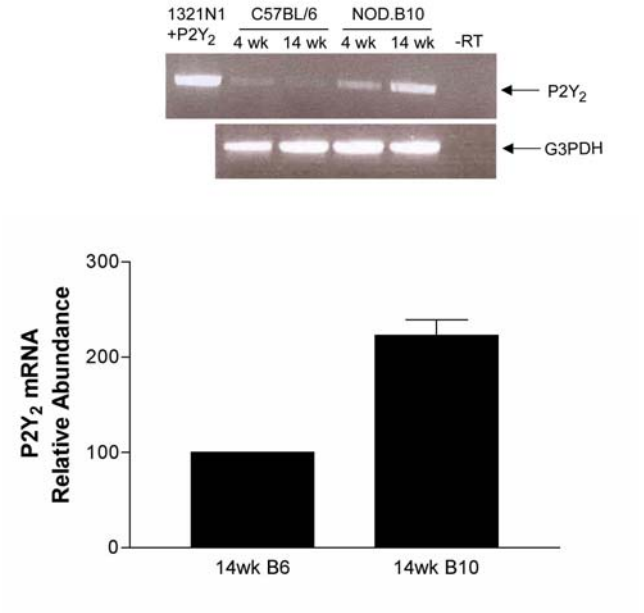
1321N1
+P2Y2
C57BL/6
4 wk
14 wk
NOD.B10
4 wk
14 wk
-RT
P2Y2
G3PDH
P2Y2 mRNA
Relative Abundance
300
200
100
0
14wk B6
14wk B10

Figure 7. Detection of $P2Y_2$ receptor mRNA in SMG slices from NOD.B10 or C57BL/6 mice by *in situ* hybridization**.** Tissue slices and *in situ* hybridization were performed as described in Methods using SMG isolated from 19 week-old **(A)** NOD.B10 or **(B)** C57BL/6 mice. Hybridization of SMG $P2Y_2$ receptor mRNA with a $P2Y_2$-specific antisense riboprobe was indicated by dark blue/purple staining **(A, B)**, whereas hybridization with a $P2Y_2$ sense riboprobe served as a control for non-specific binding to NOD.B10 SMG **(C)**. SMG slices from NOD.B10 mice treated without riboprobe indicated background staining **(D)**. Data are representative of 3 experiments. Arrows indicate ductal cells. Original magnification X 400.

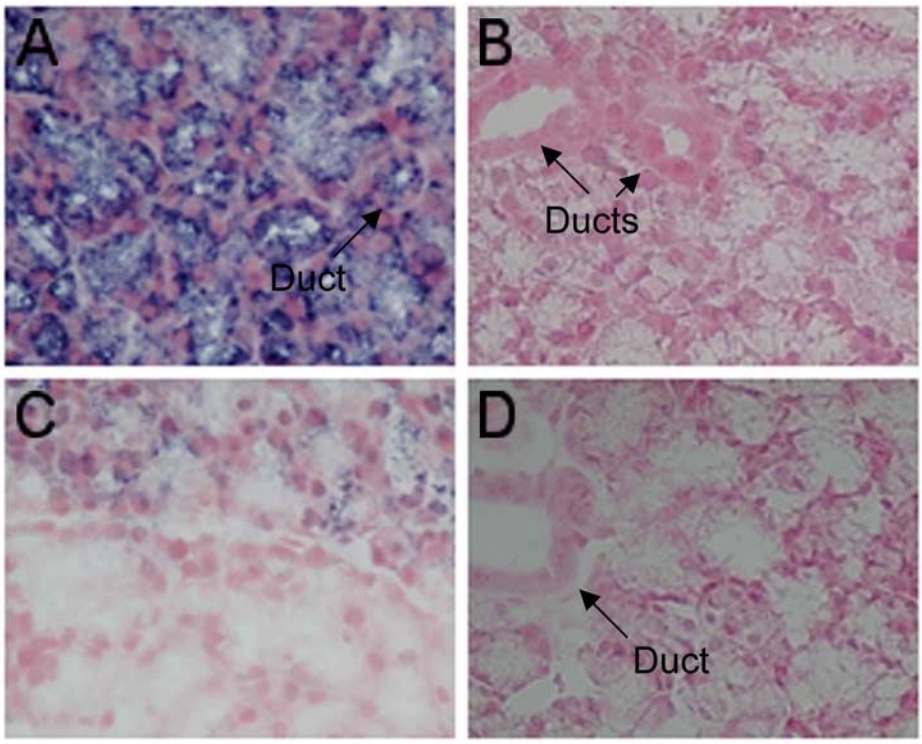
A
Duct
B
Ducts
C
D
Duct

Figure 8. Detection of $P2Y_4$ and $P2Y_6$ receptor mRNA in mouse SMG cells from NOD.B10 and C57BL/6 mice. mRNA was isolated from SMG cells of 14 week-old NOD.B10 (B10) and C57BL/6 (B6) mice and cDNA was synthesized and amplified by RT-PCR using primers specific for $P2Y_4$, $P2Y_6$, or G3PDH cDNA (see Methods). mRNA isolated from human 1321N1 cells expressing recombinant $P2Y_4$ or $P2Y_6$ receptors served as positive controls; PCR of RNA samples incubated in the absence of reverse transcriptase (-RT) served as a negative control. Data shown are representative of 3 experiments.

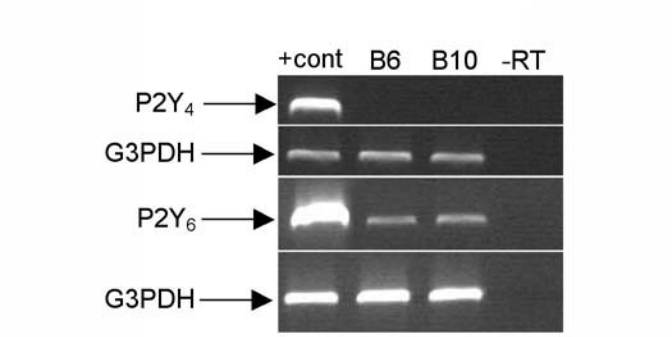
+cont
B6
B10
-RT
P2Y4
G3PDH
P2Y6
G3PDH

Age-dependent increases in $P2Y_2$ receptor activity in SMG cells from NOD.B10 but not C57BL/6 mice.

Both acinar and ductal SMG cells freshly isolated from NOD.B10 mice exhibited increases in $[Ca^{2+}]_i$ in the presence of the $P2Y_2$ receptor-selective agonist uridine 5'-triphospate (UTP) in contrast to SMG cells from C57BL/6 mice which did not respond to UTP (Figure 9A). UTP-induced increases in $[Ca^{2+}]_i$ were similar in acinar and ductal cells (data not shown), and therefore the data obtained from these two cell types were combined. UTP-induced increases in $[Ca^{2+}]_i$ were greater in SMG cells isolated from 14 week-old as compared to 4 week-old NOD.B10 mice, with an increase in $[Ca^{2+}]_i$ of 73 ± 7 nM compared to 28 ± 8 nM, respectively (Figure 9A). Furthermore, the number of UTP-responsive SMG cells from NOD.B10 mice increased between 4 and 14 weeks from 16% to 60%, respectively (Figure 10). Responses to the muscarinic cholinergic receptor agonist carbachol at a concentration used previously (1) were similar in SMG cells from both mouse lines at 4 and 14 weeks of age (Figure 9B). Consistent with the expression of $P2Y_6$ receptor mRNA (Figure 8), SMG cells from both C57BL/6 and NOD.B10 mice were equally responsive to the $P2Y_6$ receptor agonist UDP (Figure 11). The enhanced expression of $P2Y_2$ receptor mRNA (Figure 6) and calcium responses to UTP (Figure 9) in NOD.B10 mice as compared to C57BL/6 mice, along with the absence of $P2Y_4$ receptor mRNA and the presence of relatively equivalent levels of $P2Y_6$ receptor mRNA in both C57BL/6 and NOD.B10 SMG cells (Figure 8), strongly suggest that $P2Y_2$

receptors mediate the time-dependent increases in $[Ca^{2+}]_i$ in response to UTP in NOD.B10 SMG cells.

Figure 9. $P2Y_2$ receptor activity in SMG cells from NOD.B10 and C57BL/6 mice. SMG from age and sex matched NOD.B10 (B10) or C57BL/6 (B6) mice were isolated and dispersed into single cells. Then, changes in $[Ca^{2+}]_i$ in response to **(A)** UTP (100 μM) or **(B)** carbachol (100 μM) were measured in SMG cells from 4 and 14 week-old animals (see Methods). Agonist-induced changes in the $[Ca^{2+}]_i$ in responding cells are shown. Increases in $[Ca^{2+}]_i$ were expressed by subtracting basal $[Ca^{2+}]_i$ (prior to UTP addition) from the peak $[Ca^{2+}]_i$ responses to UTP. Basal levels of $[Ca^{2+}]_i$ in all cells were approximately 100 nM. Values are means ± SE of results from 6-37 responding cells from 4 animals per group.

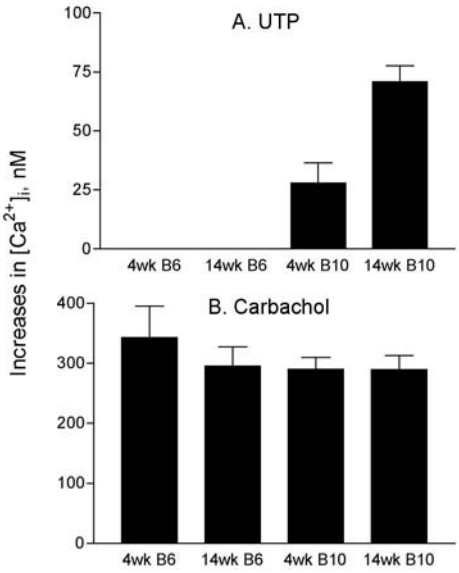
A. UTP
100
75
50
25
0
4wk B6
14wk B6
4wk B10
14wk B10
B. Carbachol
400
300
200
100
0
4wk B6
14wk B6
4wk B10
14wk B10
Increases in [Ca2+]i, nM

Figure 10. Percentage of UTP-responsive SMG cells from NOD.B10 or C57BL/6 mice. SMG cells were isolated (see Methods) and $P2Y_2$ receptor activity was measured as described in Figure 9. The percentage of SMG cells isolated from NOD.B10 (B10) or C57BL/6 (B6) mice of the indicated age that responded with changes in $[Ca^{2+}]_i$ was determined after stimulation with 100 μM UTP (see Methods).

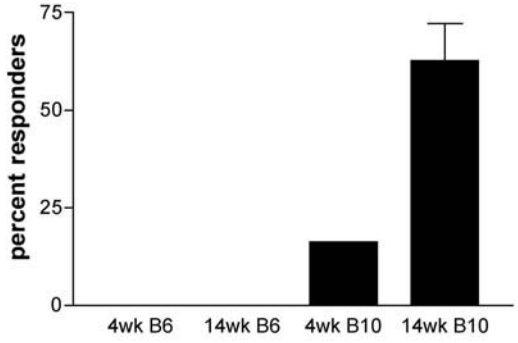
percent responders
75
50
25
0
4wk B6
14wk B6
4wk B10
14wk B10

Figure 11. $P2Y_6$ receptor activity in SMG cells from NOD.B10 and C57BL/6 mice. SMG from 14 week-old sex matched NOD.B10 (B10) or C57BL/6 (B6) mice were isolated and dispersed into single cells. Then, changes in $[Ca^{2+}]_i$ in response to UDP (10 μM and 100 μM) were measured in SMG cells. Agonist-induced changes in the $[Ca^{2+}]_i$ in responding cells are shown. Increases in $[Ca^{2+}]_i$ were expressed by subtracting basal $[Ca^{2+}]_i$ (prior to UDP addition) from the peak $[Ca^{2+}]_i$ in response to UDP. Basal $[Ca^{2+}]_i$ in all cells was approximately 100 nM.

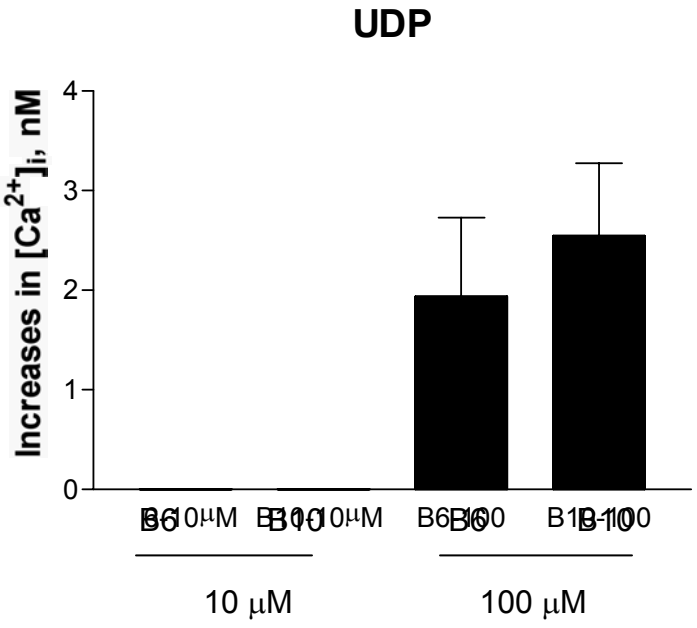
UDP
Increases in [Ca2+]i, nM
4
3
2
1
0
B6
B6
B6
B6
10 μM
100 μM

DISCUSSION

The results obtained in this study suggest that $P2Y_2$ nucleotide receptor expression is up-regulated in submandibular gland (SMG) of the NOD.B10 mouse model of the autoimmune disease Sjögren's syndrome (SS), consistent with our previous findings that the $P2Y_2$ receptor is up-regulated in salivary gland by cell dispersal and culture or by ligation of the main excretory duct [52, 54]. The $P2Y_2$ receptor also is up-regulated in activated thymocytes [57], in arteries after angioplasty [58], ischemic reperfusion injury [56], or collar-induced intimal hyperplasia [53] and in congestive heart failure [55]. In contrast to NOD.B10 SMG cells, functional $P2Y_2$ receptors are not expressed in SMG cells from normal C57BL/6 mice that do not display autoimmune exocrinopathy (AEC).

The NOD.B10 mouse is derived from the parental NOD mouse strain (that exhibits diabetes and AEC) and a major histocompatability complex (MHC) from the C57BL/10 mouse strain (that does not display diabetes or AEC), resulting in the NOD.B10 mouse that retains AEC without the complication of diabetes and thus serves as an excellent model for primary SS [18]. Similarities between human SS and murine AEC include the presence of auto-antibodies to M3 muscarinic receptors and the presence of lymphocytic infiltrates in exocrine tissue [18, 82]. A major symptom of AEC is impaired saliva secretion that begins at 8 weeks of age in the NOD.B10 mouse and is accompanied by infiltration of lymphocytes in salivary glands [18]. Other symptoms include the aberrant expression and processing of the major saliva protein, PSP, and increased expression of apoptotic cysteine proteases at 8 to 20 weeks of age [18]. Our

results indicate that $P2Y_2$ receptor expression occurs at the early stages of AEC in NOD.B10 mice, since there seems to be a relative increase in $P2Y_2$ receptor mRNA and activity between 4 to 14 weeks of age. It is interesting that the age-dependent progression of AEC did not correlate with a change in muscarinic receptor-induced intracellular calcium mobilization (using 100 μM carbachol) (Figure 9) since pilocarpine-stimulated saliva secretion is known to be impaired in AEC [82, 83]. However, the impaired saliva secretion in NOD.B10 mice is thought to be a result of the generation of M3 receptor antibodies, and the carbachol-induced increase in $[Ca^{2+}]_i$ in NOD.B10 SMG cells (Figure 9) may be due to expression of a subset of the muscarinic receptor subtypes identified in salivary gland, including the M1, M3, and/or M5 receptors [83, 84]. Alternatively, it is possible that AEC causes impairment of muscarinic receptor signaling downstream of $[Ca^{2+}]_i$ mobilization in the NOD.B10 mice, or that the reported decrease in muscarinic receptor signaling in AEC is a late event.

A possible consequence of $P2Y_2$ receptor up-regulation in salivary glands of the NOD.B10 mouse may be to provide a pathway for fluid secretion. A $P2Y_2$ receptor knockout mouse has been developed that displays reduced Ca^{2+} signaling and chloride secretion in airway epithelial cells [63, 64]. This is consistent with the previously established role for the $P2Y_2$ receptor in mediating calcium-dependent anion transport and fluid secretion in a variety of epithelial tissues, including colon, gallbladder, bile ducts, and pancreas [37] and in airway epithelium where it is accompanied by mucin glycoprotein release from epithelial goblet cells [44, 66]. In the ocular mucosa, $P2Y_2$ receptor activation increases

salt, water, and mucus secretion [65], and in rabbit conjunctival epithelium, $P2Y_2$ receptors also stimulate Cl^- and fluid transport [85].

The up-regulation of the $P2Y_2$ receptor also may contribute to the progression of AEC in NOD.B10 mice, but this remains to be determined. $P2Y_2$ receptors are known to regulate a wide variety of intracellular signaling pathways including alterations in the cytoplasmic free calcium concentration, modulation of growth factor and integrin-associated pathways, and the expression of cell-surface antigens and chemotactic proteins that bind leukocytes [40, 53, 54, 86]. Therefore, up-regulation of $P2Y_2$ receptors and its signaling pathways may well contribute to autoimmune exocrinopathy in SS, especially since $P2Y_2$ receptor agonists would likely be released from the cytoplasm of apoptotic SMG cells. In addition, $P2Y_2$ receptor up-regulation may promote SMG cell apoptosis, since previous studies indicate that $P2Y_2$ receptors mediate growth inhibition and apoptosis in human colorectal carcinoma cells [87] and human esophageal cancer cells [88].

Alternatively, $P2Y_2$ receptor up-regulation may play a role in tissue repair by stimulating mitogenesis [38]. In support of this latter hypothesis, the $P2Y_2$ receptor has been shown to activate the mitogen-activated protein kinases, ERK1/2, in salivary gland tissue [59], PC12 pheochromocytoma cells [60], C_6 glioma cells [61], EAhy 926 endothelial cells [89], human monocytic U937 cells [90], and human 1321N1 astrocytoma cells expressing heterologous $P2Y_2$ receptors [40]. Future studies should delineate the functional consequences of $P2Y_2$ receptor up-regulation in the NOD.B10 mouse and determine whether

these pathways are related to the pathophysiology of Sjögrens syndrome in humans.

CHAPTER 3

MATRIX METALLOPROTEASE- AND EGFR-DEPENDENT ERK1/2 ACTIVATION BY $P2Y_2$ NUCLEOTIDE RECEPTORS IN A HUMAN SUBMANDIBULAR GLAND CELL LINE

ABSTRACT

$P2Y_2$ nucleotide receptors ($P2Y_2Rs$) have been shown to be up-regulated in rat salivary gland in response to stress induced by ligation of the main excretory duct of the submandibular gland [52], or dispersion and culture of submandibular gland cells [54]. In addition, $P2Y_2$ receptors are up-regulated in submandibular glands from the NOD.B10 Sjögren's syndrome mouse model [91]. Recently, $P2Y_2Rs$ have been shown to transactivate growth factor receptors and their signaling pathways via RAFTK (PYK2) and src-dependent binding to SH3 binding sites in the C-terminal domain of $P2Y_2Rs$ [60, 62]. Additionally, transactivation of the epidermal growth factor receptor (EGFR) by other G protein-coupled receptors has been shown to be dependent on proteolytic cleavage of membrane ligands such as heparin binding epidermal growth factor (HBEGF) [92, 93]. However, the mechanisms whereby $P2Y_2Rs$ transactivate the EGFR in salivary gland remain unclear, and downstream signaling pathways have not been elucidated. Utilizing the human submandibular gland (HSG) cell line, we found that activation of the $P2Y_2R$ by its agonist UTP caused phosphorylation of the EGFR, the extracellular-signal regulated kinases ERK1/2, p90RSK, and the transcription factor ELK in a time-dependent manner. The EGFR inhibitor AG1478 blocked UTP-stimulated phosphorylation of the EGFR and ERK1/2. Moreover, TAPI-2, a matrix metalloprotease (ADAM17) inhibitor, and ADAM10 and ADAM17 siRNA also inhibited UTP-stimulated EGFR and ERK1/2 phosphorylation. The src inhibitor PP2 inhibited UTP-stimulated ERK1/2, but not EGFR, phosphorylation. UTP-stimulated ERK1/2

phosphorylation at 1 min was sensitive to PP2, and ERK1/2 phosphorylation at 10 min was insensitive to PP2, but sensitive to AG1478 and TAPI-2. Thus, $P2Y_2$Rs in HSG cells activate ERK1/2 by at least two separate pathways, a rapid src-dependent response and a slower src-independent response that is dependent upon metalloprotease activity and EGFR transactivation.

INTRODUCTION

The $P2Y_2$ nucleotide receptor ($P2Y_2R$) is a G_q protein-coupled receptor that is activated equipotently by extracellular ATP and UTP, leading to the activation of phospholipase C (PLC), and inositol 1,4,5-trisphosphate (IP_3)-dependent increases in $[Ca^{2+}]_i$ and the diacylglycerol (DAG)-dependent activation of PKC [32, 76]. The $P2Y_2$ nucleotide receptor is up-regulated in a variety of tissues in response to injury or stress. For example, the $P2Y_2R$ is up-regulated in response to salivary gland dispersion and culture [54], and ligation of the main rat submandibular gland excretory duct [52], and the $P2Y_2R$ is expressed in human submandibular gland (HSG) cells derived from a salivary gland tumor [94]. $P2Y_2Rs$ also are up-regulated in submandibular glands of a NOD.B10 mouse model of autoimmune exocrinopathy displaying disease symptoms similar to human Sjögren's syndrome, an autoimmune disorder characterized by lymphocytic infiltration and dysfunction of the salivary and lacrimal glands [91]. The physiological consequences of $P2Y_2R$ expression in salivary gland are unknown. However, $P2Y_2R$ up-regulation also occurs in blood vessels after balloon angioplasty and in collared carotid arteries, where it induces intimal hyperplasia and inflammation by increasing smooth muscle cell proliferation and leukocyte infiltration [53, 58, 86]. Up-regulation of the $P2Y_2R$ in salivary gland may serve to mediate similar processes.

The $P2Y_2R$ contains two SH3 binding sites (PXXP motifs) in its intracellular C-terminal domain that mediate the binding of src and the src-mediated transactivation of growth factor receptors [62, 67]. In human coronary

artery endothelial cells (HCAEC), the $P2Y_2R$ also mediates the src-dependent transactivation of vascular endothelial growth factor receptor type 2 (VEGFR-2) [67], and the subsequent up-regulation of vascular cell adhesion molecule (VCAM-1), a protein that mediates the binding of monocytes to the endothelium [67, 86]. In addition to the SH3 binding domains, the $P2Y_2R$ also contains an Arg-Gly-Asp (RGD)-sequence in its first extracellular loop that has been shown to interact with $\alpha_v\beta_3/\beta_5$ integrins [40] that regulate ATP- and UTP-induced cell chemokinesis and chemotaxis [68, 69], responses associated with inflammation [70].

The mechanisms whereby GPCRs activate MAPK cascades vary according to the type of receptor and the tissue in which the receptor is expressed. GPCRs for lysophosphatidic acid (LPA), endothelin (ET-1), thrombin, bombesin, muscarinic (M1R), and alpha (α2) adrenergic receptors activate the EGFR through the release or shedding of the EGFR ligand, HB-EGF, leading to stimulation of MAPKs [92, 93, 95, 96]. Shedding of an EGF-like ligand requires metalloprotease (i.e., sheddase) activation [97], but the specific metalloproteases involved have not been identified.

Members of the adamalysin family of proteases (ADAMs), are membrane-anchored glycoproteins with diverse functions, including the shedding of membrane-bound proteins from cells (for a review see [98]). ADAM10 and ADAM17 have been implicated in GPCR-mediated tumor cell migration [99]. ADAM10 and ADAM17 have been shown to mediate the shedding of six EGFR ligands: EGF, HB-EGF, TGFα, amphiregulin, epiregulin, and betacellulin [100].

Recently, we found that the human $P2Y_2R$ expressed in a P2YR-null cell line (human 1321N1 astrocytoma cells) mediates the proprotein convertase furin-dependent activation of ADAM10 and ADAM17 leading to the proteolytic cleavage of the transmembrane amyloid precursor protein (APP) and the release of the fragment sAPPα [101].

Other mechanisms involved in GPCR-mediated ERK1/2 activation can occur independently of the release of a soluble ligand. For example, β2 adrenergic receptors activate ERK via a pertussis toxin sensitive G protein [102], and the adapter protein β-arrestin that recruits and activates c-src [103]. In other studies, G$\beta\gamma$ subunits [104] increases in $[Ca^{2+}]_i$ [105, 106], and activation of c-src [104, 107-110], and PYK2 [107, 110] have been linked to EGFR transactivation and MAPK activation. The $P2Y_2R$ expressed in 1321N1 cells can activate ERK1/2 via transactivation of growth factor receptors or $\alpha_v\beta_3/\beta_5$ integrins [40, 62]. The present study indicates that $P2Y_2Rs$ in salivary gland cells derived from a human submandibular gland (HSG) tumor, can activate ERK1/2 by two distinct mechanisms, a rapid src-dependent, EGFR-independent response and a slower src-independent response due to activation of ADAM10, ADAM17 and the EGFR.

METHODS

Materials

All chemicals and reagents were purchased from Sigma Chemical Co. (St. Louis, MO) unless otherwise stated. Dulbecco's-modified Eagle's medium (DMEM), fetal bovine serum (FBS), and Taq DNA polymerase were obtained from Gibco BRL/Invitrogen (Carlsbad, CA). AG1478 and PP2 were purchased from Calbiochem (San Diego, CA). Tumor necrosis factor-α protease inhibitor (TAPI-2) was purchased from Peptides International (Louisville, KY). Antibodies that recognize human HBEGF, TGFα, amphiregulin (AR), and EGF and recombinant human HBEGF, TGFα, and AR were purchased from R&D systems (Minneapolis, MN). The RNeasy kit was purchased from Qiagen (Chatsworth, CA). RNase-free DNase was purchased from Ambion (Austin, TX). The cDNA synthesis kit was obtained from BD Biosciences (Palo Alto, CA). Oligonucleotide primers were purchased from Integrated DNA Technologies, Inc. (Coralville, IA).

Cell Culture

Human submandibular gland (HSG) cells were cultured in DMEM supplemented with 5% (v/v) FBS, 100 units/ml penicillin and 100 μg/ml streptomycin, and maintained at 37°C in a humidified atmosphere of 5% CO_2 and 95% air.

Measurement of EGFR, ERK1/2, p90RSK, and ELK phosphorylation

Cells were seeded on 12-well culture dishes and grown until ~ 80-90% confluence. Then, cells were incubated overnight in DMEM without serum. When indicated, cells were pretreated for 30 min with or without inhibitors or antibodies before stimulation with ligands for the indicated times. Then, the medium was removed, 2X Laemmli Lysis Buffer (200 μl) was added, samples were sonicated, boiled for 4 min, and subjected to SDS-PAGE on 7.5% (w/v) polyacrylamide gels. Proteins resolved on the gel were transferred to nitrocellulose membranes and blocked for 1 h with 5% (w/v) non-fat dry milk in Tris-buffered saline containing 0.1% (v/v) Tween-20 (TBST). Blots were incubated overnight at 4°C in TBST containing 3% (w/v) BSA, 0.02% (w/v) sodium azide, and the following rabbit antibodies (Cell Signaling Technology, Beverly, MA unless otherwise stated) at 1:1000 dilutions: anti-phospho-EGFR (Tyr 1068, an autophosphorylation site), anti-phospho-ERK1/2 (Thr202/Tyr204), anti-phospho-p90RSK (Ser 380), anti-phospho-ELK (Ser 383), anti-phospho-c-Myc (Thr58/Ser62), and anti-ERK (Santa Cruz Biotechnology, Santa Cruz, CA). Membranes were washed 3 times with TBST and incubated with horseradish peroxidase-linked goat anti-rabbit IgG antibody (1:1000 dilution; Santa Cruz Biotechnology, Santa Cruz, CA) at room temperature for 1 h. The membranes were washed 3 times with TBST, incubated with enhanced chemiluminescence reagent and the protein bands detected on X-ray film were quantified using a computer-driven scanner and Quantity One software (Bio-Rad, Hercules, CA). The intensities of phosphorylated protein bands in cells treated with ligands or other agents were normalized to total ERK (detected with anti-ERK antibody) and

expressed as a percentage of normalized data from untreated controls. Unpaired Student's *t* test was used to determine statistical significance ($p < 0.05$).

RT-PCR

Total RNA was extracted from cells using a RNeasy kit, followed by treatment with ribonuclease-free deoxyribonuclease (DNase). The quantity and quality of the RNA was assessed by spectrophotometry and agarose gel electrophoresis after DNase treatment. cDNA synthesis was performed using a first-strand cDNA synthesis kit with 1 μg of total RNA and oligo dT primer. Ten percent of the cDNA was used as template in the PCR. For amplification of $P2Y_2$ receptor cDNA, the upstream primer, 5'-CTTCAACGAGGACTTCAAGTACGTGC-3', and the downstream primer, 5'-CATGTTGATGGCGTTGAGGGTGTGG-3', were used to amplify a 778-bp fragment. For amplification of $P2Y_4$ receptor cDNA, the upstream primer, 5'-CCACCTACATGTTCCACCTGGCA-3', and the downstream primer, 5'-GAAGCAGACAGCAAAGACAGTCA-3', were used to amplify a 555-bp fragment. For amplification of $P2Y_6$ receptor cDNA, the upstream primer, 5'-TGCCACCCACCACCTGTGTCTACCG-3', and the downstream primer, 5'-AGTAGAAGAGGATGGGGTCCAGCAC-3', were used to amplify an 871-bp fragment. For amplification of G3PDH cDNA, the upstream primer, 5'-TGAAGGTCGGTGTCAACGGATTTGGC-3', and the downstream primer, 5'-CATGTAGGCCATGAGGTCCACCAC-3', were used to amplify a 983-bp

fragment. The PCR reaction contained 2.5 units of Taq polymerase, 2 mM $MgCl_2$, and 20 pmol of each primer in a 50 μl reaction volume. The PCR conditions were as follows: 1 min at 94˚C, then 30 cycles (for $P2Y_2$, G3PDH) or 35 cycles (for $P2Y_4$, $P2Y_6$) of denaturation for 1 min at 94˚C, annealing for 1 min at 60˚C, and extension for 1 min at 72˚C, followed by a 7 min extension at 72˚C. The resulting products were resolved on a 2% (w/v) agarose ethidium bromide gel. cDNA derived from total RNA isolated from human 1321N1 astrocytoma cells transfected with either $P2Y_2$, $P2Y_4$, or $P2Y_6$ receptor cDNA [71, 81] was used as a positive control. The amplified bands were visualized with ultraviolet light, and the relative densities were quantified using the Gel Doc 2000 gel documentation system (Bio-Rad, Hercules, CA).

siRNA targeting of ADAM10 and ADAM17/TACE mRNA

Transfection of cells with siRNA duplexes (Integrated DNA Technologies, Coralville, IA) to inhibit endogenous ADAM10 or ADAM17/TACE expression was performed using Lipofectamine 2000 (Invitrogen, Carlsbad, CA), according to the manufacturer's instructions. Briefly, 0.7 μg each of 3 ADAM10 or ADAM17/TACE siRNA duplexes was incubated with cells in serum-free DMEM for 6 h, and the medium was replaced with DMEM supplemented with 5% (v/v) FBS, 100 units/ml penicillin and 100 μg/ml streptomycin. Sequences of the siRNA duplexes were: ADAM10: AUUCGUAGGUUGAAAUGUCdTdT, UUCCAUUUCCACAAAUAGGdTdT, and AGCCAUUACAUAUUCCUUCdTdT;

ADAM17/TACE: AGUUUGCUUGGCACACCUUdTdT, AGUAAGGCCCAGGAGUGUdTdT, and CAUAGAGCCACUUUGGAGAdTdT. Cells were assayed for UTP-stimulated ERK1/2 phosphorylation 48 h after siRNA transfection. Silencing of targeted protein expression was confirmed by Western analysis of cell lysates using goat anti-human ADAM10 antibody (1:1000 dilution; Sigma-Aldrich, St. Louis, MO) or goat anti-human ADAM17 antibody (1:1000 dilution; Santa Cruz Biotechnology, Santa Cruz, CA). Blots were stripped and reprobed with anti-total-ERK antibody to verify the equivalence of protein loading per lane.

RESULTS

$P2Y_2$Rs mediate the phosphorylation of EGFR, ERK1/2, p90RSK, and the transcription factor ELK in HSG cells.

In HSG cells, UTP induced the dose-dependent phosphorylation of the EGFR (Figure 12) that reached a maximal level within ~10 min and returned to a basal level within 30 min (Figure 13). In contrast to EGFR phosphorylation, ERK1/2 phosphorylation was induced at low UTP concentrations (e.g., 1 μM; Figure 12) and reached a maximal level within 2 min and returned to a basal level within 60 min (Figure 13). Downstream targets of ERK, such p90RSK and the transcription factor ELK, were phosphorylated at similar UTP concentrations and with similar time courses as ERK1/2 phosphorylation (Figures 12 and 13). Phosphorylation of the transcription factor c-myc was not affected by UTP stimulation (Figure 13).

RT-PCR for mRNA to P2Y receptor subtypes activated by uridine nucleotides indicated that HSG cells express mRNA for the $P2Y_2R$ and $P2Y_6R$, but not the $P2Y_4R$ (Figure 14A). In addition, the $P2Y_6R$ agonist UDP did not cause an increase in $[Ca^{2+}]_i$ (Figure 14B), suggesting that there are no functional $P2Y_6Rs$ in HSG cells. Thus, UTP-induced activation of EGFR and ERK1/2 in HSG cells is mediated by the $P2Y_2R$ subtype.

Figure 12: Concentration-dependence of UTP-induced phosphorylation of EGFR, ERK1/2, and downstream targets of ERK1/2, p90RSK and ELK in HSG cells. HSG cells were incubated with the indicated concentration of UTP for 5 min, cell lysates were prepared and phosphorylation of EGFR, ERK1/2, ELK, and p90RSK was determined by Western analysis using specific antibodies (see Methods). Total ERK1/2 was used as a control for protein loading. Data shown are representative of results from three experiments.

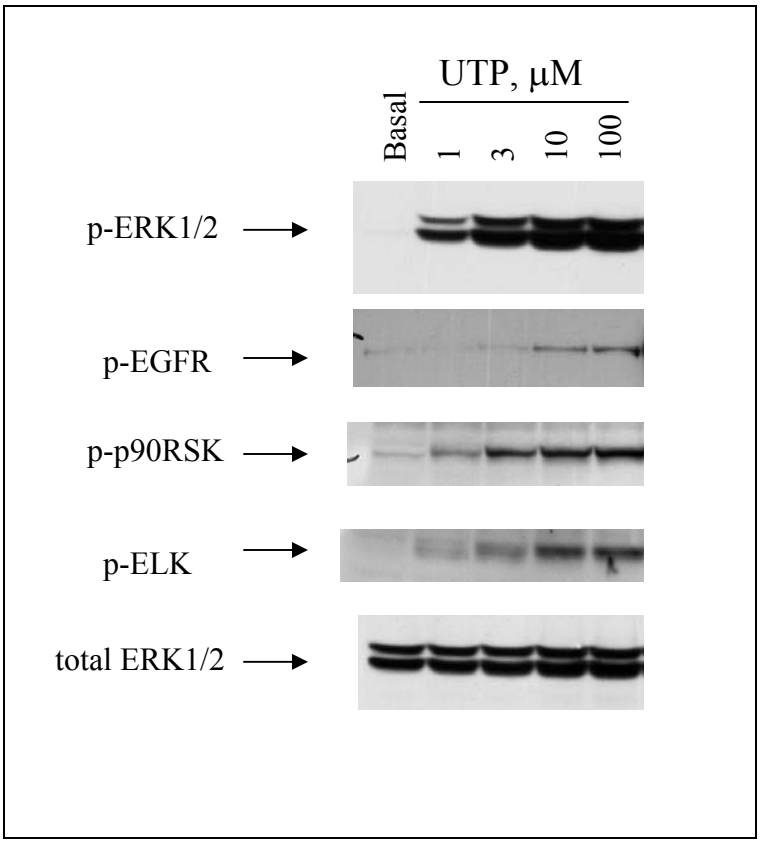
UTP, μM
Basal
1
3
10
100
p-ERK1/2
p-EGFR
p-p90RSK
p-ELK
total ERK1/2

Figure 13: Time-dependence of UTP-induced phosphorylation of EGFR, ERK1/2, and the downstream targets of ERK, p90RSK and ELK in HSG cells. HSG cells were incubated with 100 μM UTP for the indicated times, cell lysates were prepared and phosphorylation of EGFR, ERK1/2, p90RSK, and ELK was determined by Western analysis using specific antibodies (see Methods). Total ERK1/2 was used as a control for protein loading. Data shown are representative of results from three experiments.

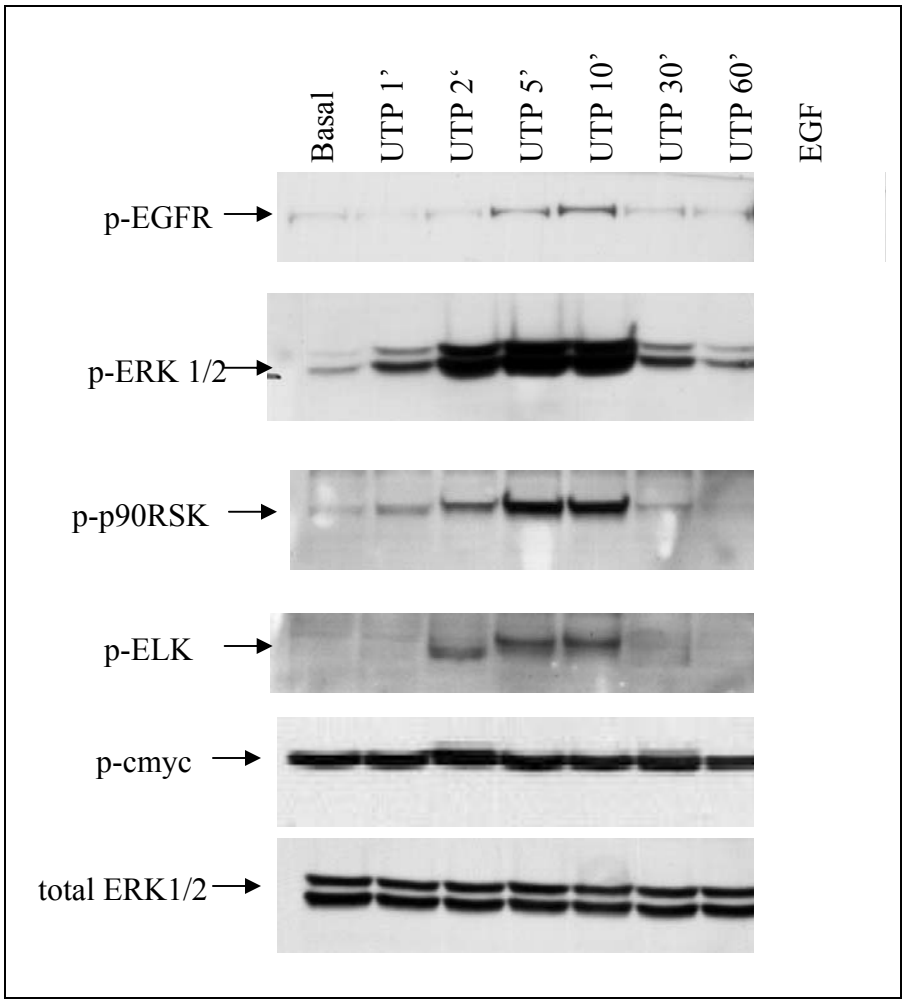
Basal
UTP 1'
UTP 2'
UTP 5'
UTP 10'
UTP 30'
UTP 60'
EGF
p-EGFR
p-ERK 1/2
p-p90RSK
p-ELK
p-cmyc
total ERK1/2

Figure 14. Detection of mRNA for the $P2Y_2R$ and $P2Y_6R$, but not $P2Y_4$ in HSG cells; detection or $P2Y_2R$ but not $P2Y_6R$ activity. (A) mRNA isolated from HSG cells was used to synthesize cDNA, followed by RT-PCR using primers specific for $P2Y_2R$, $P2Y_4R$, $P2Y_6R$, or G3PDH cDNA. Also, mRNA isolated from human 1321N1 cells expressing recombinant $P2Y_2$, $P2Y_4$, or $P2Y_6$ receptors served as positive controls; PCR of RNA samples incubated in the absence of reverse transcriptase (-RT) served as a negative control. (B) $P2Y_2$ and $P2Y_6$ receptor activity was measured in HSG cells by monitoring changes in $[Ca^{2+}]_i$ in response to UTP and ATP ($P2Y_2R$ agonists) or UDP ($P2Y_6R$ agonist). Increases in $[Ca^{2+}]_i$ indicate peak responses to nucleotides minus the basal $[Ca^{2+}]_i$ (prior to agonist addition), and represent the means +/- S.E.M. of results from three experiments.

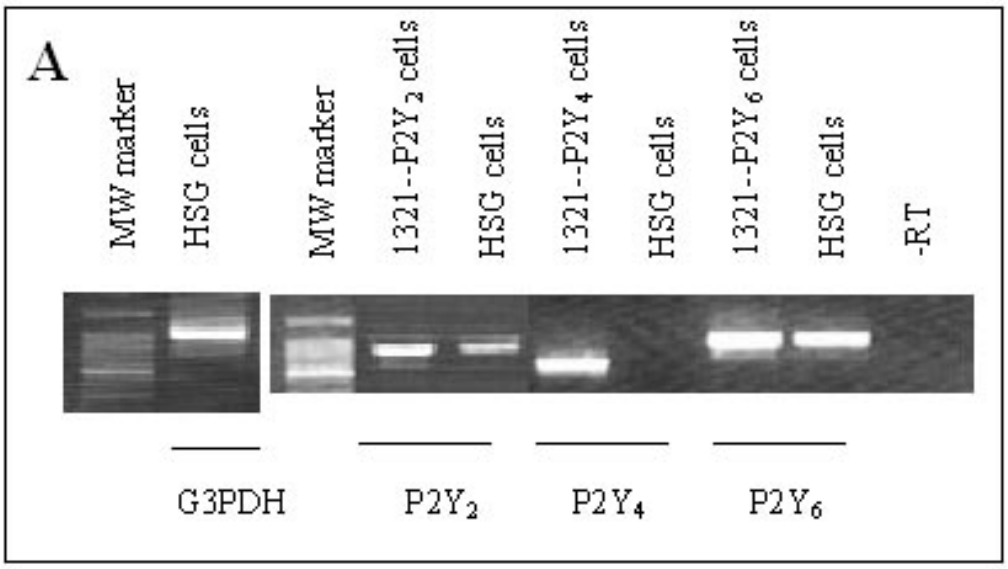
A
MW marker
HSG cells
MW marker
1321--P2Y2 cells
HSG cells
1321--P2Y4 cells
HSG cells
1321--P2Y6 cells
HSG cells
-RT
G3PDH
P2Y2
P2Y4
P2Y6

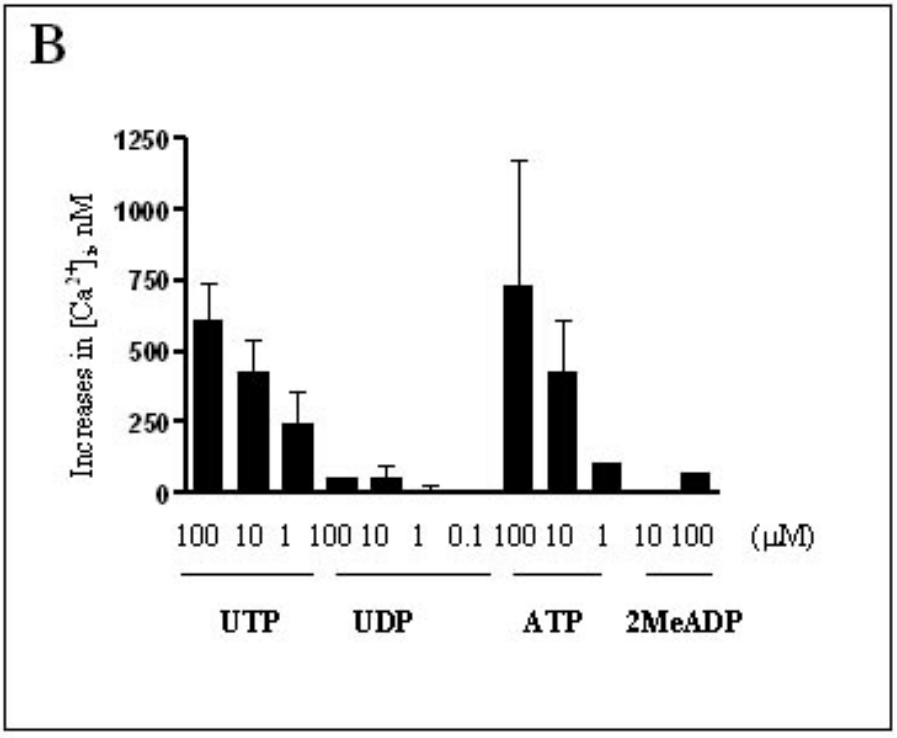
B
Increases in [Ca2+]i, nM
1250
1000
750
500
250
0
100 10 1 100 10 1 0.1 100 10 1 10 100 (μM)
UTP
UDP
ATP
2MeADP

$P2Y_2$Rs employ at least two distinct mechanisms to activate ERK1/2.

To determine whether $P2Y_2$R-mediated EGFR phosphorylation mediates ERK1/2 activation, we analyzed the effect of pretreatment of HSG cells with the EGFR autophosphorylation inhibitor, AG1478. As shown in Figure 15, AG1478 completely inhibited UTP-induced EGFR phosphorylation. In addition, AG1478 prevented ERK1/2 phosphorylation induced by a 10 min treatment with UTP, but had no effect on ERK1/2 phosphorylation induced by a 1 min UTP treatment. These data suggest that rapid $P2Y_2$R-mediated ERK1/2 activation was EGFR-independent, whereas a slower phase of ERK1/2 activation was dependent on EGFR phosphorylation. ERK1/2 phosphorylation induced by 1 or 10 min treatment of HSG cells with HBEGF and EGF can be inhibited by AG1478, providing further evidence that rapid UTP-induced ERK1/2 phosphorylation is independent of EGFR phosphorylation. Thus, UTP-induced ERK1/2 phosphorylation occurs by both a rapid EGFR-independent pathway and a slower EGFR-dependent pathway.

The $P2Y_2$R contains two SH3 binding domains in the C-terminal tail that mediate the src-dependent phosphorylation of EGFR in UTP-treated human 1321N1 astrocytoma cells expressing the recombinant $P2Y_2$R [62]. $P2Y_2$R-mediated activation of src also regulates the phosphorylation of the PDGF and VEGF receptors [62, 67]. In HSG cells preincubated with the src inhibitor PP2, ERK1/2 phosphorylation induced by a 1 min UTP treatment was significantly inhibited whereas UTP-induced ERK1/2 phosphorylation at 10 min was relatively unaffected by PP2 (Figure 16). This result suggests that src is required only for

the rapid phase of $P2Y_2R$-mediated ERK1/2 phosphorylation. Thus, $P2Y_2Rs$ mediate rapid phosphorylation of ERK1/2 by a src-dependent and EGFR-independent pathway, and a slower phase of ERK1/2 phosphorylation that is src-independent but dependent upon activation of the EGFR.

Figure 15: The EGFR autophosphorylation inhibitor AG1478 affects only the slow phase of UTP-induced ERK1/2 phosphorylation in HSG cells. HSG cells were pretreated with 3 μM AG1478 for 30 min and UTP (100 μM) was added for 1 or 10 min, whereas stimulation with the EGFR ligands EGF (100 ng/ml) or HBEGF (20 ng/ml) was used as positive controls. Cell lysates were prepared and phosphorylation of EGFR or ERK1/2 was determined by Western analysis using specific antibodies (see Methods). (**A**) Representative blots and (**B**) the means +/- S.E.M. of results from three experiments were normalized to total ERK where * indicates $p < 0.05$ (see Methods).

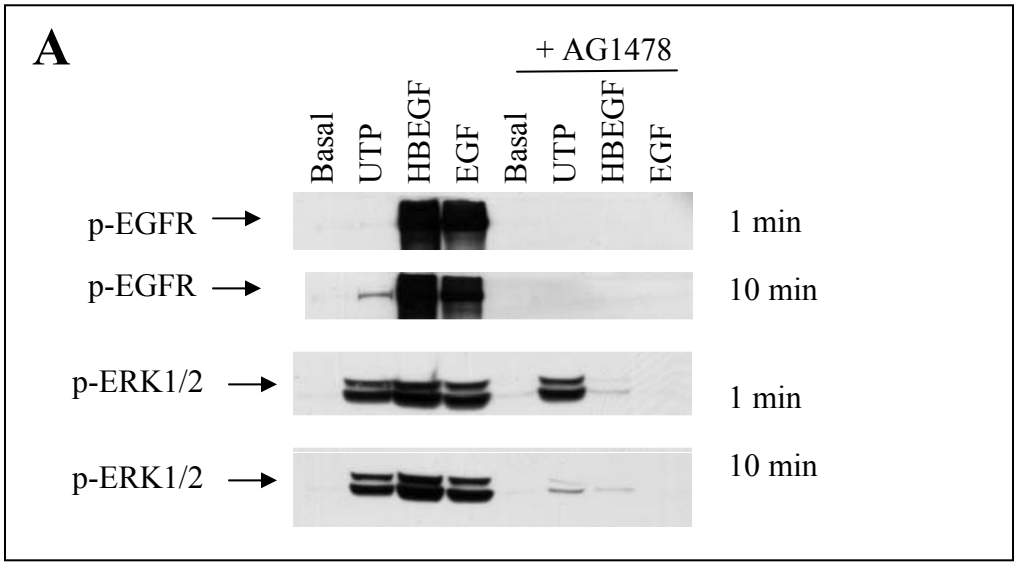
A
+ AG1478
Basal
UTP
HBEGF
EGF
Basal
UTP
HBEGF
EGF
p-EGFR
1 min
p-EGFR
10 min
p-ERK1/2
1 min
p-ERK1/2
10 min

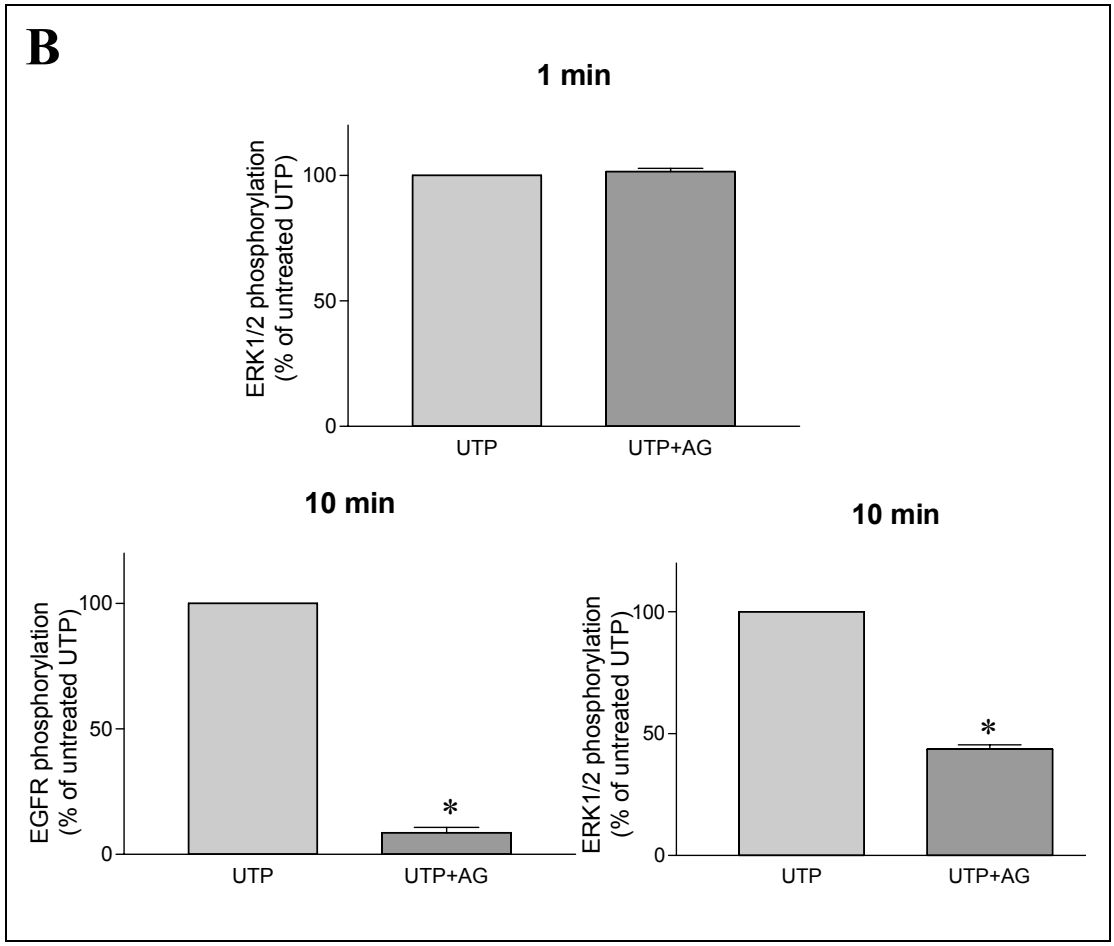
B
1 min
ERK1/2 phosphorylation (% of untreated UTP)
100
50
0
UTP
UTP+AG
10 min
EGFR phosphorylation (% of untreated UTP)
100
50
0
*
UTP
UTP+AG
10 min
ERK1/2 phosphorylation (% of untreated UTP)
100
50
0
*
UTP
UTP+AG

Figure 16: The src inhibitor PP2 affects only the rapid phase of UTP-induced ERK1/2 phosphorylation in HSG cells. HSG cells were pretreated with 10 μM PP2 for 30 min and UTP (100 μM) was added for 1 or 10 min, whereas stimulation with the EGFR ligands EGF (100 ng/ml) or HBEGF (20 ng/ml) was used as positive controls. Cell lysates were prepared and phosphorylation of EGFR or ERK1/2 was determined by Western analysis using specific antibodies (see Methods). (**A**) Representative blots and (**B**) the means +/- S.E.M. of results from three experiments were normalized to total ERK where * indicates $p < 0.05$ (see Methods).

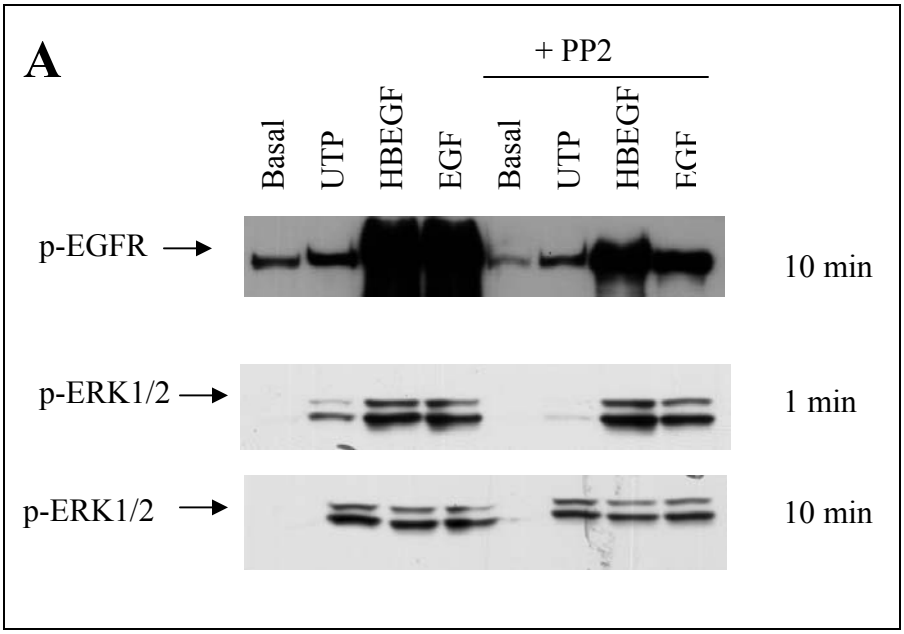
A
+ PP2
Basal
UTP
HBEGF
EGF
Basal
UTP
HBEGF
EGF
p-EGFR
10 min
p-ERK1/2
1 min
p-ERK1/2
10 min

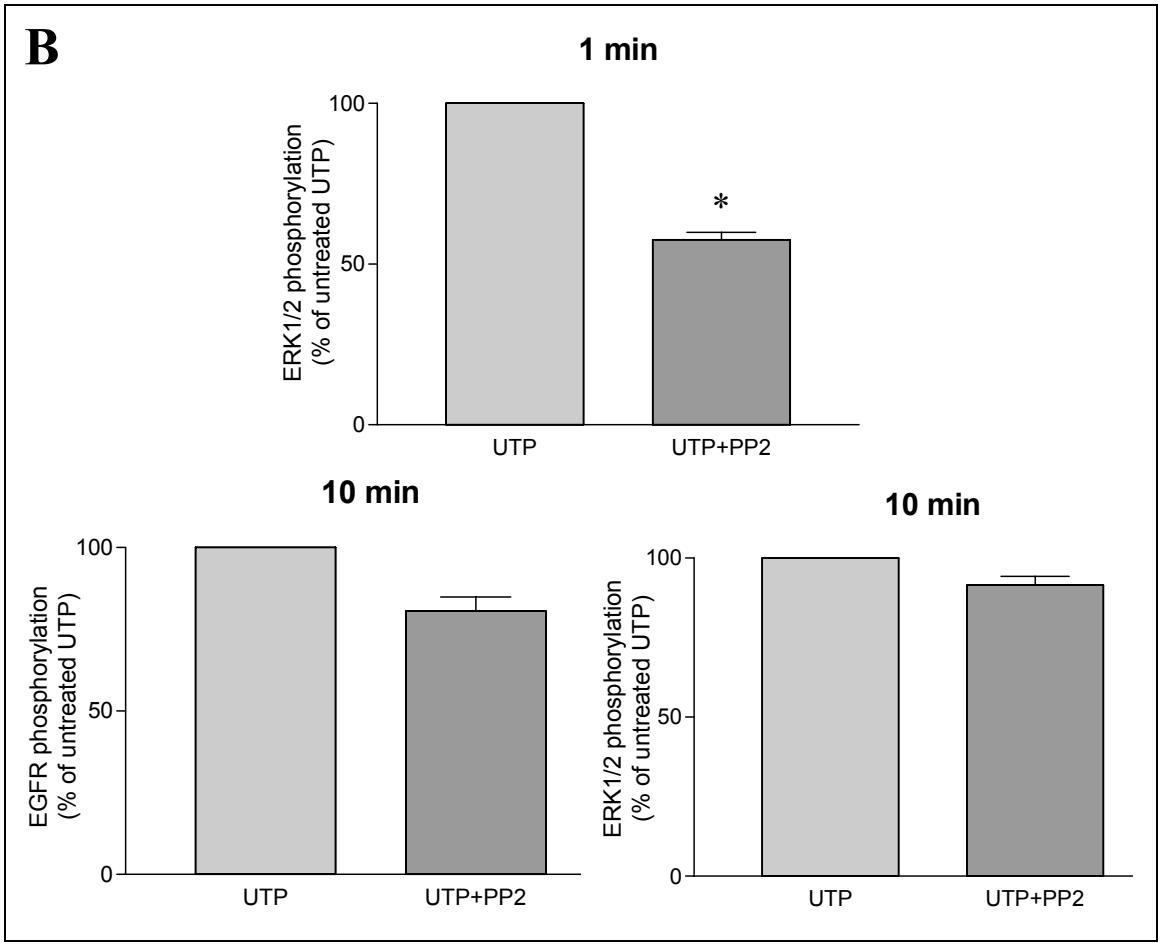
B
1 min
ERK1/2 phosphorylation (% of untreated UTP)
100
50
0
*
UTP
UTP+PP2
10 min
EGFR phosphorylation (% of untreated UTP)
100
50
0
UTP
UTP+PP2
10 min
ERK1/2 phosphorylation (% of untreated UTP)
100
50
0
UTP
UTP+PP2

$P2Y_2R$-mediated ERK1/2 phosphorylation due to EGFR transactivation requires metalloprotease activity.

Many GPCRs have been shown to transactivate the EGFR through activation of metalloproteases that generate EGFR ligands, including HBEGF [92, 93, 95]. There is evidence that specific subtypes of the ADAM family of metalloproteases are involved in the shedding of EGFR ligands [100]. Therefore, the involvement of metalloprotease activity in $P2Y_2R$-mediated EGFR and ERK1/2 phosphorylation was evaluated. TAPI-2, a selective competitive inhibitor of the metalloprotease ADAM17, partially inhibited EGFR and ERK1/2 phosphorylation induced by a 10 min treatment of HSG cells with UTP, whereas UTP-induced ERK1/2 phosphorylation at the 1 min time point was unaffected (Figure 17). Metalloproteases including ADAM10 and ADAM17 require proteolytic processing to become active [98, 111, 112] and the proprotein convertase furin has been linked to the proteolysis of adamalysins [113, 114]. Therefore, we examined the effect of the furin inhibitor, decanoyl-Arg-Val-Lys-Arg-chloromethylketone (CMK), on UTP-induced EGFR and ERK1/2 phosphorylation. Pretreatment of HSG cells with 50 μM CMK inhibited EGFR and ERK1/2 phosphorylation induced by a 10 min UTP treatment, confirming the role of a furin-like protease in $P2Y_2R$- and metalloprotease-mediated transactivation of the EGFR (Figure 18).

To determine the involvement of ADAM10 and ADAM17 in $P2Y_2R$-mediated EGFR transactivation leading to ERK1/2 phosphorylation, HSG cells were transfected with small interference RNA molecules targeting either

ADAM10 or ADAM17 mRNA. Transfection of HSG cells with ADAM10 or ADAM17 siRNA partially suppressed ERK1/2 phosphorylation induced by a 10 min UTP treatment, whereas co-transfection with both ADAM10 and ADAM17 siRNA almost completely prevented UTP-induced ERK1/2 phosphorylation (Figure 19A), demonstrating that ADAM10 and ADAM17 are involved in $P2Y_2R$-mediated EGFR transactivation and downstream ERK1/2 phosphorylation. The suppression by siRNA of ADAM10 and ADAM17 protein expression in HSG cells was confirmed by Western analysis with ADAM10- and ADAM17-specific antibodies (Figure 19B).

Figure 17: TAPI-2, a selective inhibitor of ADAM17, inhibits the EGFR-dependent phase of UTP-induced ERK1/2 phosphorylation in HSG cells. HSG cells pretreated for 30 min with 10 μM TAPI-2, a selective ADAM17/TACE inhibitor, were stimulated with UTP (100 μM) for 1 or 10 min, whereas stimulation with the EGFR ligands EGF (100 ng/ml) or HBEGF (20 ng/ml) was used as positive controls. Cell lysates were prepared and phosphorylation of EGFR or ERK1/2 was determined by Western analysis using specific antibodies (see Methods). (**A**) Representative blots and (**B**) the means +/- S.E.M. of results from three experiments were normalized to total ERK where * indicates $p < 0.05$ (see Methods).

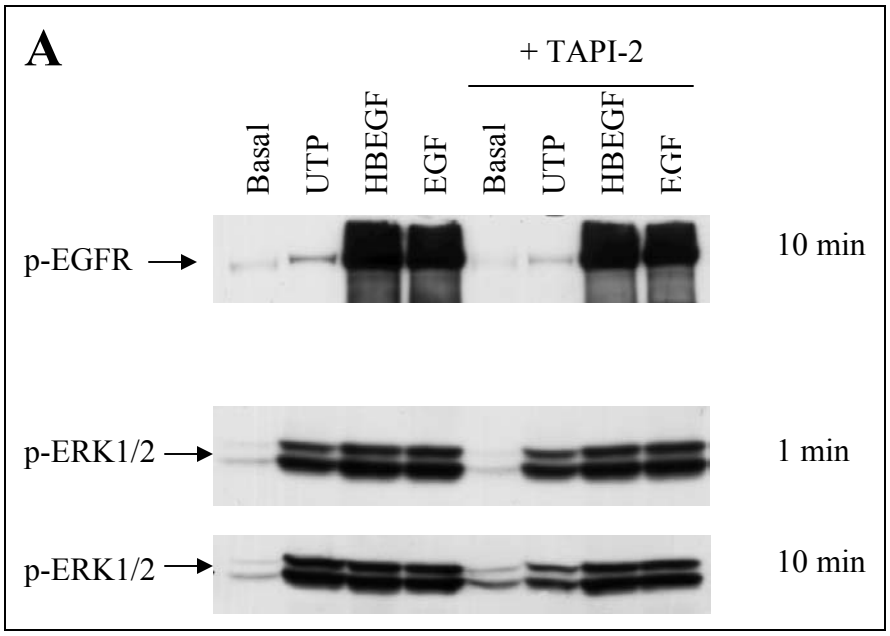
A
+ TAPI-2
Basal
UTP
HBEGF
EGF
Basal
UTP
HBEGF
EGF
p-EGFR
10 min
p-ERK1/2
1 min
p-ERK1/2
10 min

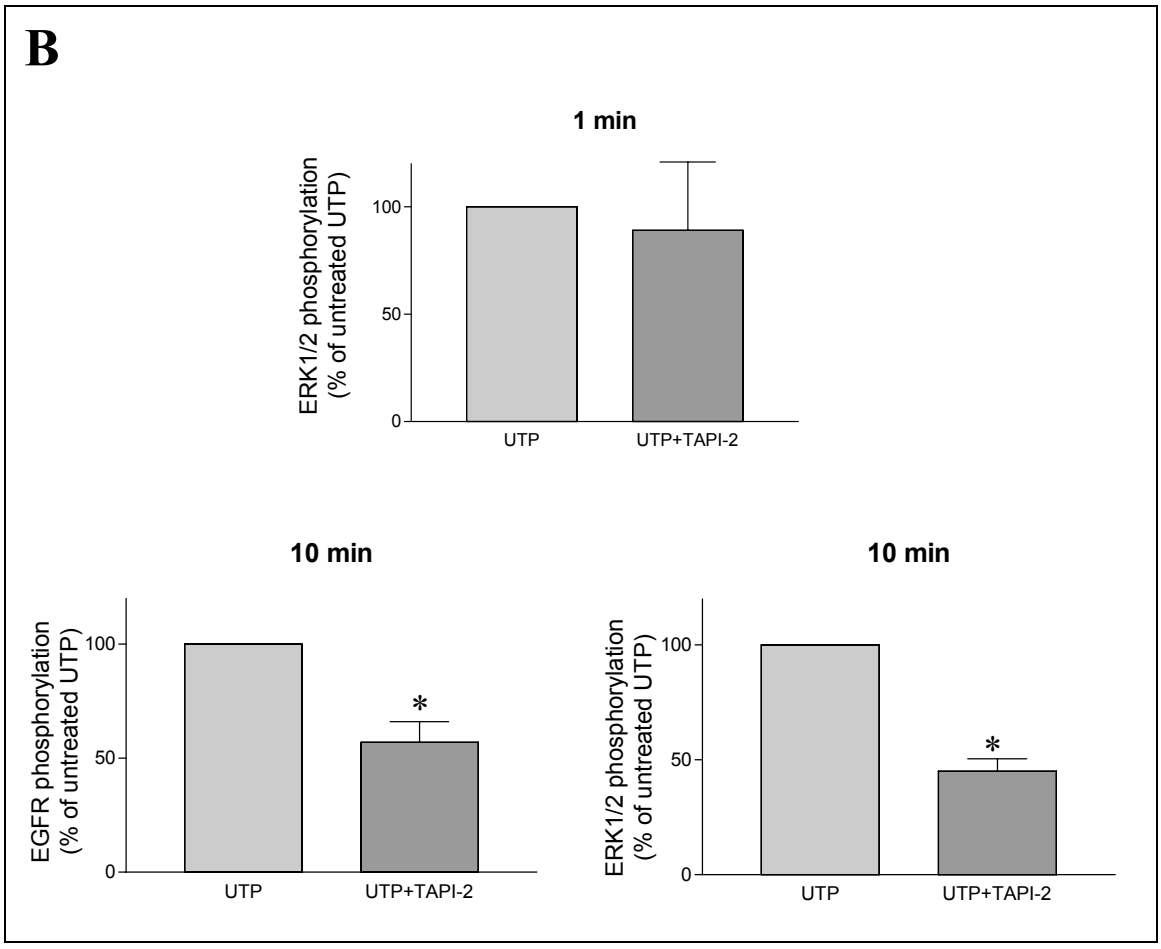
B
1 min
ERK1/2 phosphorylation (% of untreated UTP)
100
50
0
UTP
UTP+TAPI-2
10 min
EGFR phosphorylation (% of untreated UTP)
100
50
0
*
UTP
UTP+TAPI-2
10 min
ERK1/2 phosphorylation (% of untreated UTP)
100
50
0
*
UTP
UTP+TAPI-2

Figure 18. CMK, a furin inhibitor, inhibits the EGFR-dependent phase of UTP-induced ERK1/2 phosphorylation in HSG cells. HSG cells pretreated for 30 min with 50 μM CMK, were stimulated with UTP (100 μM) for 1 or 10 min, whereas stimulation with the EGFR ligands EGF (100 ng/ml) or HBEGF (20 ng/ml) was used as positive controls. Cell lysates were prepared and phosphorylation of EGFR or ERK1/2 was determined by Western analysis using specific antibodies (see Methods). Representative blots from three experiments are shown.

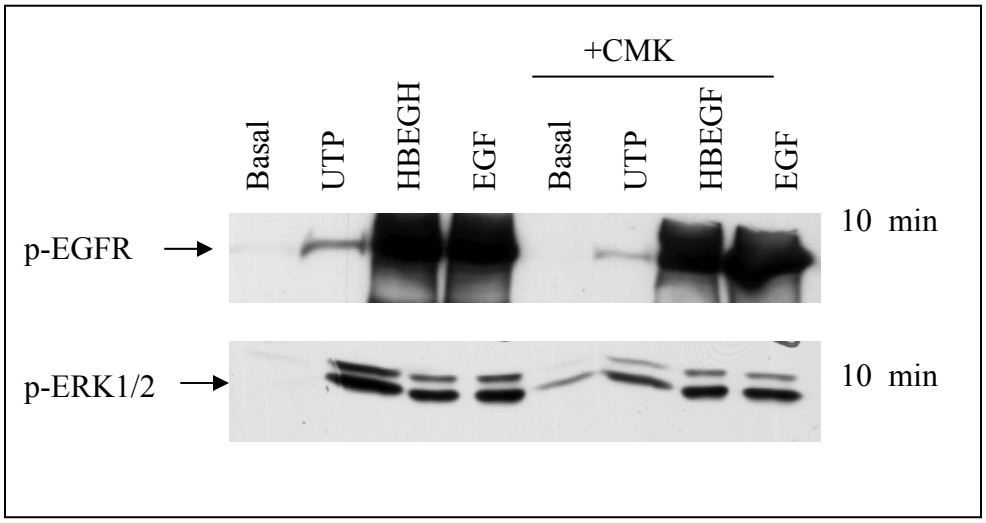
+CMK
Basal
UTP
HBEGH
EGF
Basal
UTP
HBEGF
EGF
p-EGFR
10 min
p-ERK1/2
10 min

Figure 19: ADAM10 and ADAM17 siRNAs inhibit UTP-induced ERK1/2 phosphorylation in HSG cells. HSG cells were transfected with ADAM10 and/or ADAM17 siRNA (see Methods). UTP (100 μM) was added for 10 min, and stimulation with the EGFR ligand EGF (100 ng/ml) was used as a positive control. Cell lysates were prepared and (**A**) phosphorylation of ERK1/2 and (**B**) ADAM10 and ADAM17 expression were detected by Western analysis using specific antibodies (see Methods). Data shown are representative of results from four experiments.

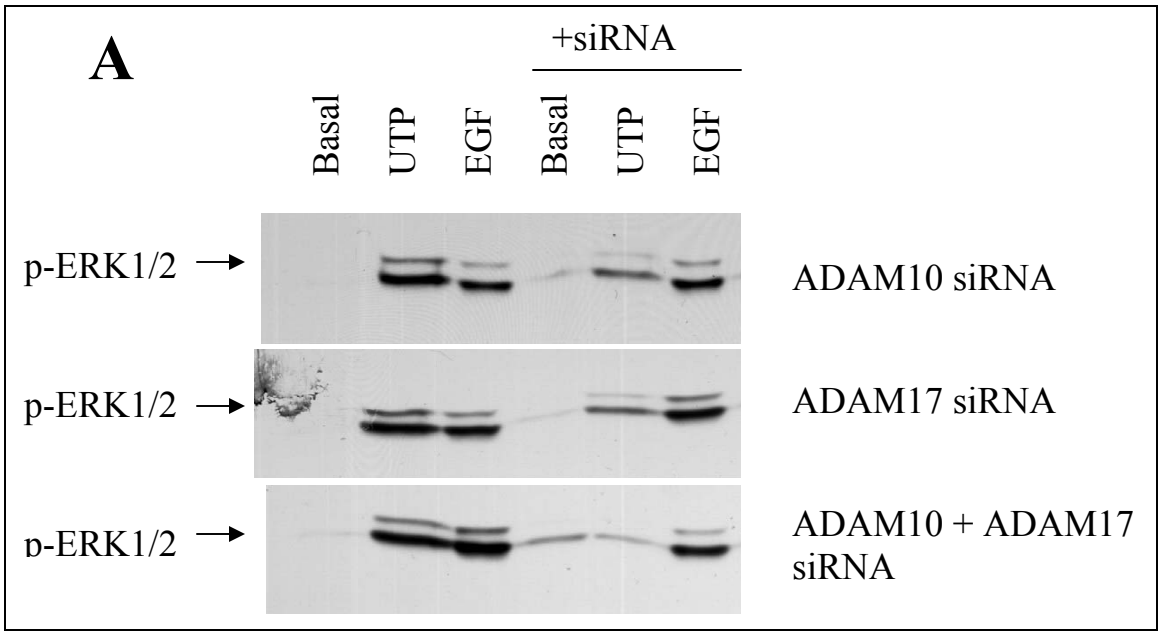
A
+siRNA
Basal
UTP
EGF
Basal
UTP
EGF
p-ERK1/2
p-ERK1/2
p-ERK1/2
ADAM10 siRNA
ADAM17 siRNA
ADAM10 + ADAM17 siRNA

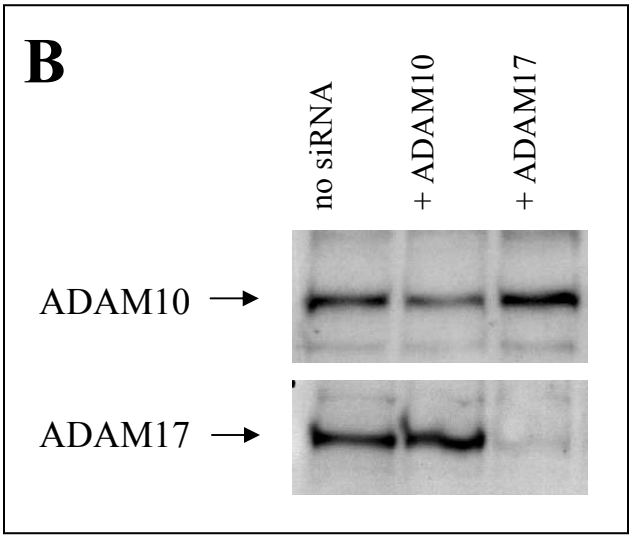
B
no siRNA
+ ADAM10
+ ADAM17
ADAM10
ADAM17

Antibodies against HBEGF, TGFα, AR, and EGF do not inhibit P2Y$_2$R-mediated EGFR transactivation.

EGFR ligands are synthesized as membrane anchored precursor proteins. Recently, six EGFR ligands have been shown to be cleaved from their precursor proteins by the metalloproteases ADAM10 and ADAM17 [100]. HBEGF has been implicated in GPCR-mediated transactivation of the EGFR [92, 93, 115]. TGFα and AR also have been shown to activate the EGFR [97, 115, 116]. EGF is abundantly expressed and secreted from salivary glands [116], making it a potential ligand for EGFR transactivation generated by P2Y$_2$R-mediated metalloprotease activation. To identify EGF-like ligands involved in P2Y$_2$R-mediated EGFR transactivation, we preincubated HSG cells with antibodies against HBEGF, TGFα, AR, or EGF for 30 min prior to UTP stimulation. Preincubation with these ligand-specific antibodies did not inhibit UTP-stimulated transactivation of the EGFR (Figure 20). However, these antibodies did inhibit EGFR phosphorylation induced by the corresponding antigens, indicating the ability of the antibodies to neutralize the effects of specific EGFR ligands (Figure 20). These results suggest that HBEGF, TGFα, AR, and EGF are not generated by activation of the P2Y$_2$R.

Figure 20: Anti-growth factor antibodies do not inhibit UTP-induced phosphorylation of the EGFR in HSG cells. HSG cells were preincubated for 60 min with (**A**) anti-HBEGF (40 μg/ml), (**B**) anti-TGFα (20 μg/ml), (**C**) anti-AR (40 μg/ml), or (**D**) anti-EGF (50 μg/ml) antibody (Ab) and then stimulated for 10 min with 100 μM UTP, HBEGF (20 ng/ml), TGFα (3 ng/ml), AR (50 ng/ml), or EGF (100 ng/ml). Cell lysates were prepared and phosphorylation of EGFR was detected by Western analysis using a specific antibody (see Methods). Data shown are representative of results from three experiments.

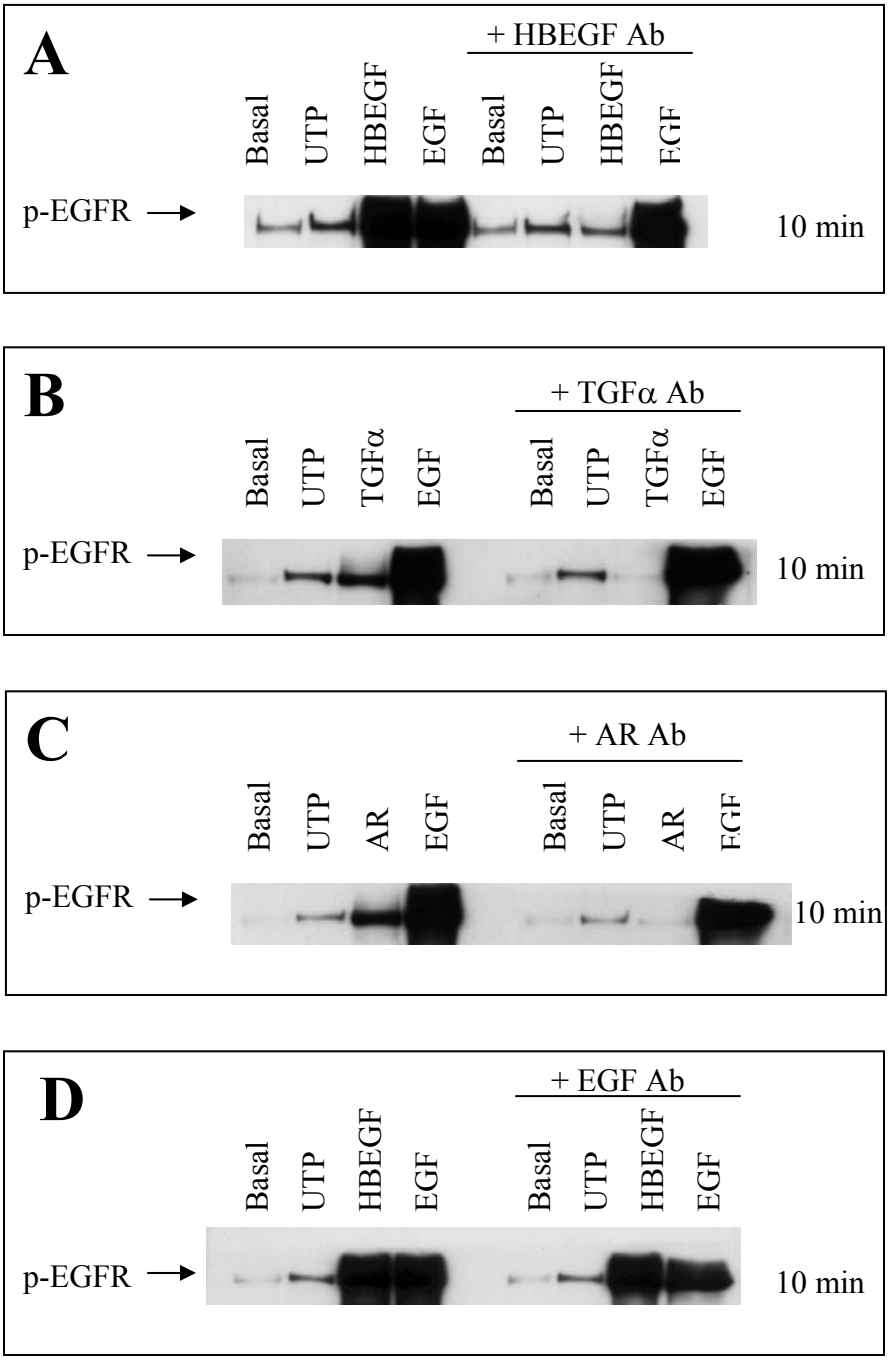
A
+ HBEGF Ab
Basal
UTP
HBEGF
EGF
Basal
UTP
HBEGF
EGF
p-EGFR
10 min
B
+ TGFα Ab
Basal
UTP
TGFα
EGF
Basal
UTP
TGFα
EGF
p-EGFR
10 min
C
+ AR Ab
Basal
UTP
AR
EGF
Basal
UTP
AR
EGF
p-EGFR
10 min
D
+ EGF Ab
Basal
UTP
HBEGF
EGF
Basal
UTP
HBEGF
EGF
p-EGFR
10 min

$P2Y_2R$-stimulated ERK1/2 phosphorylation is dependent on extracellular calcium and PKC.

The $P2Y_2R$ is known to couple to Gq protein leading to the activation of phospholipase C (PLC) and the induction of diacylglycerol (DAG)-dependent protein kinase C (PKC) activity, and inositol 1,4,5-trisphosphate (IP_3)-dependent increases in $[Ca^{2+}]_i$ due to calcium release from intracellular stores and calcium influx through plasma membrane calcium channels [25, 117]. Therefore, we determined the role of calcium mobilization and PKC activation in $P2Y_2R$-mediated EGFR transactivation and ERK1/2 phosphorylation. Results indicated that pretreatment of HSG cells with BAPTA-AM, that generates the intracellular calcium chelator BAPTA, did not affect UTP-induced ERK1/2 phosphorylation, although BAPTA significantly increased basal levels of EGFR phosphorylation (Figure 21). In contrast, EGFR and ERK1/2 phosphorylation induced by a 10 min UTP treatment was inhibited by preincubation of HSG cells in calcium-free media containing 200 μM EGTA (Figure 22). Chelation of extracellular calcium had no significant effect on ERK1/2 phosphorylation induced by a 1 min UTP treatment (Figure 22). These data suggest that extracellular Ca^{2+} is required for $P2Y_2R$-mediated EGFR transactivation and ERK1/2 phosphorylation, responses that were not modulated by the release of calcium from intracellular stores. The PKC inhibitor, GF109203, inhibited ERK1/2 phosphorylation induced by a 1 min UTP stimulation, but had no effect on UTP-induced ERK1/2 phosphorylation at the 10 min time point (Figure 23), suggesting that PKC regulates the rapid src-dependent and EGFR-independent activation of ERK1/2 via the $P2Y_2R$. Figure

24 depicts the $P2Y_2R$ signaling pathways that mediate EGFR transactivation and ERK1/2 phosphorylation in HSG cells.

Figure 21. UTP-induced ERK1/2 phosphorylation is not dependent on intracellular calcium. HSG cells were preincubated with BAPTA/AM (25 μM) for 30 min to generate the intracellular calcium chelator BAPTA, and then stimulated with 100 μM UTP for 1 or 10 min. Stimulation with EGF (100 ng/ml) was used as a positive control. Cell lysates were prepared and phosphorylation of EGFR or ERK1/2 was determined by Western analysis using specific antibodies (see Methods). Data shown are representative of results from three experiments.

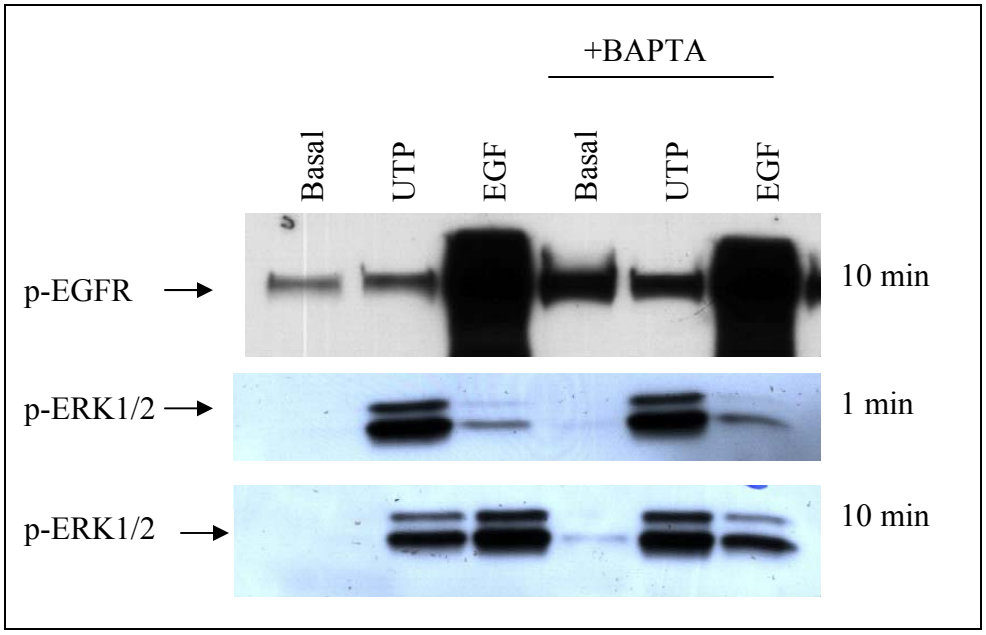
+BAPTA
Basal
UTP
EGF
Basal
UTP
EGF
p-EGFR
10 min
p-ERK1/2
1 min
p-ERK1/2
10 min

Figure 22: UTP-induced ERK1/2 phosphorylation due to EGFR transactivation is dependent on extracellular calcium. HSG cells were incubated in either calcium-containing Krebs-HEPES buffer (15 mM HEPES, pH 7.4, 120 mM NaCl, 4 mM KCl, 1.2 mM $MgSO_4$, 1.2 mM KH_2PO_4, 1 mM $CaCl_2$, and 10 mM D-glucose) or calcium-free Krebs-HEPES buffer containing 0.2 mM EGTA. Then, cells were stimulated with UTP (100 μM) or EGF (100 ng/ml) for 1 or 10 min. Cell lysates were prepared and phosphorylation of EGFR or ERK1/2 was determined by Western analysis using specific antibodies (see Methods). (**A**) Representative blots and (**B**) the means +/- S.E.M. of results from three experiments were normalized to total ERK where * indicates $p < 0.05$ (see Methods).

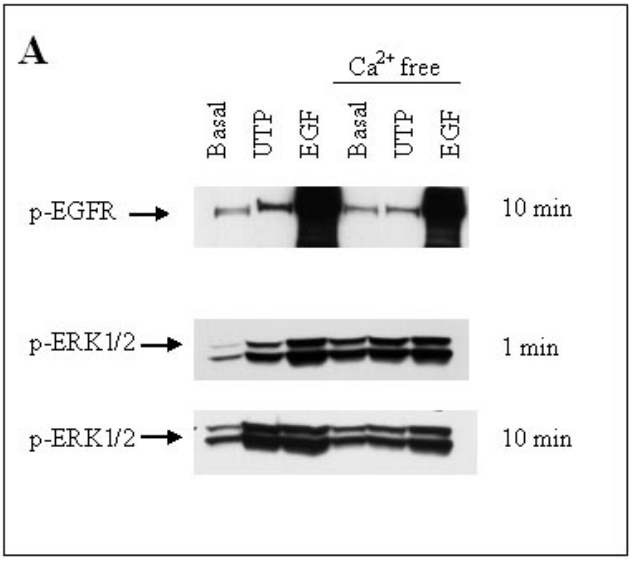
A
Ca2+ free
Basal
UTP
EGF
Basal
UTP
EGF
p-EGFR
10 min
p-ERK1/2
1 min
p-ERK1/2
10 min

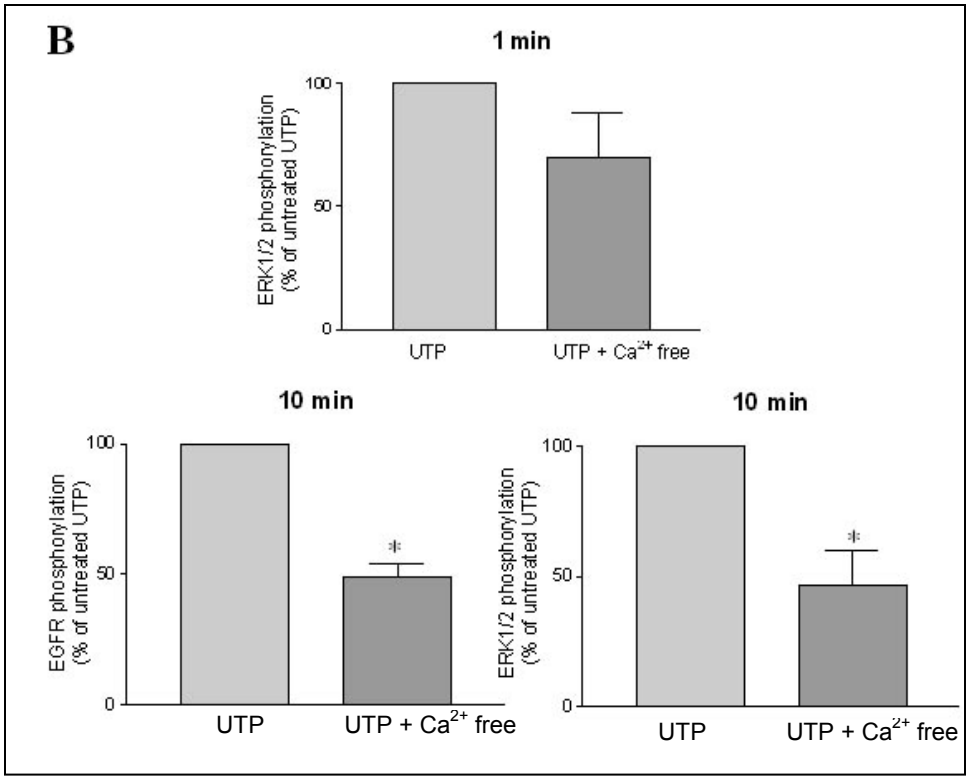
B
1 min
ERK1/2 phosphorylation (% of untreated UTP)
100
50
0
UTP
UTP + Ca2+ free
10 min
EGFR phosphorylation (% of untreated UTP)
100
50
0
*
UTP
UTP + Ca2+ free
10 min
ERK1/2 phosphorylation (% of untreated UTP)
100
50
0
*
UTP
UTP + Ca2+ free

Figure 23: Rapid UTP-induced ERK1/2 phosphorylation is dependent on PKC. HSG cells were pretreated with the PKC inhibitor GF109203 for 30 min and then stimulated with 100 μM UTP for 1 or 10 min. PMA (10 ng/ml) was used as a positive control. Cell lysates were prepared and phosphorylation of EGFR or ERK1/2 was determined by Western analysis using specific antibodies (see Methods). (**A**) Representative blots and (**B**) the means +/- S.E.M. of results from three experiments were normalized to total ERK where * indicates $p < 0.05$ (see Methods).

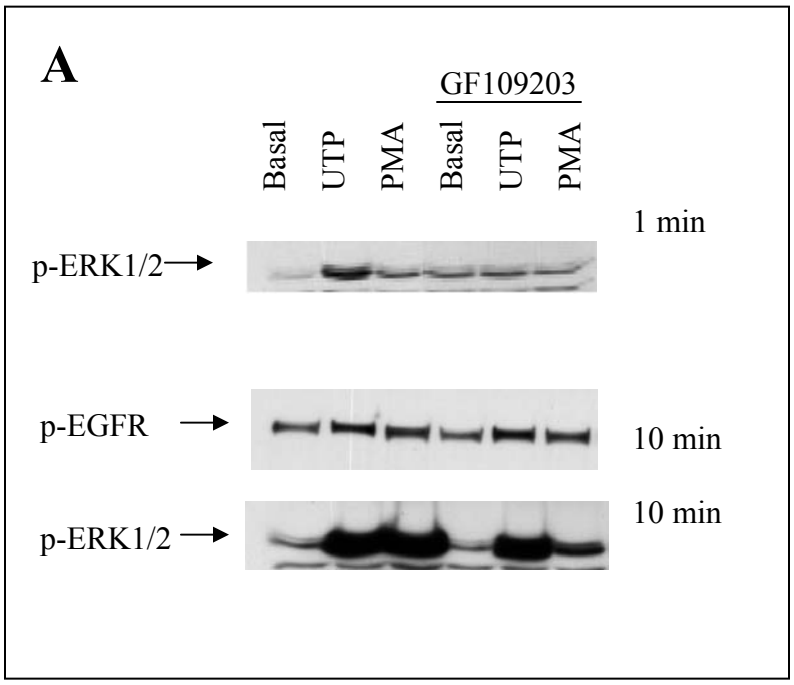
A
GF109203
Basal
UTP
PMA
Basal
UTP
PMA
1 min
p-ERK1/2
p-EGFR
10 min
p-ERK1/2
10 min

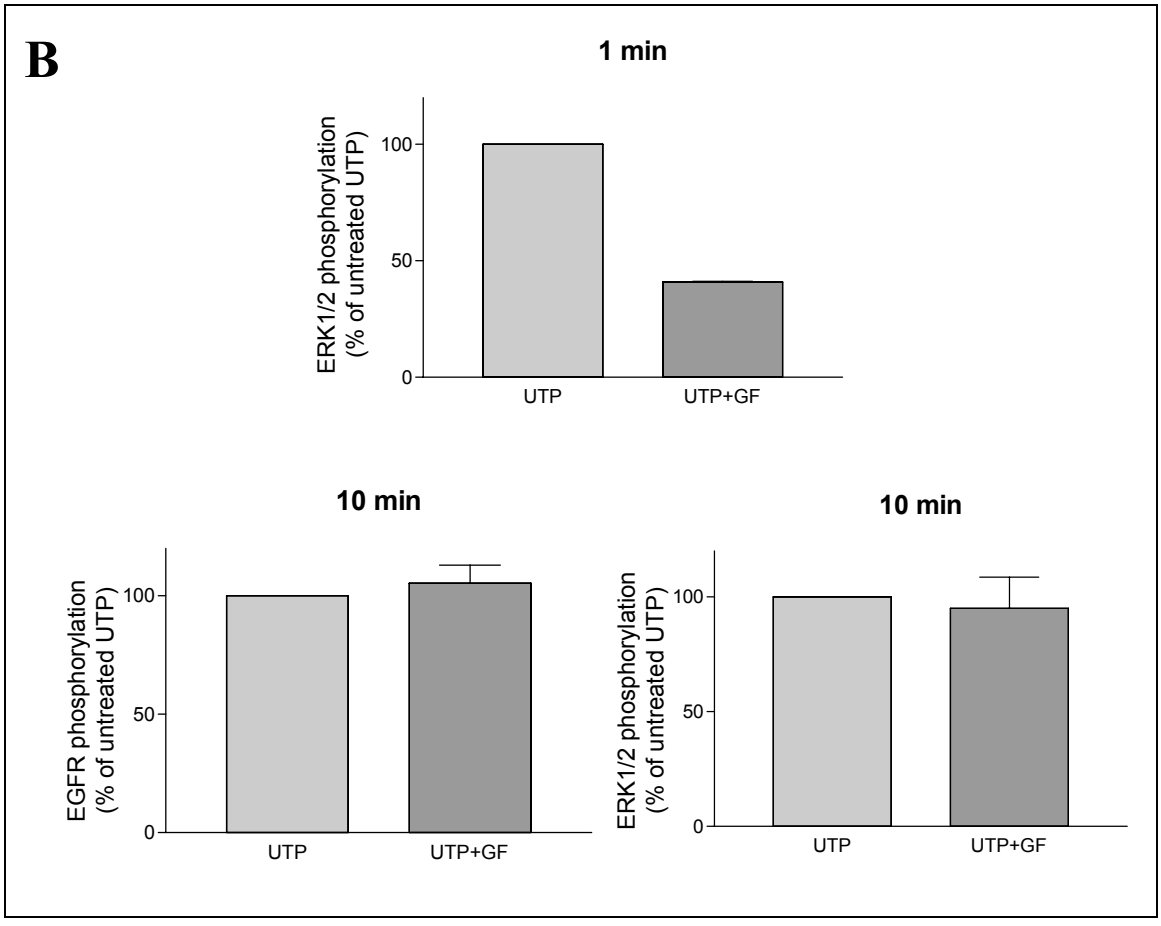
B
1 min
ERK1/2 phosphorylation (% of untreated UTP)
100
50
0
UTP
UTP+GF
10 min
EGFR phosphorylation (% of untreated UTP)
100
50
0
UTP
UTP+GF
10 min
ERK1/2 phosphorylation (% of untreated UTP)
100
50
0
UTP
UTP+GF

Figure 24: Model for $P2Y_2R$-mediated EGFR transactivation and ERK1/2 phosphorylation. Activation of the $P2Y_2R$ by ATP or UTP causes the rapid PKC- and src-dependent phosphorylation of ERK1/2, whereas ERK1/2 phosphorylation induced by longer UTP treatments is dependent upon metalloprotease (ADAM10 and ADAM17) activation and EGFR transactivation, responses modulated by extracellular calcium.

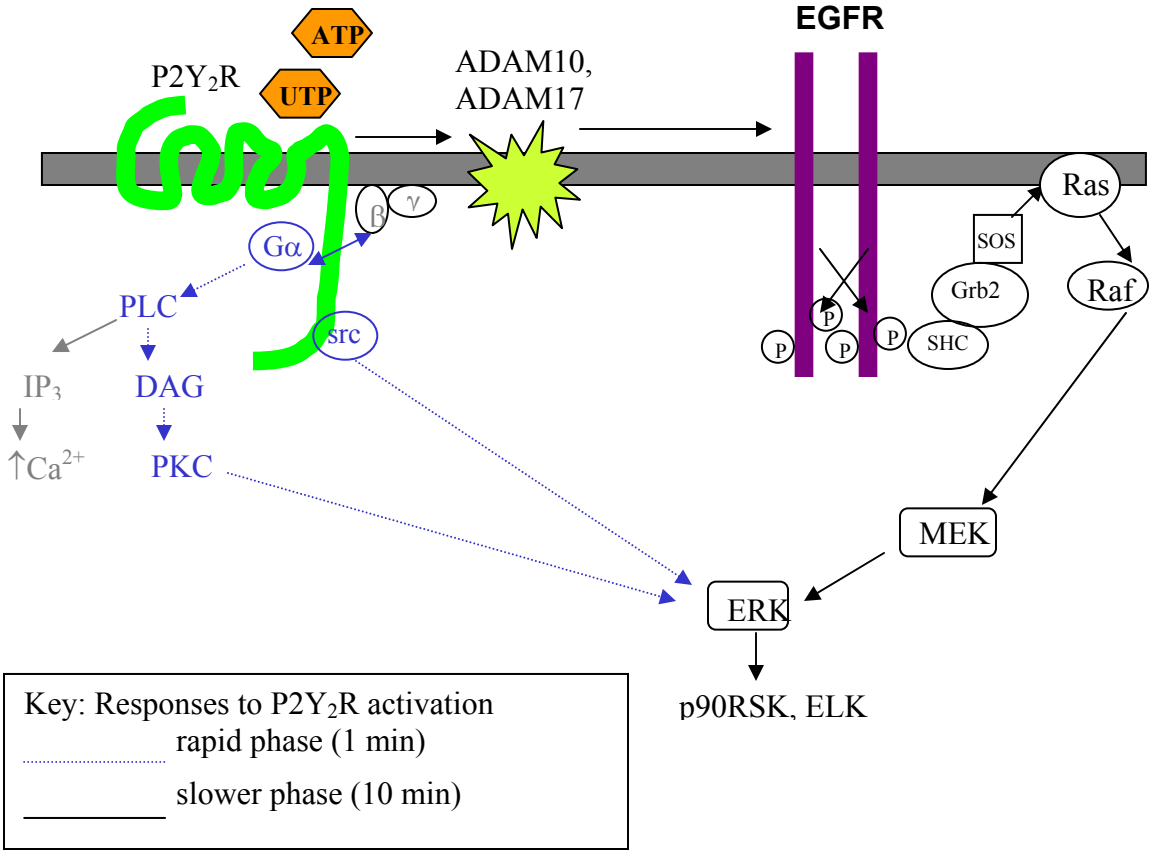
ATP
UTP
P2Y2R
ADAM10,
ADAM17
EGFR
Ras
SOS
Grb2
Raf
SHC
P
P
P
P
β
γ
Gα
PLC
src
IP3
DAG
↑Ca2+
PKC
MEK
ERK
p90RSK, ELK
Key: Responses to P2Y2R activation
rapid phase (1 min)
slower phase (10 min)

DISCUSSION

It is becoming recognized that GPCRs activate mitogen activated protein kinases (MAPKs) not only through direct coupling to heterotrimeric G proteins, but also by transactivation of signal transduction pathways associated with integrins and growth factor receptors [40, 60, 62, 67, 92, 103-105, 107, 118-120]. GPCRs have been shown to activate MAPKs such as ERK1/2 via a pertussis toxin sensitive G protein [102], the adapter protein β-arrestin and the recruitment of c-src [103], Gβγ subunits [104], increases in $[Ca^{2+}]_i$ [105, 106], activation of c-src [104, 107-110] and PYK2 [107, 110] and EGFR transactivation. Recent studies indicate that G protein-coupled $P2Y_2$ receptors for ATP and UTP can activate ERK1/2 via G_q proteins or by coupling to integrin and growth factor receptors and their signaling complexes [49, 59-62]. In this report, we demonstrate that activation of the endogenous $P2Y_2$ receptor in human submandibular gland (HSG) cells stimulates ERK1/2 phosphorylation by both a rapid src- and PKC-dependent pathway, and a slower pathway that is dependent on activation of the metalloproteases ADAM10 and ADAM17, EGFR transactivation, and extracellular calcium.

In HSG cells, rapid src- and PKC-dependent ERK1/2 phosphorylation occurs within 1 min of UTP addition (see Figure 16 and Figure 23). The $P2Y_2R$ has been shown to bind src via two SH3 binding domains in its C-terminal tail, but this mechanism has been associated with the transactivation of growth factor receptors [62, 67], a slow response in HSG cells that appears to be src-

independent (see Figure 16). Nonetheless, src plays a role in the activation of ERK by other GPCRs [95, 121]. Our observation that $P2Y_2R$-mediated EGFR phosphorylation is not src-dependent in HSG cells depends upon an anti-EFGR antibody that is specific for an autophosphorylation site (tyrosine 1068) on the EGFR that serves as the binding site for Grb2/SH2, and results in Ras activation through a Grb2/Sos signaling mechanism [122]. In a previous study demonstrating src-dependent EGFR transactivation by the $P2Y_2R$, [62], the anti-EGFR antibody used recognized a src-dependent phosphorylation site (tyrosine 992) on the EGFR, which is a direct binding site for PLCγ and results in activation of PLCγ signaling pathways [123]. Therefore, it appears that both src-dependent and src-independent mechanisms of $P2Y_2R$-mediated EGFR transactivation exist, although in HSG cells autophosphorylation of the EGFR via $P2Y_2R$ activation is src-independent. Since PKC is also involved in the rapid phase of UTP-induced ERK1/2 activation (see Figure 23), it is likely that PKC activity is regulated by the $P2Y_2R$ via G_q-mediated activation of PLC and the generation of diacylglycerol [32, 40]. Further study is needed to determine whether src activity is modulated by PKC in HSG cells, or whether src activation is due to $P2Y_2R$-mediated transactivation of integrin signaling pathways, as has been previously described [40].

Although src-independent, the $P2Y_2R$ in HSG cells mediates slow ERK1/2 phosphorylation via transactivation of the EGFR (see Figure 15). Transactivation of growth factor receptors is a common mechanism by which GPCRs signal to ERK1/2 [92, 93, 95]. EGFR transactivation by a GPCR can occur through

shedding of an EGF-like ligand (for a review see [124]), whereas other studies demonstrate that GPCRs can activate EGFR in a ligand-independent manner [102-110]. Our results with HSG cells show that TAPI-2 (see Figure 17), a selective ADAM17/TACE inhibitor, and ADAM10 and ADAM17 siRNAs (see Figure 19) inhibit UTP-induced EGFR and ERK1/2 phosphorylation, indicating for the first time that these metalloproteases are involved in the delayed phase of EGFR-dependent ERK1/2 activation mediated by the $P2Y_2R$. Although $P2Y_2R$ activation rapidly increases $[Ca^{2+}]_i$ through G_q-dependent stimulation of PLC [25, 117], our results show that chelation of intracellular calcium by BAPTA had no effect on UTP-induced ERK1/2 activation (see Figure 21) whereas depletion of extracellular calcium partially inhibited UTP-induced EGFR transactivation and ERK1/2 phosphorylation at the 10 min time point (see Figure 22). Thus, extracellular calcium may be required for activation of metalloproteases or other proteins involved in $P2Y_2R$-mediated EGFR transactivation and ERK1/2 phosphorylation.

UTP-induced activation of the metalloproteases ADAM10 and ADAM17 could generate EGF-like ligands that stimulate EGFR transactivation. EGF is highly expressed in salivary gland tissues [125], however to our knowledge, the presence of other EGF-like ligands in HSG cells has not been documented. RT-PCR analyses confirmed the presence of HB-EGF, TGFα, and AR mRNA expression in HSG cells (data not shown). In addition, HB-EGF and EGF induced EGFR activation and ERK1/2 phosphorylation in HSG cells (Figures 15-18 and 20). However, antibodies directed against EGF, HB-EGF, TGFα, and AR

had no effect on UTP-induced EGFR phosphorylation, although they prevented EGFR phosphorylation induced by their corresponding antigen (Figure 20). ADAM10 and ADAM17, members of the adamalysin family of proteases (ADAMs), have been implicated in GPCR- and growth factor-mediated tumor cell migration [99]. Additionally, ADAM10 and ADAM17 have been shown to induce the release of EGF, HB-EGF, TGFα, amphiregulin, epiregulin, and betacellulin [100]. Thus, it remains plausible that UTP-induced activation of ADAM10 and ADAM17 in HSG cells could generate an as yet unidentified EGFR ligand that induces ERK1/2 phosphorylation through transactivation of the EGFR. We recently found that ADAM10 and ADAM17 activation by the $P2Y_2R$ expressed in 1321N1 astrocytoma cells leads to cleavage of the amyloid precursor protein (APP) thereby generating sAPPα [101], a peptide that is not known to activate the EGFR.

$P2Y_2R$-mediated EGFR transactivation and ERK1/2 phosphorylation may play a role in stress- and disease-related responses in salivary gland cells, where the $P2Y_2R$ is up-regulated. Furthermore, it is possible that $P2Y_2R$-induced transactivation of the EGFR may amplify signals induced by EGF or EGF-like ligands in chronic disease states. It has been shown that $P2Y_2R$-induced ERK1/2 activation leads to cell proliferation [35, 126-128], which may play a role in the repair of damaged tissue, although this remains to be determined. The $P2Y_2R$ has also been shown to promote inflammatory responses in a variety of cell and tissue types [53, 129-131]. $P2Y_2R$ up-regulation in endothelial cells promotes vascular inflammation due to increased expression of vascular cell

adhesion molecule-1 (VCAM-1) that promotes the binding of monocytes to endothelium through a mechanism involving $P2Y_2R$-mediated transactivation of vascular endothelial growth factor receptor-2 (VEGFR-2). In the NOD.B10 mouse model of Sjögren's syndrome, an autoimmune disease involving lymphocytic cell infiltration leading to salivary gland degeneration [18], $P2Y_2R$ expression is up-regulated in comparison to normal C57BL/6 mice [91]. It is intriguing to postulate that $P2Y_2R$ up-regulation in salivary gland regulates the expression of cell adhesion molecules that promote the binding of lymphocytes. Moreover, the ADAM10 and ADAM17 metalloproteases activated by $P2Y_2Rs$ are known to generate the cytokines TNFα and IL-1 [98]. Therefore, it is possible that $P2Y_2R$-induced metalloprotease activity may enhance salivary gland degeneration by amplifying inflammatory responses to nucleotides. Thus, the studies described in this chapter encourage further attempts to determine the function of $P2Y_2Rs$ in salivary gland, and suggest that $P2Y_2Rs$ may be novel targets for the treatment of salivary gland pathologies.

CHAPTER 4

CONCLUDING REMARKS

The extracellular nucleotides, ATP, ADP, UTP, and UDP, elucidate a wide range of physiological responses through activation of 15 P2 nucleotide receptor subtypes belonging to two families, GPCRs and ligand-gated ion channels. Among the G protein-coupled P2Y receptors, the $P2Y_2$ subtype is distinguished by its ability to be equipotently activated by ATP and UTP and mediates the $G_{q/11}$–dependent activation of phospholipase C (PLC) to generate the second messengers diacylglycerol and inositol 1,4,5-trisposphate (IP_3) that respectively stimulate PKC and release of calcium from intracellular organelles [32, 76]. In submandibular gland (SMG) cells isolated from rat salivary glands, the $P2Y_2R$ is the only UTP-responsive receptor expressed [38], and mediates a UTP-induced increase in $[Ca^{2+}]_i$, a response that increases with time of SMG cell culture [54]. $P2Y_2Rs$ are also up-regulated in ligated salivary glands [52].

In chapter two of this dissertation, we show that $P2Y_2Rs$ are up-regulated in the NOD.B10 mouse model of Sjögren's syndrome, an autoimmune disease of the salivary gland that decreases saliva production due to lymphocytic infiltration into the gland [7]. Since no specific $P2Y_2R$ antibodies exist, we demonstrated $P2Y_2R$ mRNA up-regulation by RT-PCR with cDNA derived from NOD.B10 SMG cell mRNA, and by *in situ* hybridization of SMG tissue slices from NOD.B10 mice, in comparision to normal C57BL/6 mice, using $P2Y_2$-specific anti-sense riboprobes. $P2Y_2R$ mRNA up-regulation in SMG of NOD.B10 mice correlated

with UTP-induced increases in $[Ca^{2+}]_i$, a measure of $P2Y_2R$ activity. Other results indicate that $P2Y_2R$ up-regulation increased with disease progression. These findings support previous suggestions that $P2Y_2R$ up-regulation may play a role in salivary gland tissue responses to stress and injury seen in two other models of $P2Y_2R$ up-regulation in salivary glands [52, 54].

The fact that $P2Y_2Rs$ are up-regulated under stress conditions in many types of tissues [53, 55-58], leads us to postulate that $P2Y_2Rs$ may play a role in the wound healing process. In salivary glands, $P2Y_2Rs$ could regulate saliva secretion through activation of signaling cascades that lead to increases in $[Ca^{2+}]_i$ and activation of Ca^{2+}-activated Cl^- channels. Thus, expression of $P2Y_2Rs$ could potentially be beneficial to SS patients by increasing saliva flow, although chronic expression and activation of $P2Y_2Rs$ may lead to prolonged inflammatory responses that promote gland degeneration.

$P2Y_2Rs$ in other cell types can activate ERK1/2 through transactivation of EGFR [60], PDGFR [54], and VEGFR [67], and SH3 binding domains in the $P2Y_2R$ have been shown to mediate the src-dependent transactivation of these growth factor receptors [62]. Chapter three of this dissertation describes studies demonstrating that EGFR transactivation by the $P2Y_2R$ in human salivary gland (HSG) cells leads to the time-dependent phosphorylation of ERK1/2 and the downstream targets of ERK1/2, p90RSK and the transcription factor ELK, suggesting that activated $P2Y_2Rs$ may regulate gene expression in salivary gland tissue. Other results demonstrate that $P2Y_2R$-mediated EGFR transactivation is dependent on ADAM10 and ADAM17 metalloprotease activities and extracellular

calcium, and occurs more slowly than src-dependent, EGFR-independent ERK1/2 activation in HSG cells that is modulated by PKC. This study marks the first description of ADAM10 and ADAM17 involvement in $P2Y_2R$-mediated EGFR transactivation, and describes the most complete characterization to date of $P2Y_2R$ functions in salivary gland cells.

Taken together, the fact that $P2Y_2Rs$ are up-regulated in many different types of stressed tissues to activate the signal transduction pathways mentioned above, may provide clues as to the consequence of $P2Y_2R$ up-regulation in salivary gland. In support of a role for the $P2Y_2R$ in regulating the expression of pro-inflammatory molecules, $P2Y_2R$ up-regulation and activation in endothelial cells increases the expression of vascular cell adhesion molecule-1 (VCAM-1) that facilitates the binding of monocytes to endothelium [86]. Similarly, $P2Y_2R$ regulation of cell adhesion molecule expression in salivary gland may be related to Sjögren's syndrome, an autoimmune disease where binding and infiltration of lymphocytes leads to gland degeneration.

In addition to studies demonstrating that $P2Y_2Rs$ can activate responses associated with inflammation [53, 129-131], $P2Y_2R$ activation can induce proliferation of MCF-7 breast cancer cells [35], A549 lung cancer cells [126] HeLa cervical cancer cells [127], and human epidermal keratinocytes [128]. Conversely, the $P2Y_2R$ may be responsible for apoptosis of human endometrial HEC-1A and Ishikawa cancer cell lines [132] and colorectal HT-29 and Colo320 DM carcinoma cell lines [87, 133]. In salivary gland cells, preliminary studies suggest that $P2Y_2R$ activation does not induce apoptosis, since cleaved

caspase-3 levels, a marker of apoptosis, do not increase with UTP stimulation (Figure 25). Staurosporine, an inducer of apoptosis [134], increased levels of cleaved caspase-3 in salivary gland cells (Figure 25).

Figure 25. $P2Y_2Rs$ do not mediate cleavage of pro-caspase-3 in HSG cells. HSG cells in serum-free medium were treated with UTP (100 μM or 1 mM) or staurosporine (1 μM) for 2 or 8 h. Cell lysates were prepared and cleaved caspase-3 and total caspase-3 levels were determined by Western analysis using specific antibodies from Cell Signaling Technology (Beverly, MA). Data shown are representative of results from three experiments.

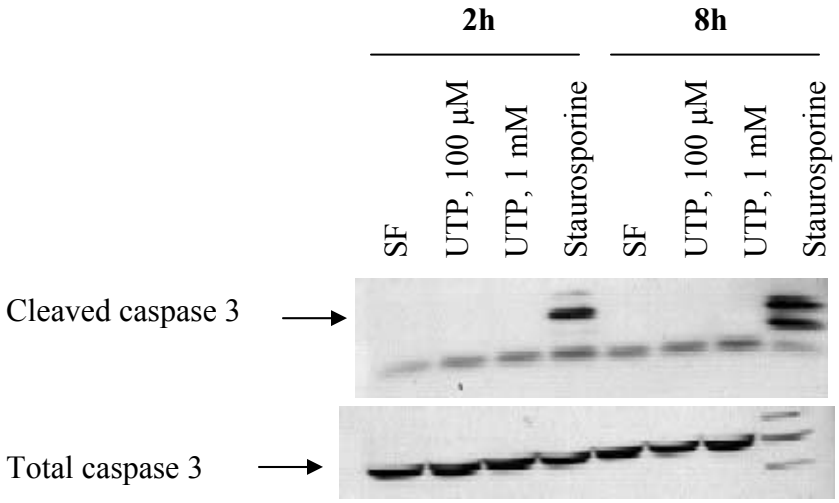
2h
8h
SF
UTP, 100 μM
UTP, 1 mM
Staurosporine
SF
UTP, 100 μM
UTP, 1 mM
Staurosporine
Cleaved caspase 3
Total caspase 3

Beyond understanding the function of $P2Y_2$Rs in salivary gland, it is also imperative that we define the mechanisms controlling $P2Y_2$R up-regulation. Since $P2Y_2$Rs are up-regulated under stress-induced conditions, it is plausible that these receptors could be either negatively or positively targeted in therapies. If $P2Y_2$Rs play a beneficial role by inducing apoptosis of tumor cells, increased saliva flow in Sjögren's syndrome, or tissue repair, stimulation of $P2Y_2$R up-regulation could be therapeutic. Published reports indicate that $P2Y_2$Rs can be up-regulated by treatment of vascular smooth muscle cells with cytokines including IL-1β in combination with TNFα or IFNγ [135]. Alternatively, if $P2Y_2$Rs play a detrimental role by promoting chronic inflammation for example, then inhibiting the signaling pathways that control $P2Y_2$R up-regulation may prove beneficial. Previously published data indicate that the MEK inhibitor, PD98059, partially blocks $P2Y_2$R up-regulation in isolated rat SMG cells cultured for 24 h, suggesting that ERK1/2 may play a role in regulating $P2Y_2$R expression [59]. Preliminary experiments suggest that resveratrol, an anti-oxidant found in grapes and grape products, such as grape juice and red wine, inhibits $P2Y_2$R up-regulation in 48 h-old rat SMG cell cultures (Figure 26), suggesting that a combination of resveratrol and PD98059 may be an effective way to minimize $P2Y_2$R expression in salivary gland cells. Further work is necessary to define the mechanisms whereby resveratrol inhibits $P2Y_2$R expression, but it seems likely that this anti-oxidant prevents activation of transcriptional events induced by oxidative stress or related conditions.

Figure 26. Effect of resveratrol on $P2Y_2R$ agonist-induced increases of $[Ca^{2+}]_i$ and $P2Y_2R$ mRNA expression in rat SMG cells after 48 h in culture. Resveratrol (1-100 μM) was added to SMG incubated in Krebs-HEPES medium prior to the preparation of dispersed cell aggregates, as previously described [59]. **(A)** Cells were assayed for changes in $[Ca^{2+}]_i$ in response to UTP (100 μM) or carbachol (100 μM), using approximately equal numbers of cells from each preparation. Increases in $[Ca^{2+}]_i$ were expressed after subtracting the basal $[Ca^{2+}]_i$ from the peak increase in $[Ca^{2+}]_i$ induced by UTP or carbachol (Carb). Values are means +/- SEM of results from 3 experiments. **(B)** $P2Y_2R$ mRNA levels were determined by RT-PCR of cDNA derived from mRNA of SMG cells cultured with or without resveratrol (1-75 μM; Res) for 48 h; PCR of RNA samples incubated in the absence of reverse transcriptase (-RT) served as a negative control. Samples were electrophoresed on a 2% (w/v) agarose ethidium bromide gel and bands were visualized under UV light. Data shown are representative of results from two experiments (see Chapter 2 for methods).

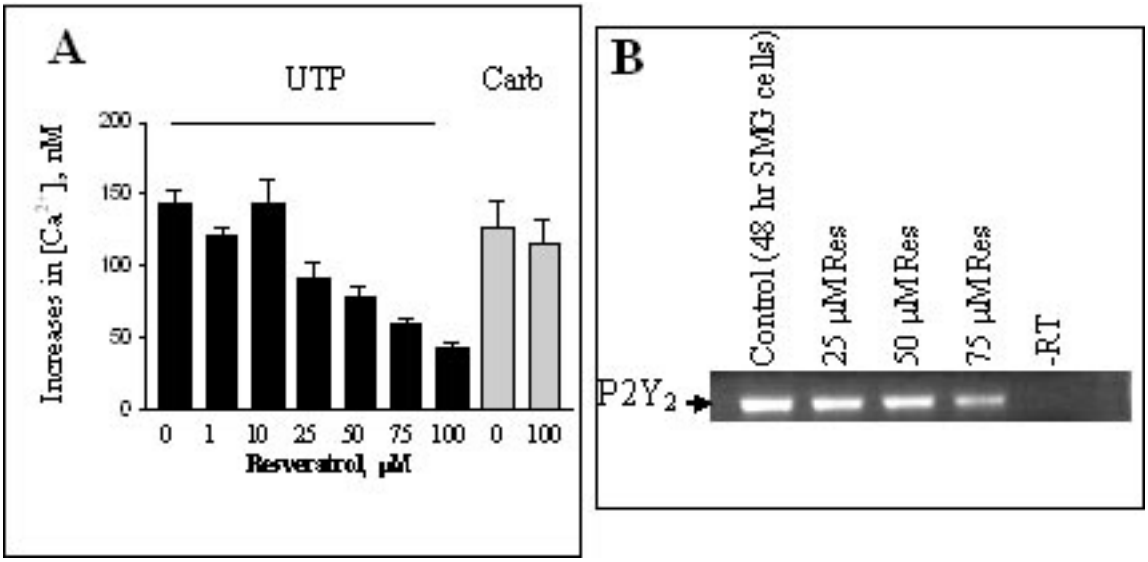
A
UTP
Carb
Increases in [Ca2+], nM
200
150
100
50
0
0 1 10 25 50 75 100 0 100
Resveratrol, μM
B
Control (48 hr SMG cells)
25 μM Res
50 μM Res
75 μM Res
-RT
P2Y2

Further studies are needed to define the signaling pathway that mediates UTP-induced EGFR transactivation in HSG cells, such as the identification of an EGF-like ligand generated by metalloproteases coupled to $P2Y_2R$ activation. Although our experiments have utilized anti-EGF ligand antibodies to suggest that these ligands play no role in UTP-induced EGFR transactivation, results from studies with dominant negative constructs or siRNA to inhibit ligand generation would be more conclusive. The potential involvement of EGF-like ligands such as betacellulin and epigen in UTP-induced EGFR transactivation remains to be examined, although these ligands have not been associated with GPCR-mediated EGFR transactivation to date. Potentially, there are other growth factor receptors, for example FGFR and PDGFR, that are expressed in salivary gland tissues and worthy of investigation as potential targets of activated $P2Y_2Rs$. Moreover, since both $P2Y_2Rs$ and ADAM metalloproteases have integrin binding domains [40, 98, 111], and since $P2Y_2Rs$ are known to activate integrin-dependent signaling events [40], the role of integrins in salivary gland functions mediated by the $P2Y_2R$ should be investigated.

Further studies are needed to link pro-inflammatory responses to $P2Y_2R$ activation in salivary gland with the autoimmune disease Sjögren's syndrome (SS). Preliminary data demonstrate that $P2Y_2R$ activation in HSG cells and cultured rat SMG cells increases VCAM-1 expression and U937 monocyte and Jurkat lymphocyte binding to SMG cells (Olga Baker, unpublished results), and lymphocyte infiltration into salivary gland has been associated with SS [7].

Experiments to demonstrate lymphocyte adherence to UTP-stimulated SMGs from the NOD.B10 mouse model of SS could provide further support for the hypothesis that $P2Y_2$Rs play a role in SS. Moreover, since the ADAM metalloproteases activated by $P2Y_2$Rs generate pro-inflammatory cytokines [98], it should be investigated whether release of cytokines from HSG cells contributes to the effects of UTP.

To clarify the mechanisms involved in regulation of $P2Y_2$R expression, studies are currently being performed to identify the transcription factor binding sites in the 5'-flanking region of the $P2Y_2$R gene. This information should help elucidate the signaling pathways that mediate $P2Y_2$R gene expression. Finally, other studies underway will examine whether SMG cell culture-induced $P2Y_2$R up-regulation can be inhibited in SMG isolated from resveratrol-fed rats compared to rats fed a normal diet.

In conclusion, studies in this dissertation provide evidence that $P2Y_2$Rs are up-regulated in salivary glands of the NOD.B10 mouse model of Sjögren's syndrome, and provide novel insights into the signaling pathways activated by $P2Y_2$Rs in salivary gland cells. More work is needed to elucidate the physiological consequences of $P2Y_2$R activation in salivary glands, such as the involvement in autoimmune and inflammatory processes. Moreover, elucidation of the mechanisms that control $P2Y_2$R expression may prove to be therapeutically useful in the treatment of a variety of diseases linked to $P2Y_2$R expression, including SS, atherosclerosis, cystic fibrosis and cancer [35, 43, 44, 53, 91, 136, 137].

References cited

1. Whelton, H. (1996) The anatomy and physiology of salivary glands in *Saliva and oral health* (Edgar, W. M. & O'Mullane, D. M., eds) pp. 1-9, The British Dental Association, London.

2. Nusair, S. & Rubinow, A. (1999) The use of oral pilocarpine in xerostomia and Sjögren's syndrome, *Semin Arthritis Rheum. 28*, 360-367.

3. Tortora, G. J. & Grabowski, S. R. (1996) *Principles of Anatomy and Physiology*, 8th edn, Harper Collins College Publishers, New York.

4. Edgar, W. M. & O'Mullane, D. M. (1996) *Saliva and oral health*, 2nd edn, British Dental Association, Great Britain.

5. Carlsson, M. (1999). Henrik Sjogren - A medical and historical presentation. Paper presented at the *State of the Art Lectures on Sjögren's syndrome*, Jönköping, Sweden.

6. Tsianos, E. B., Vasakos, S., Drosos, A. A., Malamou-Mitsi, V. D. & Moutsopoulos, H. M. (1986) The gastrointestinal involvement in primary Sjögren's syndrome, *Scand J Rheumatol. 61*, 151-155.

7. Fox, R. I. & Kang, H. I. (1992) Pathogenesis of Sjögren's syndrome, *Rheum Dis Clin North Am. 18*, 517-538.

8. Humphreys-Beher, M. G., Peck, A. B., Dang, H. & Talal, N. (1999) The role of apoptosis in the initiation of the autoimmune response in Sjögren's syndrome, *Clin Exp Immunol. 116*, 383-387.

9. Bacman, S., Sterin-Borda, L., Camusso, J. J., Arana, R., Hubscher, O. & Borda, E. (1996) Circulating antibodies against rat parotid gland M3 muscarinic receptors in primary Sjögren's syndrome, *Clin Exp Immunol. 104*, 454-459.

10. Bacman, S., Perez Leiros, C., Sterin-Borda, L., Hubscher, O., Arana, R. & Borda, E. (1998) Autoantibodies against lacrimal gland M3 muscarinic

acetylcholine receptors in patients with primary Sjögren's syndrome, *Invest Ophthalmol Vis Sci. 39*, 151-156.

11. Humphreys-Beher, M. G. & Peck, A. B. (1999) New concepts for the development of autoimmune exocrinopathy derived from studies with the NOD mouse model, *Arch Oral Biol. 44*, S21-S25.

12. Konttinen, Y. T., Hukkanen, M., Kemppinen, P., Segerberg, M., Sorsa, T., Malmstrom, M., Rose, S., Itescu, S. & Polak, J. M. (1992) Peptide-containing nerves in labial salivary glands in Sjögren's syndrome, *Arthritis Rheum. 35*, 815-820.

13. Konttinen, Y. T., Sorsa, T., Hukkanen, M., Segerberg, M., Kuhlefelt-Sundstrom, M., Malmstrom, M. & Polak, J. M. (1992) Topology of innervation of labial salivary glands by protein gene product 9.5 and synaptophysin immunoreactive nerves in patients with Sjögren's syndrome, *J Rheumatol. 19*, 30-37.

14. Tornwall, J., Konttinen, Y. T., Tuominen, R. K. & Tornwall, M. (1997) Protein kinase C expression in salivary gland acinar epithelial cells in Sjögren's syndrome, *Lancet. 349*, 1814-1815.

15. Greenspan, J. S., Daniels, T. E., Talal, N. & Sylvester, R. A. (1974) The histopathology of Sjogren's syndrome in labial salivary gland biopsies, *Oral Surg Oral Med Oral Pathol. 37*, 217-229.

16. Pedersen, A. M., Reibel, J. & Nauntofte, B. (1999) Primary Sjögren's syndrome (pSS): subjective symptoms and salivary findings, *J Oral Pathol Med. 28*, 303-311.

17. Kino-Ohsaki, J., Nishimori, I., Morita, M., Okasaki, K., Yamamoto, Y., Onishi, S. & Hollingsworth, M. A. (1997) Serum antibodies to carbonic anhydrase I and II in patients with idiopathic chronic pancreatitis and Sjögren's syndrome, *Gastroenterology. 112*, 1054-1056.

18. Robinson, C. P., Yamachika, S., Bounous, D. I., Brayer, J., Jonsson, R., Holmdahl, R., Peck, A. B. & Humphreys-Beher, M. G. (1998) A novel NOD-derived murine model of primary Sjögren's syndrome, *Arthritis Rheum. 41*, 150-156.

19. Robinson, C. P., Cornelius, J., Bounous, D. I., Yamamoto, H., Humphreys-Beher, M. G. & Peck, A. B. (1998) Characterization of the changing lymphocyte populations and cytokine expression in the exocrine tissues of autoimmune NOD mice, *Autoimmunity. 27*, 29-44.

20. Humphreys-Beher, M. G., Hu, Y., Nakagawa, Y., Wang, P.-L. & Purushotham, K. R. (1994) Utilization of the NOD mouse as an animal model for the study of secondary Sjögren's syndrome, *Adv Exp Med Biol. 350*, 631-636.

21. Hu, Y., Nakagawa, Y., Purushotham, K. R. & Humphreys-Beher, M. G. (1992) Functional changes in salivary glands of autoimmune disease-prone NOD mice, *Am J Physiol Endocrinol Metab. 263*, E607-E614.

22. Robinson, C. P., Yamamoto, H., Peck, A. B. & Humphreys-Beher, M. G. (1996) Genetically programmed development of salivary gland abnormalities in the NOD (Nonobese Diabetic)-scid mouse in the absence of detectable lymphocytic infiltration: a potential trigger for Sialoadenitis of NOD mice, *Clin Immunol Immunopathol. 79*, 50-59.

23. Humphreys-Beher, M. G., Yamachika, S., Yamamoto, H., Maeda, N., Nakagawa, Y., Peck, A. B. & Robinson, C. P. (1998) Salivary gland changes in the NOD mouse model for Sjögren's syndrome: is there a non-immune genetic trigger?, *Eur J Morphol. 36*, 247-251.

24. Serreze, D. V., Chapman, H. D., Varnum, D. S., Hanson, M. S., Reifsnyder, P. C., Richard, S. D., Fleming, S. A., Leiter, E. H. & Schultz, L. D. (1996) B lymphocytes are essential for the initiation of T cell-mediated autoimmune diabetes: analysis of a new "speed congenic" stock of NOD.Igmnull mice, *J Exp Med. 184*, 2049-2053.

25. Ralevic, V. & Burnstock, G. (1998) Receptors for purines and pyrimidines, *Pharmacol Rev. 50*, 413-492.

26. Boarder, M. R. & Hourani, S. M. O. (1998) The regulation of vascular function by P2 receptors: multiple sites and multiple receptors, *Trends Pharmacol Sci. 19*, 99-107.

27. Harden, T. K., Lazarowski, E. R. & Boucher, R. C. (1997) Release, metabolism and interconversion of adenine and uridine nucleotides: implications for G protein-coupled P2 receptor agonist selectivity, *Trends Pharmacol Sci. 18*, 43-46.

28. King, B. F., Townsend-Nicholson, A. & Burnstock, G. (1998) Metabatropic receptors for ATP and UTP: exploring the correspondence between native and recombinant nucleotide receptors, *Trends Pharmacol Sci. 19*, 506-514.

29. Kunapuli, S. P. & Daniel, J. L. (1998) P2 receptor subtypes in the cardiovascular system, *Biochem J. 336*, 513-523.

30. Abbrachio, M. P. & Burnstock, G. (1994) Purinoceptors: are there families of P2X and P2Y purinoceptors?, *Pharmacol Ther. 64*, 455-475.

31. Bean, B. P. (1992) Pharmacology and electrophysiology of ATP-activated ion channels, *Trends Pharmacol Sci. 13*, 87-90.

32. Dubyak, G. R. & El-Moatassim, C. (1993) Signal transduction via P2-purinergic receptors for extracellular ATP and other nucleotides, *Am J Physiol Cell Physiol. 265*, C577-C606.

33. North, R. A. (1996) P2X purinoceptor plethora, *Semin Neurosci. 8*, 187-194.

34. Buell, G., Collo, G. & Rassendren, F. (1996) P2X receptors: an emerging channel family, *Eur J Neurosci. 8*, 2221-2228.

35. Dixon, C. J., Bowler, W. B., Fleetwood, P., Ginty, A. F., Gallagher, J. A. & Carron, J. A. (1997) Extracellular nucleotides stimulate proliferation in MCF-7 breast cancer cells via P2-purinoceptors, *Br J Pharmacol. 75*, 34-39.

36. Marteau, F., Le Poul, E., Communi, D., Communi, D., Labouret, C., Savi, P., Boeynaems, J.-M. & Gonzalez, N. S. (2003) Pharmacological characterization of the human $P2Y_{13}$ receptor, *Mol Pharmacol. 64*, 104-112.

37. Burnstock, G. & Williams, M. (2000) P2 purinergic receptors: modulation of cell function and therapeutic potential, *J Pharmacol Exp Ther. 295*, 862-869.

38. Turner, J. T., Landon, L. A., Gibbons, S. J. & Talamo, B. R. (1999) Salivary gland P2 nucleotide receptors, *Crit Rev Oral Biol Med. 10*, 210-224.

39. Kim, H. D., Bowen, J. W., James-Kracke, M. R., Landon, L. A., Camden, J. M., Burnett, J. E. & Turner, J. T. (1996) Potentiation of regulatory volume

decrease by P2U purinoceptors in HSG-PA cells, *Am J Physiol Cell Physiol. 270*, C89-C97.

40. Erb, L., Liu, J., Ockerhausen, J., Kong, Q., Garrad, R. C., Griffin, K., Neal, C., Drugh, B., Santiago-Perez, L. I., Gonzalez, F. A., Gresham, H. D., Turner, J. T. & Weisman, G. A. (2001) An RGD sequence in the $P2Y_2$ receptor interacts with $\alpha v\beta 3$ integrins and is required for G_o-mediated signal transduction, *J Cell Biol. 153*, 491-501.

41. Garritsen, A., Zhang, Y. & Cooper, D. M. (1992) Purinergic receptor regulation of signal transduction in NC-20 cells, *Mol Pharmacol. 41*, 743-749.

42. Schulze-Lohoff, E., Bitzer, M., Ogilvie, A. & Sterzel, R. B. (1995) P2U-purinergic receptor activation mediates inhibition of cAMP accumulation in cultured renal mesangial cells, *Ren Physiol Biochem. 18*, 219-230.

43. Parr, C. E., Sullivan, D. M., Paradiso, A. M., Lazarowski, E. R., Burch, L. H., Olsen, J. C., Erb, L., Weisman, G. A., Boucher, R. C. & Turner, J. T. (1994) Cloning and expression of a human P2U nucleotide receptor, a target for cystic fibrosis pharmacotherapy, *Proc Natl Acad Sci U S A. 91*, 3275-3279.

44. Clarke, L. L. & Boucher, R. C. (1992) Chloride secretory response to extracellular ATP in human normal and cystic fibrosis nasal epithelia, *Am J Physiol Cell Physiol. 263*, C348-C356.

45. Hiruma, H. & Bourque, C. W. (1995) P2 purinoceptor-mediated depolarization of rat supraoptic neurosecretory cells in vitro, *J Physiol (Lond). 489*, 805-811.

46. Purkiss, J. R. & Boarder, M. R. (1992) Stimulation of phosphatidate synthesis in endothelial cells in response to P2-receptor activation: Evidence for phospholipase C and phospholipase D involvement, phosphatidate and diacylglycerol interconversion and the role of protein kinase C, *Biochem J. 287*, 31-36.

47. Pfeilschifter, J. & Merriweather, C. (1993) Extracellular ATP and UTP activation of phospholipase D is mediated by protein kinase C-ε in rat renal mesangial cells, *Br J Pharmacol. 110*, 847-853.

48. Neary, J. T., Kang, Y., Bu, Y., Yu, E., Akong, K. & Peters, C. M. (1999) Mitogenic signaling by ATP/P2Y purinergic receptors in astroctyes: involvement of a calcium-independent protein kinase C, extracellular signal-regulated protein kinase pathway distinct from the phosphatidylinositol-specific phospholipase C/calcium pathway, *J Neurosci. 19*, 4211-4220.

49. Patel, V., Brown, C., Goodwin, A., Wilkie, N. & Boarder, M. R. (1996) Phosphorylation and activation of p42 and p44 mitogen-activated protein kinase are required for the P2 purinoceptor stimulation of endothelial prostacyclin production, *Biochem J. 320*, 221-116.

50. Huwiler, A., van Rossum, G., Wartmann, M. & Pfeilschifter, J. (1997) Stimulation by extracellular ATP and UTP of the stress-activated protein kinase cascade in rat renal mesangial cells, *Br J Pharmacol. 120*, 807-812.

51. Malam-Souley, R., Seye, C., Gadeau, A. P., Loirand, G., Pillois, X., Campan, M., Pacaud, P. & Desgranges, C. (1996) Nucleotide receptor P2U partially mediates ATP-induced cell cycle progression of aortic smooth muscle cells, *J Cell Physiol. 166*, 57-65.

52. Ahn, J. S., Camden, J. M., Schrader, A. M., Redman, R. S. & Turner, J. T. (2000) Reversible regulation of $P2Y_2$ nucleotide receptor expression in the duct-ligated rat submandibular gland, *Am J Physiol Cell Physiol. 279*, C286-C294.

53. Seye, C., Kong, Q., Erb, L., Garrad, R. C., Krugh, B., Wang, M., Turner, J. T., Sturek, M., Gonzalez, F. A. & Weisman, G. A. (2002) Functional $P2Y_2$ nucleotide receptors mediate uridine 5'-triphosphate-induced intimal hyperplasia in collared rabbit carotid arteries, *Circulation. 106*, 2720-2726.

54. Turner, J. T., Weisman, G. A. & Camden, J. M. (1997) Up-regulation of $P2Y_2$ nucleotide receptors in rat salivary gland cells during short-term culture, *Am J Physiol Cell Physiol. 273*, C1100-C1107.

55. Hou, M., Malmsjö, M., Möller, S., Pantev, E., Bergdahl, A., Zhai, X.-H., Sun, X.-Y., Hedner, T., Edvinsson, L. & Erlinge, D. (1999) Increase in cardiac $P2X_1$- and $P2Y_2$-receptor mRNA levels in congestive heart failure, *Life Sci. 65*, 1195-1206.

56. Kishore, B. K., Wang, Z., Rab, H., Haq, M. & Soleimani, M. (1998) Upregulation of $P2Y_2$ purinoceptor during ischemic reperfusion injury (IRI): possible relevance to diuresis of IRI (Abstract), *J Am Soc Nephrol. 9*, 581.

57. Koshiba, M., Apasov, S., Sverdlov, V., Chen, P., Erb, L., Turner, J. T., Weisman, G. A. & Sitkovsky, M. V. (1997) Transient up-regulation of $P2Y_2$ nucleotide receptor mRNA expression is an immediate early gene response in activated thymocytes, *Proc Natl Acad Sci U S A. 94*, 831-836.

58. Seye, C. I., Gadeau, A. P., Daret, D., Dupuch, F., Alzieu, P., Capron, L. & Desgranges, C. (1997) Overexpression of the $P2Y_2$ purinoceptor in intimal lesions of the rat aorta, *Arterioscler Thromb Vasc Biol. 17*, 3602-3610.

59. Ahn, J. S., Camden, J. M. & Turner, J. T. (2001) Involvement of the ERK1/2 signaling pathway in up-regulation of $P2Y_2$ nucleotide receptors during short-term culture of salivary gland cells, *Int J Oral Biol. 26*, 31-37.

60. Soltoff, S. P. (1998) Related adhesion focal tyrosine kinase and the epidermal growth factor receptor mediate the stimulation of mitogen-activated protein kinase by the G-protein-coupled $P2Y_2$ receptor, *J Biol Chem. 273*, 23110-23117.

61. Tu, M.-T., Luo, S.-F., Wang, C.-C., Chien, C.-S., Chiu, C.-T., Lin, C.-C. & Yang, C.-M. (2000) $P2Y_2$ receptor-mediated proliferation of C6 glioma cells via activation of Ras/Raf/MEK/MAPK pathway, *Br J Pharmacol. 129*, 1481-1489.

62. Liu, J., Liao, Z., Camden, J. M., Griffin, K., Garrad, R. C., Santiago-Perez, L. I., Gonzalez, F. A., Seye, C., Weisman, G. A. & Erb, L. (2004) Src homology 3 binding sites in the $P2Y_2$ nucleotide receptor interact with src and regulate activities of src, proline-rich tyrosine kinase 2, and growth factor receptors, *J Biol Chem. 279*, 8212-8218.

63. Homolya, L., Watt, W. C., Lazarowski, E. R., Koller, B. H. & Boucher, R. C. (1999) Nucleotide-regulated calcium signaling in lung fibroblasts and epithelial cells from normal and $P2Y_2$ receptor (-/-) mice, *J Biol Chem. 274*, 26454-26460.

64. Cressman, B. L., Sazorowski, E., Homolya, L., Boucher, R. C., Koller, B. H. & Grubb, B. R. (1999) Effect of loss of $P2Y_2$ receptor gene expression on nucleotide regulation of murine epithelial Cl^- transport, *J Biol Chem. 274*, 26461-26468.

65. Yerxa, B. R. (2001) Therapeutic use of nucleotides in respiratory and ophthalmic diseases, *Drug Dev Res. 52*, 196-201.

66. Stutts, M. J. & Boucher, R. C. (1999) Cystic fibrosis gene and functions of CFTR: implications of dysfunctional ion transport for pulmonary pathogenesis in *Cystic Fibrosis in Adults* (Yankaskas, J. R. & Knowles, M. R., eds) pp. 3-25, Lippincott-Raven, Philadelphia.

67. Seye, C., Yu, N., Gonzalez, F. A., Erb, L. & Weisman, G. A. (2004) The $P2Y_2$ nucleotide receptor mediates vascular cell adhesion molecule-1 expression through interaction with VEGF receptor-2 (KDR/Flk-1), *J Biol Chem. 279*, 35679-35686.

68. Weerasinghee, D., McHugh, K. P., Ross, F. P., Brown, E. J., Gisler, R. H. & Imhof, B. A. (1998) A role for the $\alpha v\beta 3$ integrin in the transmigration of monocytes, *J Cell Biol. 142*, 595-607.

69. Jones, J. I., Prevette, T., Gockerman, A. & Clemmons, D. R. (1996) Ligand occupancy of the $\alpha V\beta 3$ integrin is necessary for smooth muscle cells to migrate in response to insulin-like growth factor I, *Proc Nat Acad Sci U S A. 93*, 2482-2487.

70. Murdoch, C. & Finn, A. (2000) Chemokine receptors and their role in inflammation and infectious diseases, *Blood. 95*, 3032-3043.

71. Erb, L., Garrad, R. C., Wang, T., Quinn, T., Turner, J. T. & Weisman, G. A. (1995) Site-directed mutagenesis of P2U purinoceptors. Positively charged amino acids in transmembrane helices 6 and 7 affect agonist potency and specificity, *J Biol Chem. 270*, 4185-4188.

72. Lazarowski, E. R. & Boucher, R. C. (2001) UTP as an extracellular signaling molecule, *News Physiol Sci. 16*, 1-5.

73. Schwiebert, E. M. & Zsembery, A. (2003) Extracellular ATP as a signaling molecule for epithelial and other cells, *Biochim Biophys Acta. 1615*, 7-32.

74. Soltoff, S. P., McMillian, M. K., Cragoe, E. J., Cantley, L. C. & Talamo, B. R. (1990) Effects of extracellular ATP on ion transport systems and $[Ca^{2+}]_i$ in rat parotid acinar cells, *J Gen Physiol. 95*, 319-346.

75. McMillian, M. K., Soltoff, S. P., Cantley, L. C. & Talamo, B. R. (1987) Extracellular ATP elevates intracellular free calcium in rat parotid acinar cells, *Biochem Biophys Res Commun. 149*, 523-530.

76. Harden, T. K., Boyer, J. L. & Nicholas, R. A. (1995) P2-purinergic receptors: subtype-associated signaling responses and structure, *Annu Rev Pharmacol Toxicol. 35*, 541-579.

77. Park, M. K., Garrad, R. C., Weisman, G. A. & Turner, J. T. (1997) Changes in $P2Y_1$ nucleotide receptor activity during the development of rat salivary glands, *Am J Physiol Cell Physiol. 272*, C1388-C1393.

78. Amsallem, H., Metioui, M., VandenAbeele, A., Elyamani, A., Moran, A. & Dehaye, J. P. (1996) Presence of a metabatropic and an ionotropic purinergic receptor on rat submandibular ductal cells, *Am J Physiol Cell Physiol. 271*, C1546-C1555.

79. Robinson, C. P., Cornelius, J., Bounous, D. I., Yamamoto, H., Humphreys-Beher, M. G. & Peck, A. B. (1998) Infiltrating lymphocyte populations and cytokine production in the salivary and lacrimal glands of autoimmune NOD mice in *Lacrimal Gland, Tear Film, and Dry Eyes Syndromes 2* (Sullivan, D. A., ed) pp. 493-497, Plenum Press, New York.

80. Turner, J. T. & Camden, J. M. (1990) The influence of vasoactive intestinal peptide receptors in dispersed acini from rat submanidibular gland on cyclic AMP production and mucin release, *Arch Oral Biol. 35*, 103-108.

81. Nguyen, T., Erb, L., Weisman, G. A., Marchese, A., Heng, H. Q., Garrad, R. C., George, S. R., Turner, J. T. & Dowd, B. F. (1995) Cloning, expression, and chromosomal localization of the human uridine nucleotide receptor gene, *J Biol Chem. 270*, 30845-30848.

82. Nguyen, K.-H. T., Brayer, J., Cha, S., Diggs, S., Yasunari, U., Hilal, G., Peck, A. B. & Humphreys-Beher, M. G. (2000) Evidence for antimuscarinic acetylcholine receptor antibody-mediated secretory dysfunction in NOD mice, *Arthritis Rheum. 43*, 2297-2306.

83. Yamamoto, H., Simms, N. E., Macauley, S. P., Nguyen, K.-H. T., Nakagawa, Y. & Humphreys-Beher, M. G. (1996) Alterations in the secretory response of non-obese diabetic (NOD) mice to muscarinic receptor stimulation, *Clin Immunol Immunopathol. 78*, 245-255.

84. Tobin, G., Giglio, D. & Gotrick, B. (2002) Studies of muscarinic receptor subtypes in salivary gland function in anaesthetized rats, *Auton Neurosci. 100*, 1-9.

85. Li, Y., Kuang, K., Yerxa, B. R., Wen, Q., Rosskothen, H. & Fischbarg, J. (2001) Rabbit conjunctival epithelium transports fluid, and $P2Y_2$ receptor agonists stimulate Cl- and fluid secretion., *Am J Physiol Cell Physiol. 281*, C595-C602.

86. Seye, C. I., Yu, N., Jain, R., Kong, Q., Minor, T., Newton, J., Erb, L., Gonzalez, F. A. & Weisman, G. A. (2003) The $P2Y_2$ nucleotide receptor mediates UTP-induced vascular cell adhesion molecule-1 expression in coronary artery endothelial cells, *J Biol Chem. 278*, 24960-24965.

87. Hopfner, M., Maaser, K., Barthel, B., von Lampe, B., Hanski, C., Riecken, E. O., Zeitz, M. & Scherubl, H. (2001) Growth inhibition and apoptosis induced by $P2Y_2$ receptors in human colorectal carcinoma cells: involvement of intracellular calcium and cyclic adenosine monophospate, *Int J Colorectal Dis. 16*, 154-166.

88. Maaser, K., Hopfner, M., Kap, H., Sutter, A. P., Barthel, B., von Lampe, B., Zeitz, M. & Scherubl, H. (2002) Extracellular nucleotides inhibit growth of human oesophageal cancer cells via $P2Y_2$ receptors, *Br J Cancer. 86*, 636-644.

89. Graham, A., McLees, A., Kennedy, C., Gould, G. W. & Plevin, R. (1996) Stimulation by the nucleotides ATP and UTP of mitogen-activated protein kinase in EAhy 926 endothelial cells, *Br J Pharmacol. 117*, 1341-1347.

90. Santiago-Perez, L. I., Flores, R. V., Santos-Berrios, C., Chorna, L. E., Krugh, B., Garrad, R. C., Erb, L., Weisman, G. A. & Gonzalez, F. A. (2001) $P2Y_2$ nucleotide receptor signaling in human monocytic cells: activation, desensitization, and coupling to mitogen-activated protein kinases, *J Cell Physiol. 187*, 196-208.

91. Schrader, A. M., Camden, J. M. & Weisman, G. A. (2005) $P2Y_2$ nucleotide receptor up-regulation in the NOD.B10 mouse model of Sjögren's syndrome, *Arch Oral Biol. 50*, 533-540.

92. Prenzel, N., Zwick, E., Daub, H., Leserer, M., Abraham, R., Wallasch, C. & Ullrich, A. (1999) EGF receptor transactivation by G-protein-coupled receptors requires metalloproteinase cleavage of proHB-EGF, *Nature. 402*, 884-888.

93. Pierce, K. L., Tohgo, A., Ahn, S., Field, M. E., Luttrell, L. M. & Lefkowitz, R. J. (2001) Epidermal growth factor (EGF) receptor-dependent ERK activation by G protein-coupled receptors, *J Biol Chem. 276*, 23155-23160.

94. Yu, H. & Turner, J. T. (1991) Functional studies in the human submandibular duct cell line, HSG-PA, suggest a second salivary gland receptor subtype for nucleotides, *J Pharmacol Exp Ther. 259*, 1344-1350.

95. Daub, H., Wallasch, C., Lankenau, A., Herrlich, A. & Ullrich, A. (1997) Signal characteristics of G protein-transactivated EGF receptor, *EMBO J. 16*, 7032-7044.

96. Kalmes, A., Vesti, B. R., Daum, G., Abraham, J. R. & Clowes, A. W. (2000) Heparin blockade of thrombin-induced smooth muscle cell migration involves inhibition of epidermal growth factor (EGF) receptor transactivation by heparin-binding EGF-like growth factor, *Circ Res. 87*, 92-98.

97. Harris, R. C., Chung, E. & Coffey, R. J. (2003) EGF receptor ligands, *Exp Cell Res. 284*, 2-13.

98. Seals, D. F. & Courtneidge, S. A. (2003) The ADAMs family of metalloproteases: multidomain proteins with multiple functions, *Genes Dev. 17*, 7-30.

99. Schafer, B., Gschwind, A. & Ullrich, A. (2004) Multiple G-protein-coupled receptor signals converge on the epidermal growth factor receptor to promote migration and invasion, *Oncogene. 23*, 991-999.

100. Sahin, U., Weskamp, G., Kelly, K., Zhou, H.-M., Higashiyama, S., Peschon, J., Hartmann, D., Saftig, P. & Blobel, C. P. (2004) Distinct roles for ADAM10 and ADAM17 in ectodomain shedding of six EGFR ligands, *J Cell Biol. 164*, 769-779.

101. Camden, J. M., Schrader, A. M., Camden, R. E., Gonzalez, F. A., Erb, L., Seye, C. & Weisman, G. A. (2005) $P2Y_2$ nucleotide receptors enhance α-secretase-dependent amyloid precursor protein processing, *J Biol Chem. in press*.

102. Daaka, Y., Luttrell, L. M. & Lefkowitz, R. J. (1997) Switching of the coupling of the β_2-adrenergic receptor to different G proteins by protein kinase A, *Nature. 390*, 88-91.

103. Luttrell, L. M., Ferguson, S. S., Daaka, Y., Miller, W. E., Maudsley, S., Della, R. G., Lin, F., Kawakatsu, H., Owada, K., Luttrell, D. K., Caron, M. G. &

Lefkowitz, R. J. (1999) Beta-arrestin-dependent formation of beta2 adrenergic receptor-Src protein kinase complexes, *Science. 283*, 655-661.

104. Luttrell, L. M., Della Rocca, G. J., van Biesen, T., Luttrell, D. K. & Lefkowitz, R. J. (1997) Gβγ subunits mediate src-dependent phosphorylation of the epidermal growth factor receptor, *J Biol Chem. 272*, 4637-4644.

105. Zwick, E., Daub, H., Aoki, N., Yamaguchi-Aoki, Y., Tinhofer, I., Maly, K. & Ullrich, A. (1997) Critical role of calcium- dependent epidermal growth factor receptor transactivation in PC12 cell membrane depolarization and bradykinin signaling, *J Biol Chem. 272*, 24767-24770.

106. Keely, S. J., Uribe, J. M. & Barrett, K. E. (1998) Carbachol stimulates transactivation of epidermal growth factor receptor and mitogen-activated protein kinase in T84 cells, *J Biol Chem. 273*, 27111-27117.

107. Keely, S. J., Calandrella, S. O. & Barrett, K. E. (2000) Carbachol-stimulated transactivation of epidermal growth factor receptor and mitogen-activated protein kinase in T84 cells is mediated by intracellular Ca^{2+}, PYK-2, and p60src, *J Biol Chem. 275*, 12619-12625.

108. Maudsley, S., Pierce, K. L., Zamah, A. M., Miller, W. E., Ahn, S., Daaka, Y., Lefkowitz, R. J. & Luttrell, L. M. (2000) The β_2-adrenergic receptor mediates extracellular signal-regulated kinase activation via assembly of a multi-receptor complex with the epidermal growth factor receptor, *J Biol Chem. 275*, 9572-9580.

109. Eguchi, S., Numaguchi, K., Iwasaki, H., Matsumoto, T., Yamakawa, T., Utsunomiya, H., Motley, E. D., Kawakatsu, H., Owada, K. M., Hirata, Y., Marumo, F. & Inagami, T. (1998) Calcium-dependent epidermal growth factor receptor transactivation mediates the angiotensin II-induced mitogen-activated protein kinase activation in vascular smooth muscle cells, *J Biol Chem. 273*, 8890-8896.

110. Dikic, I., Tokiwa, G., Lev, S., Courtneidge, S. A. & Schlessinger, J. (1996) A role of Pyk2 and src in linking G-protein-coupled receptors with MAP kinase activation, *Nature. 383*, 547-550.

111. Allinson, T. M. J., Parkin, E. T., Turner, A. J. & Hooper, N. M. (2003) ADAMs family members as amyloid precursor protein α-secretases, *Journal of Neuroscience Research. 74*, 342-352.

112. Kheradmand, F. & Werb, Z. (2002) Shedding light on sheddases: role in growth and development, *Bioessays. 24*, 8-12.

113. Anders, A., Gilbert, S., Garten, W., Postina, R. & Fahrenholz, F. (2001) Regulation of the α-secretase ADAM10 by its prodomain and proprotein convertases, *FASEB J. 15*, 1837-1839.

114. Anderson, E. D., VanSlyke, J. K., Thulin, C. D., Jean, F. & Thomas, G. (1997) Activation of the furin endoprotease is a multiple-step process: requirements for acidification and internal propeptide cleavage, *The EMBO Journal. 16*, 1508-1518.

115. Schafer, B., Marg, B., Gschwind, A. & Ullrich, A. (2004) Distinct ADAM metalloproteases regulate G protein-coupled receptor-induced cell proliferation and survival, *J Biol Chem. 279*, 47929-47938.

116. Hinkle, C. L., Sunnarborg, S. W., Loiselle, D., Parker, C. E., Stevenson, M., Russell, W. E. & Lee, D. C. (2004) Selective roles for tumor necrosis factor α-converting enzyme/ADAM17 in the shedding of the epidermal growth factor receptor ligand family: the juxtamembrane stalk determines cleavage efficiency, *J Biol Chem. 279*, 24179-24188.

117. Weisman, G. A., Turner, J. T. & Fedan, J. S. (1996) Structure and function of P2 purinoceptors, *J Pharmacol Exp Ther. 277*, 1-9.

118. Short, S. M., Boyer, J. L. & Juliano, R. L. (2000) Integrins regulate the linkage between upstream and downstream events in G protein-coupled receptor signaling to mitogen-activated protein kinase, *J Biol Chem. 275*, 12970-12977.

119. Della Rocca, G. J., Maudsley, S., Daaka, Y., Lefkowitz, R. J. & Luttrell, L. M. (1999) Pleiotropic coupling of G protein-coupled receptors to the mitogen-activated protein kinase cascade, *J Biol Chem. 274*, 13978-13984.

120. Boarder, M. R., Weisman, G. A., Turner, J. T. & Wilkinson, G. F. (1995) G protein-coupled P2 purinoceptors: from molecular biology to fuctional responses, *Trends Pharmacol Sci. 16*, 133-9.

121. Daub, H., Weiss, F. U., Wallasch, C. & Ullrich, A. (1996) Role of transactivation of the EGF receptor in signalling by G-protein-coupled receptors, *Nature. 379*, 557-560.

122. Batzer, A. G., Rotin, D., Urena, J. M., Skolnick, E. Y. & Schlessinger, J. (1994) Hierarchy of binding sites for Grb2 and Shc for the epidermal growth factor receptor, *Mol Cell Biol. 14*, 5192-5201.

123. Rotin, D., Margolis, B., Mohammadi, M., Daly, R. J., Daum, G., Li, N., Fischer, E. H., Burgess, W. H., Ullrich, A. & Schlessinger, J. (1992) Sh2 domains prevent tyrosine dephosphorylation of the EGF receptor: identification of Tyr 992 as the high-affinity binding site for SH2 domains of phospholipase Cγ, *EMBO J. 11*, 559-567.

124. Pierce, K. L., Luttrell, L. M. & Lefkowitz, R. J. (2001) New mechanisms in heptahelical receptor signaling to mitogen activated protein kinase cascades, *Oncogene. 20*, 1532-1539.

125. Pascall, J. C. (1997) Post-transcriptional regulation of gene expression by androgens: recent observations from the epidermal growth factor gene, *J Mol Endocrinol. 18*, 177-180.

126. Schafer, R., Sedehizade, F., Welte, T. & Reiser, G. (2003) ATP- and UTP-activated P2Y receptors differently regulate proliferation of human lung epithelial tumor cells, *Am J Physiol Lung Cell Mol Physiol. 285*, L376-385.

127. Muscella, A., Elia, M. G., Greco, S., Storelli, C. & Marsiagliante, S. (2003) Activation of $P2Y_2$ receptor induces c-FOS protein through a pathway involving mitogen-activated protein kinases and phosphoinositide 3-kinases in HeLa cells, *J Cell Physiol. 195*, 234-240.

128. Greig, A. V., Linge, C., Terenghi, G., McGrouther, D. A. & Burnstock, G. (2003) Purinergic receptors are part of a functional signaling system for proliferation and differentiation of human epidermal keratinocytes, *J Invest Dermatol. 120*, 1007-1015.

129. Brambilla, R., Burnstock, G., Bonazzi, A., Ceruti, S., Cattabeni, F. & Abbrachio, M. P. (1999) Cyclo-oxygenase-2 mediates P2Y receptor-induced reactive astrogliosis, *Br J Pharmacol. 126*, 563-567.

130. Brambilla, R. & Abbrachio, M. P. (2001) Modulation of cyclooxygenase-2 and brain reactive astrogliosis by purinergic P2 receptors, *Ann N Y Acad Sci. 939*, 54-62.

131. Xu, J., Chalimoniuk, M., Shu, Y., Simonyi, A., Sun, A. Y., Gonzalez, F. A., Weisman, G. A., Wood, W. G. & Sun, G. Y. (2003) Prostaglandin E2 production in astrocytes: regulation by cytokines, extracellular ATP, and oxidative agents, *Prostaglandins Leukot Essent Fatty Acids. 69*, 437-48.

132. Katzur, A. C., Koshimizu, T.-A., Tomic, M., Schultze-Mosgau, A., Ortmann, O. & Stojilkovic, S. S. (1999) Expression and responsiveness of $P2Y_2$ receptors in human endometrial cancer cell lines, *J Clin Endocrinol Metab. 84*, 4085-4091.

133. Hopfner, M., Lemmer, K., Jansen, A., Hanski, C., Riecken, E.-O., Gavish, M., Mann, B., Buhr, H., Glassmeier, G. & Scherubl, H. (1998) Expression of functional P2-purinergic receptors in primary cultures of human colorectal carcinoma cells, *Biochem Biophys Res Commun. 251*, 811-817.

134. Belmokhtar, C. A., Hillion, J. & Segal-Bendirdjian, E. (2001) Staurosporine induces apoptosis through both caspase-dependent and caspase-independent mechanisms, *Oncogene. 20*, 3354-3362.

135. Hou, M., Möller, S., Edvinsson, L. & Erlinge, D. (2000) Cytokines induce upregulation of vascular $P2Y_2$ receptors and increased mitogenic responses to UTP and ATP, *Arterioscler Thromb. 20*, 2064-2069.

136. Kellerman, D., Evans, R., Mathews, D. & Shaffer, C. (2002) Inhaled $P2Y_2$ receptor agonists as a treatment for patients with cystic fibrosis lung disease, *Adv Drug Deliv Rev. 54*, 1463-1474.

137. Weisman, G. A., Garrad, R. C., Erb, L. J., Otero, M., Gonzalez, F. A. & Clarke, L. L. (1998) Structure and function of $P2Y_2$ nucleotide receptors in cystic fibrosis (CF) epithelium, *Adv Exp Med Biol. 431*, 417-424.